Synthesis and Carbon Dioxide Adsorption Properties of Amine Modified Particulate Silica Aerogel Sorbents

by

Nicholas Linneen

A Dissertation Presented in Partial Fulfillment
of the Requirements for the Degree
Doctor of Philosophy

Approved July 2014 by the
Graduate Supervisory Committee:

Jerry Lin, Chair
Robert Pfeffer
Mary Lind
Kaushal Rege
David Nielsen
James Anderson

ARIZONA STATE UNIVERSITY

August 2014

ABSTRACT

Post-combustion carbon capture is a viable option for reducing CO2 greenhouse gas emissions, and one potentially promising technology for this route is adsorption using chemically and physically based sorbents. A number of exceptional CO2 sorbents materials have been prepared including metal organic frameworks, zeolites, and carbon based materials. One particular group of capable materials are amine based solid sorbents that has shown to possess high adsorption capacities and favorable adsorption kinetics. A key variable in the synthesis of an amine based sorbent is the support which acts as the platform for the amine modification. Aerogels, due to their high porosities and surface areas, appear to be a promising support for an amine modified CO2 sorbent. Therefore, in order to develop a commercially viable CO2 sorbent, particulate aerogels manufactured by Cabot Corporation through an economical and proprietary ambient drying process were modified with amines using a variety of functionalization methods. Two methods of physical impregnation of the amino polymer TEPA were performed in order to observe the performance as well as understand the effects of how the TEPA distribution is affected by the method of introduction. Both samples showed excellent adsorption capacities but poor cyclic stability for lack of any covalent attachment. Furthermore the method of TEPA impregnation seems to be independent on how the polymer will be distributed in the pore space of aerogel. The last two methods utilized involved covalently attaching amino silanes to the surface silanols of the aerogel. One method was performed in the liquid phase under anhydrous and hydrous conditions. The materials developed through the hydrous method have much greater adsorption capacities relative to the anhydrous sample as a result of the greater amine content present in the hydrous

sample. Water is another source of silylation where additional silanes can attach and polymerize. These samples also possessed stable cyclic stability after 100 adsorption/regeneration cycles. The other method of grafting was performed in the gas phase through ALD. These samples possessed exceptionally high amine efficiencies and levels of N content without damaging the microstructure of the aerogel in contrast to the liquid phase grafted sorbents.

The following chapters are modified versions of papers published or accepted for publication:

Chapter 2

Linneen N., Lin Y. S., Pfeffer R., (2013). CO_2 Capture using Particulate Silica Aerogel Immobilization with Tetraethylenepentamine. *Microporous and Mesoporous Materials, 176,* 123-131.

Chapter 3

Linneen N., Lin Y. S., Pfeffer R., (2013). Amine Distribution and Carbon Dioxide Sorption Performance of Amine Coated Silica Aerogel Sorbents: Effect of Synthesis Methods. *Industrial & Engineering Chemistry, 52,* 14671-14679.

Chapter 4

Linneen N., Lin Y. S., Pfeffer R., (2014) Influence of Synthesis Conditions on CO_2 Adsorption Performance of Amine Grafted Particulate Silica Aerogels. *Chemical Engineering Journal* (Accepted for Publication)

ACKNOWLEDGMENTS

I would like to take this opportunity to thank my family for their love and support while I pursued my degree, particularly my mother who gave me the drive and encouragement to keep persevering toward my goal.

I would like to thank my advisors Dr. Jerry Lin and Dr. Robert Pfeffer for allowing me to become a part of their group and for introducing me to the research world. Dr. Lin and Dr. Pfeffer gave me the opportunity to do leading research in important and influential topics. With the understanding and skills on how to conduct research and think like a scientist gained from collaborating with them, I know it will nothing but facilitate my future endeavors.

I would like to thank Dr. Nielsen, Dr. Rege, Dr. Lind, and Dr. Anderson for their willingness to serve on my committee and lend their expertise. I would also like to thank greatly Fred Pena for his constant hard work and support in the research, safety, and maintenance of Dr. Lin's laboratory.

Finally, I would like to thank all the current and former group members in Dr. Lin's group that I have had the pleasure to work with: Dr. Matthew Anderson, Dr. Shriya Seshadri, Dr. Carrie Eggen, Dr. Haibing Wang, Dr. Jose Ortiz-Landeros, Dr. Ding Wang, Teresa Rosa, Dr. Bo Lu, Xiaoli Ma, Alex Kasik, Defei Liu, Yang Liu, Dr. Xueliang Dong, Joshua James, Huifeng Zhang, and Stewart Mann.

I also highly appreciate the National Science Foundation for the financial support of this work.

TABLE OF CONTENTS

Page

CHAPTER Page

CHAPTER Page

APPENDIX Page

LIST OF TABLES

Table Page

LIST OF FIGURES

Figure Page

Figure Page

Figure Page

Figure Page

Figure Page

CHAPTER 1

GENERAL INTRODUCTION

1.1 Carbon Dioxide Capture Background

As is well known in the academic and scientific community, global emissions of carbon dioxide from anthropogenic point sources has resulted with convincing evidence in significant climate changes around the world. Atmospheric and oceanic average temperatures are rising, Arctic sea ice as well as mountain glaciers and snow coverage in both hemispheres are diminishing, consequently leading to increasing sea levels and ocean acidification (Bosch et al., 2007; Hofmann, Butler, & Tans, 2009). Such climate alterations are compromising major coral reef as well as terrestrial ecosystems which have serious influences on global biodiversity and the socioeconomic status of nations across the globe (Diffenbaugh & Field, 2013; Hoegh-Guldberg et al., 2007; Hughes et al., 2003). Therefore it is imperative that these major carbon dioxide anthropogenic emissions be reduced to prevent any further climate and ecological damage.

The point sources of interest are the fossil fueled power and industrial sectors releasing 13,375 $MtCO_2$ per year, approximately 60% of the total global CO_2 emissions (Bradshaw et al., 2005). Methods of CO_2 emission reduction are 1) more efficient uses of energy, 2) alternative fuels and energy resources, and 3) CO_2 capture and sequestration (CCS) technologies. Presently, the most practical methods to be implemented on large scales are CCS technologies. Main technologies of interest are cryogenic distillation (Hart & Gnanendran, 2009), membranes (Du, Park, Dal-Cin, & Guiver, 2012; Favre, 2011), adsorption (Choi, Drese, & Jones, 2009; Q. Wang, Luo, Zhong, & Borgna, 2011), and absorption (Puxty et al., 2009; M. Wang, Lawal, Stephenson, Sidders, & Ramshaw,

2011) which can be integrated in a pre-combustion, post-combustion, or oxy-fuel combustion setting (Kanniche et al., 2010). CO_2 capture in a post combustion setting is currently the most feasible due to its ease of plant modification and current experience of such systems. Pre-combustion capture requires an extensive reconstruction of the existing plant and are very complex where as oxy-fuel systems are more costly to retrofit relative to post-combustion and may need additional purification steps for transport (Notz, Tönnies, McCann, Scheffknecht, & Hasse, 2011).

Among the CSS technologies for post combustion, adsorption and absorption appear to be the most competitive. Cryogenic distillation to separate CO_2 from a post combustion flue gas is difficult and expensive. Membrane purification of CO_2 in gas mixtures such as natural gas has made significant advances (Adewole, Ahmad, Ismail, & Leo, 2013) but for conditions present in flue gas where CO_2 partial pressures are low (approximately 0.05 – 0.15 bar) membrane separation would be difficult and require very large, high surface area modules. Therefore the two promising candidates are adsorption using physical or chemical solid sorbents, or absorption using amine based aqueous alkaline solutions.

Liquid absorption (a.k.a. amine scrubbing) is a very well understood and practiced method of CO_2 capture in dilute systems. The fundamental process was first patented in 1930 and since the 1980's amine scrubbing has been used to separate CO_2 from small scale power plants in which there are currently four coal based plants of which have power outputs up to 30MW and more than 20 other CO_2 emitting plants that use amine scrubbing systems that use a 20-30% monoethanol amine aqueous solutions (Rochelle, 2009). The technology, though possibly the first generation of CCS to be integrated, has a

number of economic and human health threatening issues. Current systems have low CO_2 absorption capacities (kg CO_2 absorbed per kg absorbent), have a high propensity to corrode equipment, degrade due to thermal and chemical instabilities, require large amounts of energy for regeneration, need very large equipment units, and generate toxic by-products (Yeh, Pennline, & Resnik, 2004; Yu, 2012). It is these significant disadvantages that have led many academics and industrial scientists into investigating the use of solid adsorbents for post combustion capture.

Ideally, in order to be competitive with amine scrubbing systems the sorbent should lead to a 30-50% energy reduction required for operation, achieve a delta loading (i.e., the adsorption capacity achieved after a regeneration cycle) of at least 3.0 mmol of CO_2/g under flue gas conditions, be able to adsorb and desorb within a narrow temperature range (40-110 ^oC), have the stability to be regenerated and reach full capacity for a large number of cycles, and be durable in the presence of water vapor and other acid flue gas species (e.g., SO_x, NO_x) (Drage et al., 2012). Solid sorbents that have the potential to meet these criteria, both physical and chemical, include carbon based, zeolites, metal organic frameworks (MOF), and amine based. Carbon sorbents have extremely high surface areas, low cost, thermally stable, and can be easily customized to meet textural specifications. However, due to weak physical interactions with CO_2, carbon based materials do not perform well in flue gas temperatures (40-80 ^oC) and partial pressure (0.05-0.15 bar) (Q. Wang et al., 2011). Zeolites (i.e., porous crystalline aluminosilicates) have been extensively studied for CO_2 separations and perform quite well due to the stronger interaction with CO_2 through ion-dipole interactions (Montanari & Busca, 2008), but due to the presence of water vapor (0.1-0.15 bar) and other gases in

flue gas, their selectivities over CO_2 are low (X Xu, Song, Andresen, Miller, & Scaroni, 2003). MOF's are fairly new developed crystalline materials that are primarily composed of metal clusters connected through organic linkers that are extremely tailorable. These materials can posses open metal ion sites which can strongly adsorb CO_2, some having heats of adsorption up to 90 kJ/mol, and look to be a very promising material (Demessence, D'Alessandro, Foo, & Long, 2009).

Another very promising candidate and the main focus of this study is amine based solid sorbents. Similar to liquid amine scrubbing systems, these sorbents utilize reactive amine based compounds to covalently bind to CO_2 reversibly. Figure 1.1 reveals the potential of these sorbents within the flue gas operating range.

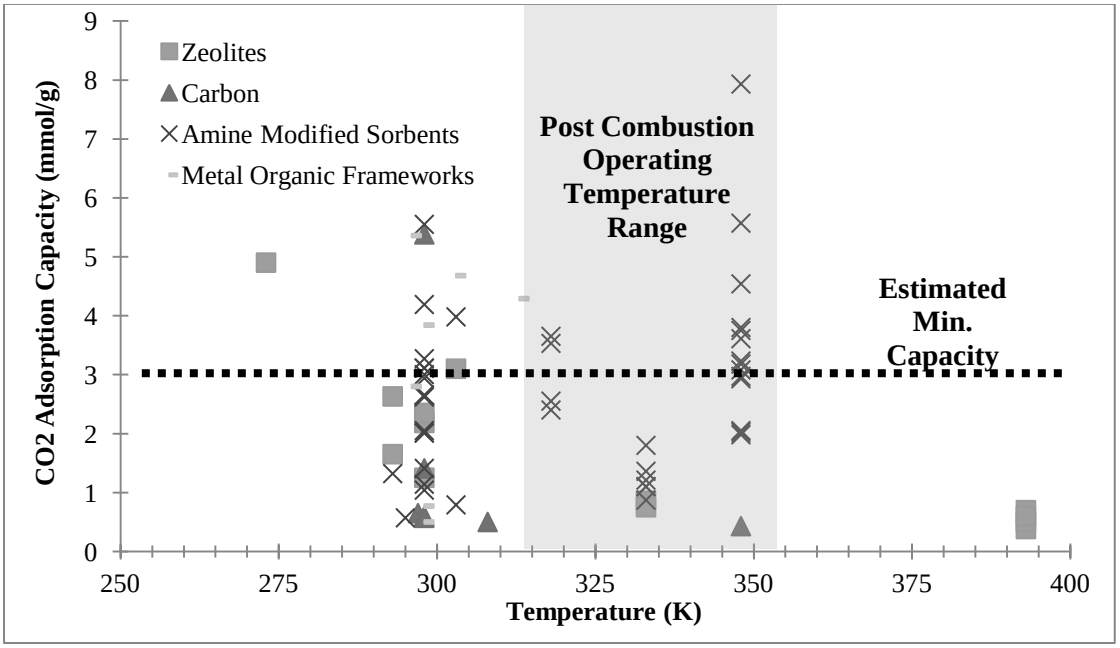

Figure 1.1: Adsorption Capacities of Various CO_2 Adsorbents Materials Tested under Simulated Flue Gas Conditions with Respect to Temperature (5-15 vol% CO_2, 5-10 vol% H_2O, 75-90 vol% N_2; 1 bar, 40 – 80 ^oC).Red Region is the Ideal Adsorption Temperature Operating Range (Drage et al., 2012).

Much of what the scientific community knows about the reaction mechanism and kinetics of amine-CO_2 chemistry has been understood by investigating aqueous amine scrubbing systems. The general consensus is that CO_2 binds to amines via two pathways to form carbamates and bicarbonates. Equation (1.1) & (1.2) shows the pathway of carbamate formation which has been reported and reviewed by several groups (Caplow, 1968; Danckwerts, 1979; Mahajani & Joshi, 1988; Versteeg, Van Dijck, & Van Swaaij, 1996b). The amine first binds to CO_2 through the unpaired electrons on nitrogen to form a zwitterionic intermediate followed by deprotonation of another free amine to form carbamate and ammonium species. This pathway leads to a stoichiometric amine:CO_2 ratio of 2:1 meaning the highest theoretical amine efficiency possible to attain in an adsorption process is 50% (i.e., moles of CO_2 adsorbed per mol of N). Unlike primary and secondary amines, tertiary amines due to thermodynamic instabilities and high steric hinderance cannot directly react with CO_2 as described by Eq. (1.1) & (1.2) unless under extremely high pH conditions (Donaldson & Nguyen, 1980; Jorgensen & Faurholt, 1954).

$$RNH_2 + CO_2 \Leftrightarrow RNH_2^+ COO^- \quad (1.1)$$

$$RNH_2^+ COO^- + RNH_2 \Leftrightarrow RNHCOO^- + RNH_3^+ \quad (1.2)$$

$$RNH_2 + CO_2 + H_2O \Leftrightarrow HCO_3^- + RNH_3^+ \quad (1.3)$$

The second pathway, Eq. (1.3) forms bicarbonate where primary, secondary, and also tertiary amines are utilized as a proton acceptor, or even a catalyst, for the hydration of CO_2 (Donaldson & Nguyen, 1980; Savage, Sartori, & Astarita, 1984). Specifically for tertiary or sterically hindered amines, the hydration of CO_2 occurs through a base-catalyzed hydration mechanism due to chemical instability (Donaldson & Nguyen, 1980;

Vaidya & Kenig, 2007). The formation of bicarbonate leads to an amine:CO_2 stoichiometric ratio of 1:1 and therefore it would be much more advantageous practically and economically for pathway two to be followed. However, between the two pathways carbamate formation is much more favorable because of its faster reaction kinetics and greater thermal stability leading to greater energy requirements for amine regeneration and reduced amine efficiencies (D.-H. Lee et al., 2008; Sartori & Savage, 1983; Versteeg, Van Dijck, & Van Swaaij, 1996a). This has led to increased research in absorption applications toward standard molar enthalpies and standard molar entropies of carbamates formed from amines with different geometries and stereochemical properties (Conway et al., 2012, 2013; Fernandes et al., 2012). However, in regards to amine based solid adsorption research, the major focus has been on methods of modification of a variety of amines on a wide range of porous supports.

The majority of research has had its primary focus on two methods of amine modification; wet impregnation and covalent grafting. The wet impregnation method is generally performed by mixing an amino polymer, commonly polyethyleneimine (PEI), with a volatile organic solvent (e.g., methanol, ethanol, acetone). The solid support of choice, which is commonly some porous siliceous material, is then added into this solution, mixed until fully saturated, and placed under heat and/or vacuum to remove the organic solvent leaving the polymer held within the pore space by weak intermolecular forces.

1.2 Amine Impregnated Solid Sorbents

The first to utilize this method was Xiaochun Xu, Song, Andresen, Miller, & Scaroni, (2002) who prepared a PEI impregnated MCM-41 ordered mesoporous silica

sorbent. Deeming the concept of the prepared sorbent a “molecular basket”, a key characteristic of this “molecular basket” is that there exists an optimum temperature for adsorption. Contradictory to classical sorbents, this form of sorbent carries with it a temperature dependent diffusional limitation along with the classical thermodynamic constraint. Consequently, this leads to an optimum in which at a certain temperature the combined rates of adsorption/desorption from the binding sites and the CO_2 diffusion rate through the liquid polymer are maximized. Since this work, many groups have explored a wide range of siliceous supports discovering several ways in which the nature of the support, solvent used for impregnation, additives, and amine type influences the performance of the adsorbent.

A significant variable above others is the textural properties of the support in which the polymer is impregnated (Barbosa et al., 2011; Chen, Son, You, Ahn, & Ahn, 2010; Chen, Yang, Ahn, & Ryoo, 2009; Heydari-gorji, Belmabkhout, & Sayari, 2011; Heydari-gorji, Yang, & Sayari, 2011; Kuwahara, Kang, Copeland, Bollini, et al., 2012; Kuwahara, Kang, Copeland, Brunelli, et al., 2012; S.-H. Liu, Wu, Lee, & Liu, 2009; Qi et al., 2011; Qi, Fu, Choi, & Giannelis, 2012; Son, Choi, & Ahn, 2008; Subagyono, Liang, Knowles, Webley, & Chaffee, 2011; Xingrui Wang, Li, Liu, & Hou, 2011; W. Yan, Tang, Bian, Hu, & Liu, 2012; X. Yan, Zhang, Zhang, Yang, & Yan, 2011; X. Yan, Zhang, Zhang, Qiao, et al., 2011; M. B. Yue, Chun, Cao, Dong, & Zhu, 2006; Ming Bo Yue et al., 2008). Son et al., (2008) prepared a number of ordered mesoporous silica (OMS) supports with a range of pore volumes, pore diameters, and surface areas where then a 600 Mw PEI was impregnated by wet impregnation. They observed that for equal PEI loading of 50 wt%, the adsorption capacity and amine efficiency increased with

increasing average pore diameter. Furthermore, each one of these materials achieved a higher adsorption capacity and faster adsorption kinetics relative to pure PEI, and the supports possessing a 3D pore structure rather to a 2D ordered network had faster adsorption kinetics. Chen et al., (2010) went further to explore PEI impregnated hexagonal mesoporous silicas (HMS) with varying textural properties and found very similar results with adsorption capacity increasing with increasing pore diameter. The HMS with higher pore volumes achieved higher adsorption capacities with equivalent loadings (45 wt%). The higher pore volume supports were capable of being impregnated with larger amounts of PEI (up to 60 wt%) and achieved a 4.2 mmol/g adsorption capacity at 75 ^{o}C with pure CO_2 without affecting the amine efficiency. The higher pore volume supports have the potential of retaining more polymer, and coupled with the larger pore diameter, it allows for higher nitrogen content to be loaded with a more efficient distribution. However, beyond a certain loading the amine completely fills the pores and begins to consolidate on the exterior of the particle leading to poor efficiencies and adsorption capacities.

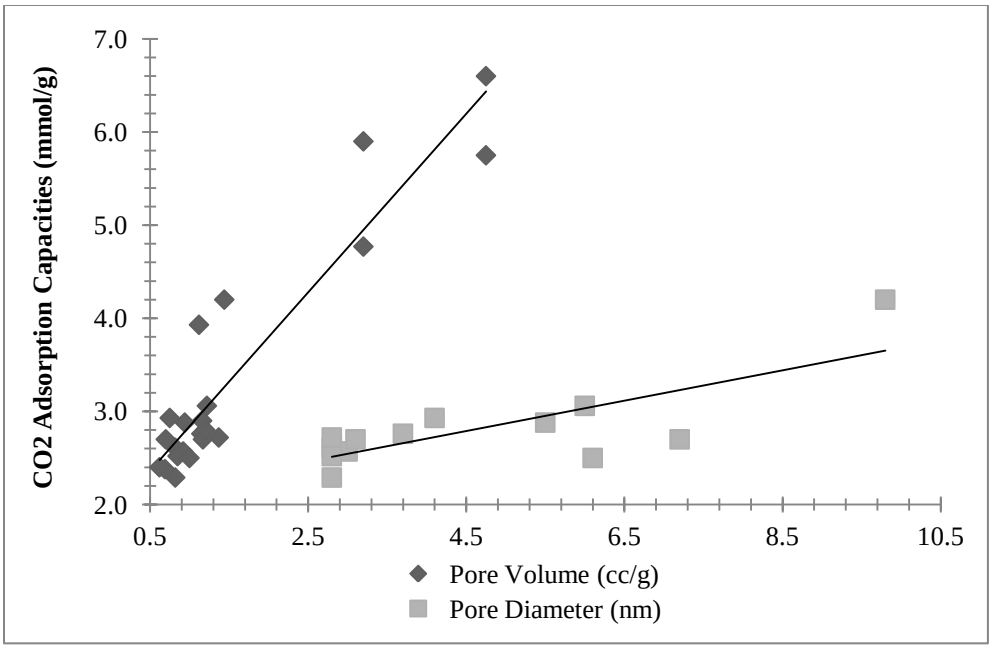

Figure 1.2: Summary of the Influences of Pore Volume and Pore Diameter on CO_2 Adsorption Capacity of a Number of PEI Impregnated Silica Supports.

These results led toward developing higher porosity supports with favorable pore diameters and structures including hierarchical silica monoliths (Chen et al., 2009), nanocomposite mesoporous capsules (Qi et al., 2011), and a number of pore-expanded (Franchi, Harlick, & Sayari, 2005; Heydari-gorji, Belmabkhout, et al., 2011; X. Yan, Zhang, Zhang, Yang, et al., 2011) and mesocelluar foams (Qi et al., 2012; Subagyono, Liang, Knowles, Webley, et al., 2011; W. Yan et al., 2012; X. Yan, Zhang, Zhang, Qiao, et al., 2011) leading to larger CO_2 adsorption capacities. Figure 1.2 summarizes the pore diameter and pore volume trends of a number of silica supports.

The pore length of the porous silica is also a key variable in attaining a high performing CO_2 adsorbent. Heydari-gorji, Yang, et al., (2011) prepared four different OMS supports with similar pore sizes but with various pore lengths ranging from 40 to 0.2 μm in diameter. With all of them loaded with near equivalent amounts of PEI (~50

wt%), the supports with the smaller pores attained the highest adsorption capacities, greatest amine efficiencies and fastest adsorption kinetics. Furthermore, the smaller pore led to a lowering of the optimum adsorption temperature for highest capacity. Such results further verify the subsequent CO_2 mass transport limitations through the liquid polymer present in impregnated supports. The short pore length as well as a larger pore diameter results in thinner polymer layers and greater amine distributions leading to more efficient adsorption site availability that causes the rise in kinetics, capacity and a fall in the optimum adsorption temperature.

For that reason, it's evident that for wet impregnated sorbents, an efficient distribution of the polymeric amine is vital toward obtaining fast adsorption kinetics and large adsorption capacities. Alternative methods of obtaining these favorable distributions other than using the appropriate support have been explored using as-prepared OMS materials(Heydari-gorji, Belmabkhout, et al., 2011; Heydari-Gorji & Sayari, 2011; Xingrui Wang et al., 2011; M. B. Yue et al., 2006; Ming Bo Yue et al., 2008) and organic additives (Meth, Goeppert, Prakash, & Olah, 2012; Tanthana & Chuang, 2010; J. Wang et al., 2012; X Xu et al., 2003; Xue, Wu, Zhou, & Zhou, 2012). An as-prepared OMS is an OMS with no post-treatment such as calcination or ethanol washes to remove the surfactant layer attached to the pore walls used during synthesis. These remaining hydrophobic scaffolds within the pore space are found to enhance the adsorption performance of the amine impregnated sorbent relative to an equivalently loaded calcined analogue. One of the first to discover this phenomena was Yue et al., (2006) who prepared a as-prepared SBA-15 impregnated with tetraethylenepentamine (TEPA). They found that the as-prepared TEPA impregnated sample achieved a higher adsorption

capacity as the calcined sample with an equivalent loading suggesting that the presences of this scaffold is interacting with the distribution of TEPA and/or aiding the adsorption process between the CO_2 and amino groups. Later Yue et al., (2008) again further investigates this phenomena with a as-prepared MCM-41 that was synthesized with different surfactants in order to understand the scaffold role in the CO_2 adsorption mechanism. They discovered that the surfactant leading to a larger micelle creating a larger pore yielded the highest adsorption capacity. Furthermore, when the surfactant was impregnated along with the TEPA inside a template free support rather to impregnating pure TEPA inside an as-prepared support, the sample impregnated with a TEPA/surfactant mixture gave a poorer result. This discovery implied that the "spoke" like arrangement of the surfactant inside the as-prepared support would allow the TEPA to be dispersed efficiently within these palisades structures allowing amine binding sites to be readily available for CO_2 capture. The amine efficiencies jump from approximately 0.25 mol CO_2/mol N to around 0.35 mol CO_2/mol N. Similar results were found when working with pore expanded (PE) MCM-41 and MSU-1 which also agree that the micelle structure creates a much more efficient distribution of the amino polymer that allows a higher degree of availability for CO_2 to find and adhere (Heydari-gorji, Belmabkhout, et al., 2011; Heydari-Gorji & Sayari, 2011; Xingrui Wang et al., 2011).

Others have also obtained higher performance with the use of surfactants but utilized as an additive to form an amine/surfactant blend to impregnate. These commonly yield adsorbents that enhance CO_2 adsorption performance not because of their ability to distribute amines more efficiently within the support pore, but because they reduce the viscosity, chemically stabilize the amine, and/or play a facilitating role in the CO_2 amine

adsorption mechanism. Tanthana & Chuang, (2010) prepared a polyethyleneglycol (PEG)/ TEPA impregnated fumed silica and found that the –OH moieties on PEG acted as a stabilizing agent for the amine during cyclic tests. Wang et al., (2012) mixed PEI with common surfactants such as Span80, CTAB, and STAB used for synthesizing OMS supports and impregnated them in hierarchical porous silica (HPS). They discovered that the surfactants incorporated reduced the viscosity of the PEI leading to an increased diffusion capability in CO_2 transport. This led the sorbents possessing enhanced adsorption capacities and even worked well at near room temperatures. Furthermore, these surfactants showed to increase the thermal cyclic stability of the sorbents due to their electrostatic interactions with the PEI.

Another influential variable to the performance of wet impregnated sorbents is the nature of the amino polymer. There has been a wide range of amines utilized for wet impregnation but the most common polymer is PEI. Traditionally, the best amino polymers are those which carry the largest number of amine groups per unit weight of polymer. Figure 1.3 shows some of the most commonly used amines for impregnation. However, this is not always the case because of other factors such has CO_2-amine chemistry and adsorption kinetics. M. Gray, Champagne, Fauth, Baltrus, & Pennline, (2008) impregnated polymethylmethacrylate beads with 1,8-diazabicyclo-[5.4.0]-undec-7-ene (DBU) and found that, under humid conditions, led to a much greater amine efficiency relative to common PEI compounds due to its inherent amidine. Though the amine to weight ratio of DBU is much lower than PEI, the nature of the conjugated amidine of DBU leads to the quick formation of bicarbonate rather than the slower route

taken by secondary and primary amines as mentioned earlier and therefore can potentially have a higher adsorption capacity under humid conditions relative to PEI.

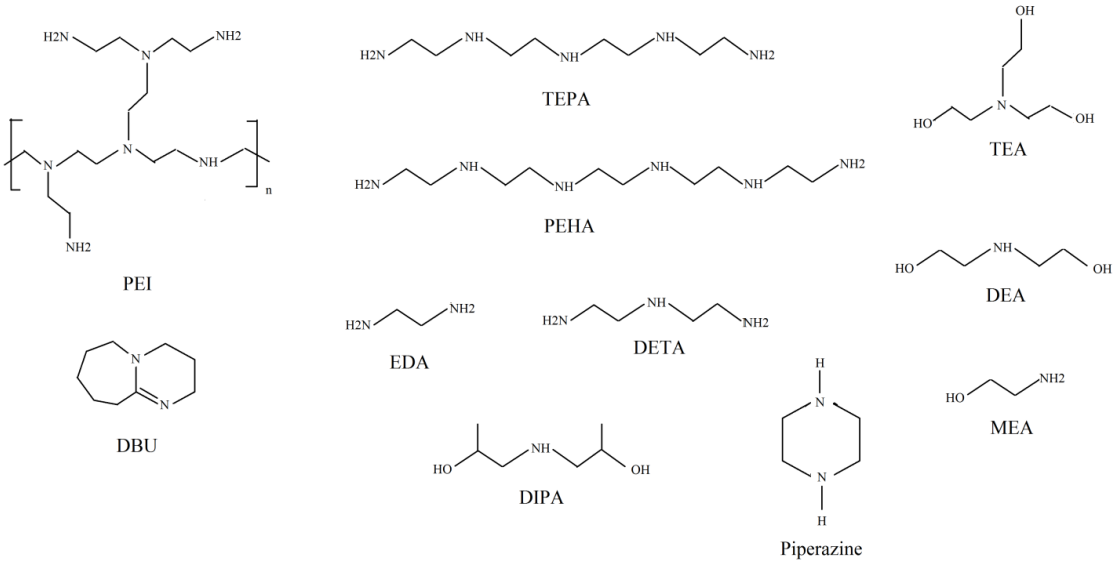

Figure 1.3: Summary Illustration of Common Organic Amines Utilized for Wet Impregnation (PEI = Polyethyleneimine; TEPA = Tetraethylenepentamine; TEA = Triethanolamine; DBU = 1,8-diazabicycloundec-7-ene; EDA = Ethylenediamine; DETA = Diethylenetriamine; DEA = Diethanolamine; DIPA = Diisopropanolamine; MEA = Monoethanolamine).

S. Lee, Filburn, Gray, Park, & Song, (2008) screened a number of amines including monoethanolamine (MEA), TEPA, ethylenediamine (EDA) and acrylnitrile treated TEPA and EDA which essentially binds multiple TEPA or EDA molecules together to form a large multiple branched amino polymer. Of these amines, TEPA and EDA attained the highest overall adsorption capacities. However, in terms of cyclic stability and working capacity (i.e., the adsorption capacity after a regeneration cycle), the acrylnitrile treated TEPA and EDA performed the best. Plaza et al., (2008) impregnated diethylenetriamine (DETA), diisopropanolamine (DIPA), triethanolamine

(TEA), pentaethylenehexamine (PEHA), and PEI into an alumina support. Of the amine tested the best performing in terms of adsorption capacity was DETA. Furthermore, Goeppert, Meth, Prakash, & Olah, (2010) tested PEI, TEPA, PEHA, MEA, and diethanolamine (DEA) and found similar results as Ruberia and Filburn, where TEPA achieved the greatest adsorption capacity under similar conditions tested. These results and others (Chen et al., 2009; Subagyono, Liang, Knowles, & Chaffee, 2011; J. Zhao, Simeon, Wang, Luo, & Hatton, 2012), show that the amino polymers with lower molecular weights (near ~200 Da) achieve the best CO_2 adsorption capacities. This trend is a result of the balance between the molecular weight and number of amine groups per molecule. As mentioned before, these amino polymers tend to impede CO_2 diffusion due to their high viscosities, and the higher the molecular weight of these polymers, even though the N to molecular weight ratio increases with molecular weight, the greater the viscosity which leads to slower adsorption kinetics. TEPA and the like achieve the best performance in terms of capacity because they possess a high N ratio as well as a lower viscosity. However, there is also an inherent problem with lower viscosity amino polymers as discussed below.

Cyclic stability is a key feature of an ideal sorbent that needs to be addressed if it is to be implemented in a practical industrial application. The impregnated sorbents, due to their lack of any covalent or strong attachment, are unstable during cyclic adsorption/regeneration tests because of the evaporation of the polymer from the support (Heydari-gorji, Belmabkhout, et al., 2011; Y. Liu et al., 2010; Olea, Sanz-Pérez, Arencibia, Sanz, & Calleja, 2013; Qi et al., 2011, 2012; Sie, 2012). This effect is more pronounced for low molecular weight amino polymers due to their higher vapor

pressures. TEPA for instance, though it may be the best amine in terms of kinetics and adsorption capacity, is thermally unstable and evaporates during regeneration cycles very easily leading to a rapid drop in the working adsorption capacity. Figure 1.4 illustrates this showing the cyclic stability of a variety of amino polymers. Though these sorbents have been tested with varying adsorption and regeneration conditions, the higher molecular weight polymers have much lower vapor pressures causing them to be more stable, but they have greater viscosities and therefore result in slower kinetics and smaller adsorption capacities.

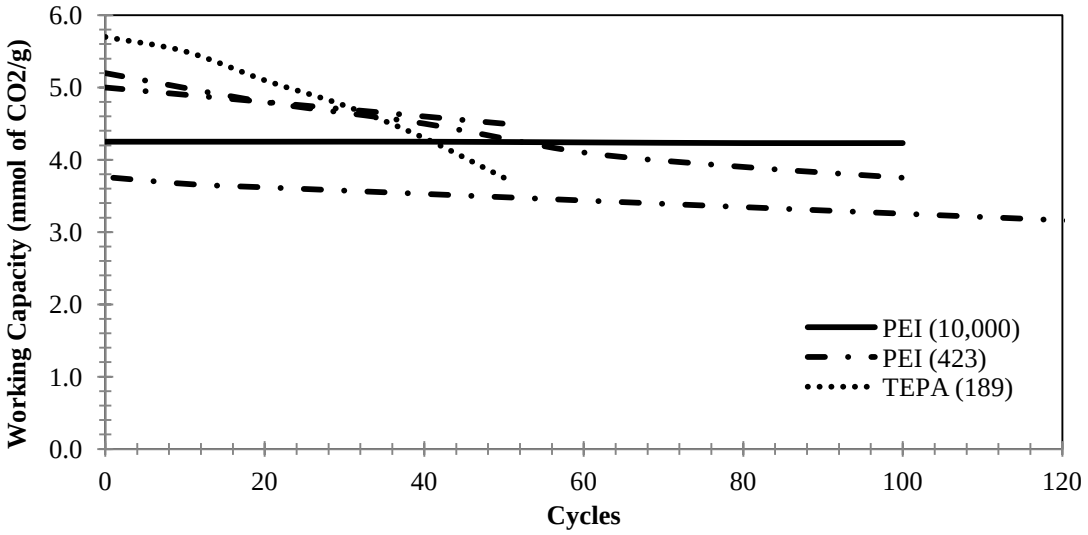

Figure 1.4: Cyclic Stability of Common Amino Polymers. These Sorbents were Regenerated under Different Conditions.

1.3 Amine Grafted Solid Sorbents

Unlike wet impregnated amine based sorbents, covalently amine grafted materials possess a greater cyclic stability. Such stability is a result of the amine's strong anchorage to the surface of the support. The most common method of grafting is through silane hydrolysis and/or condensation to the surface of some metal oxide support, typically

silica. Methods of introducing covalently bounded amine compounds to the surface vary but can be placed into two main categories; co-condensation and post-modification.

Co-condensation methods involve the simultaneous hydrolysis and condensation of the amine and the metal alkoxy precursor resulting in a rigid metal oxide structure with the amine embedded within the microstructure. The most common precursors involve amino-silane compounds such as those in Figure 1.5 and orthosilicates (e.g., tetraethylorthosilicate, TEOS). Generally, the amine and silica precursors are mixed with or without a surfactant of some sort, depending on whether an amorphous silica or an OMS is desired, together with a solution of an organic solvent (e.g., ethanol) and water. These solutions are heated to moderate temperatures to age, developing into sols and then soon precipitate to form OMS particles or an amorphous gel. These solidified materials are then filtered and/or dried (gels are commonly supercritically dried, S.C.). Acids/bases aren't often utilized as a catalyst as is common in sol-gel processing due to the inherent basicity of the amine precursors which themselves catalyze the polymerization(Brinker & Scherer, 1990).

Post-modification methods are similar to wet impregnation methods in that the amine modification is done after the preparation of the support. Typically for this method, the support is mixed with an anhydrous solution of the amino-silane and an organic solvent. The mixture is then heated for a certain period of time to allow the amino-silane to condense onto the surface of the silica support. It is much simpler relative to the co-condensation method and generally yields slightly better results.

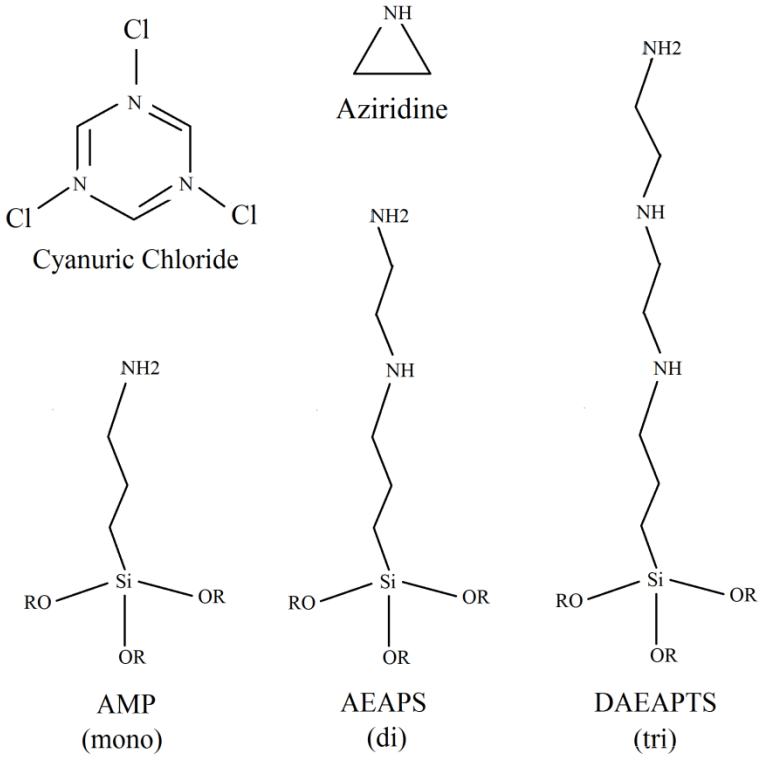

Figure 1.5: Common Amino Compounds Used in Covalent Grafting Methods.

Figure 1.6 shows the comparison between co-condensation and post-modification methods in terms of their amine content and adsorption capacity. The general trend is the higher the amine content, the greater the adsorption capacity. The post-modification route is generally more efficient due to the nature of the method. Because the amino-silane and silioxane precursors are mixed at once in the co-condensation route, a portion of the amine is trapped in the developing microstructure during condensation and therefore not available for adsorption (Klinthong, Chao, & Tan, 2013). Furthermore, it is difficult to obtain large amine loadings with co-condensation because of the inherent precursor basicity. The large amount of amino precursor results in a larger pH, which catalyzes the polymerization unfavorably leading to poor porosities and structure character for adsorption. However, S.-N. Kim, Son, Choi, & Ahn, (2008) showed that through the use

of anionic surfactants, one can achieve an amine distribution that is more efficient where the surfactants are both concurrently developing a OMS while positioning the amino-silanes normal to the surface of the silica. This route is being explored more and shows to have promising potential(Hao, Chang, Xiao, Zhong, & Zhu, 2011; Hao, Zhang, Zhong, & Zhu, 2012; Yokoi, Yoshitake, Yamada, Kubota, & Tatsumi, 2006).

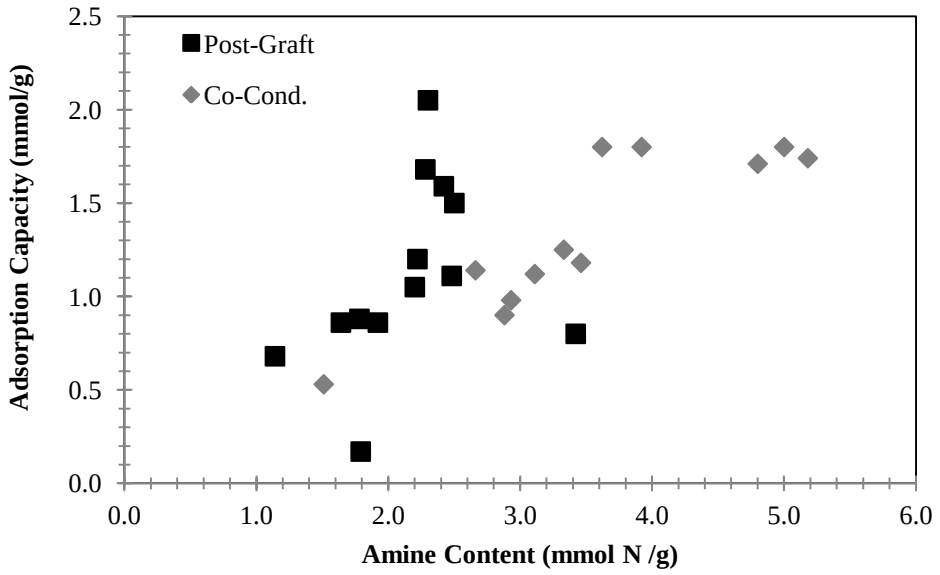

Figure 1.6: Comparison of Post-modification and Co-condensation using a Mono Amine. (Adsorption Conditions were around 25 ^{o}C and 100% CO_2 at 1bar)

Post modification is the simplest method of the two with greater tailorability and therefore has been more extensively studied for a CO_2 sorbent. The amino-silane AMP (Figure 1.4), a mono amine, is the most studied amino-silane for grafting silica based supports (Aquino et al., 2013; Araki, Doi, Sano, Tanaka, & Miyake, 2009; Aziz, Hedin, & Bacsik, 2012; Aziz, Zhao, & Hedin, 2011; Bai, Liu, Gao, Yang, & Li, 2012; A. C. Chang, Chuang, Gray, & Soong, 2003; F.-Y. Chang, Chao, Cheng, & Tan, 2009; Gil, Tiscornia, de la Iglesia, Mallada, & Santamaría, 2011; M. L. Gray et al., 2005; Gui, Yap,

Chai, & Mohamed, 2013; Hao et al., 2011, 2012; He et al., 2012; Hiyoshi, Yogo, & Yashima, 2005; C.-H. Huang, Klinthong, & Tan, 2013; H. Y. Huang, Yang, Chinn, & Munson, 2003; S. Kim, Ida, Guliants, & Lin, 2005; S.-N. Kim et al., 2008; Klinthong et al., 2013; Knowles, Graham, Delaney, & Chaffee, 2005; Ko, Shin, & Choi, 2011; Kumar, Labhsetwar, Meshram, & Rayalu, 2011; Leal, 1995; W. Li et al., 2010; Loganathan, Tikmani, & Ghoshal, 2013; Mello, Phanon, Silveira, Llewellyn, & Ronconi, 2011; Nik, Nohair, & Kaliaguine, 2011; Rezaei et al., 2013; Yang, Kim, Kim, & Ahn, 2012; Zelenak, Halamova, Gaberova, Bloch, & Llewellyn, 2008; Zeleňák et al., 2008; G. Zhao, Aziz, & Hedin, 2010). The main variables of grafting to achieve high N content are the surface area of the support and the surface silanol concentration. Other variables, such as the anhydrous grafting conditions (i.e., temperature, time of grafting, silane concentration, etc.) does play a role but has little influence relative to the former. However, as shall be noted later, when hydrous grafting is performed the temperature of grafting does play a significant role.

The surface area coupled with surface silanol concentration plays a major role for this will determine the number of tethers per unit area and the overall number of tethers per unit weight of sorbent. Silanol content is critical for it is the active moiety on the support silica surface that anchors the amino-silane. Wang & Yang, (2011) revealed this using extracted SBA-15 rather than calcined SBA-15 as a support for grafting. Grafting a mono amine, the extracted SBA-15 nearly doubled in adsorption capacity relative to the calcined support. The extracted support had more silanol content since calcination tends to lead to hydroxylation of the surface reducing the –OH surface concentration. Furthermore, Wei et al., (2008) took calcined SBA-16 and boiled it in distilled water to

further hydrolyze the surface. The boiled support achieved both higher amine content and thus a higher CO_2 capacity relative to the calcined support.

Coupled to the surface silanol concentration, higher N content can be achieved with higher surface areas. Figure 1.7 shows the significance of the surface area from a range of support with roughly the same silanol concentration, surface amine density, and similar adsorption conditions (Aquino et al., 2013; Aziz et al., 2012; Gil et al., 2011; H. Y. Huang et al., 2003; S. Kim et al., 2005; Knowles et al., 2005; Ko et al., 2011; Loganathan et al., 2013; Mello et al., 2011). Clearly the greater the surface area, the greater the number of tethers retained, and the higher the adsorption capacity.

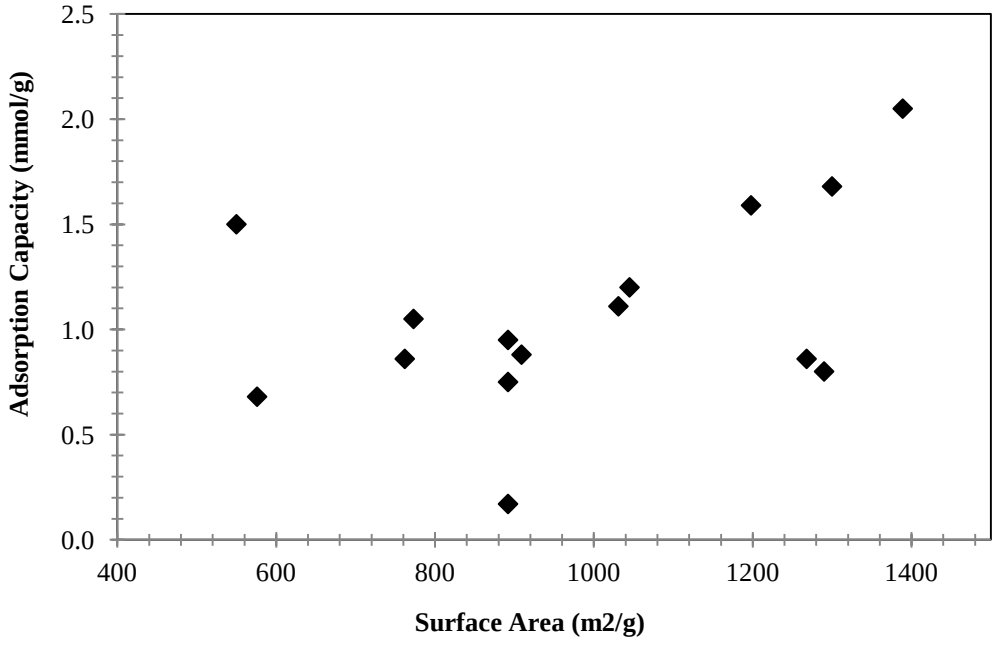

Figure 1.7: The Correlation between Surface Area and Adsorption Capacity.

One very significant variable, closely associated with the silanol density, is the amine density; Figure 1.8 illustrates the significance. This quantity, assuming an homogenous layer, is commonly calculated by dividing the total amine content per gram

by the surface area before modification. As discussed in Section 1.1, CO_2 requires two amines to form the thermodynamically favored carbamate and ammonium products. Therefore it is vital that these two amines be in close proximity in order to effectively bind CO_2. This is extremely crucial when using mono amine silanes since there is only a single amine present per tether distinct from AEAPS (di amine) and DAEAPTS (tri amine). Young & Notestein, (2011) grafted silica and TiO_2 doped silica with AMP and investigated the baseline amine concentration required for the formation of ammonium and carbamates species. They found that the minimum required surface density is 0.9 amine per nm^2. This is an indication that one must have a support carrying a silanol concentration of approximately 1.0 OH per nm^2 or greater to possess a selective CO_2 sorbent. Later Aziz et al., (2012) revealed that the threshold density was not 1.0 but approximately 1.5-2.0 amine per nm^2. However, they suggest that the variation in the results is also due to pore curvature and amine homogeneity. Regardless, for mono-amine grafting it is vital that a high silanol content and amine density is achieved to achieve selective CO_2 adsorptive properties.

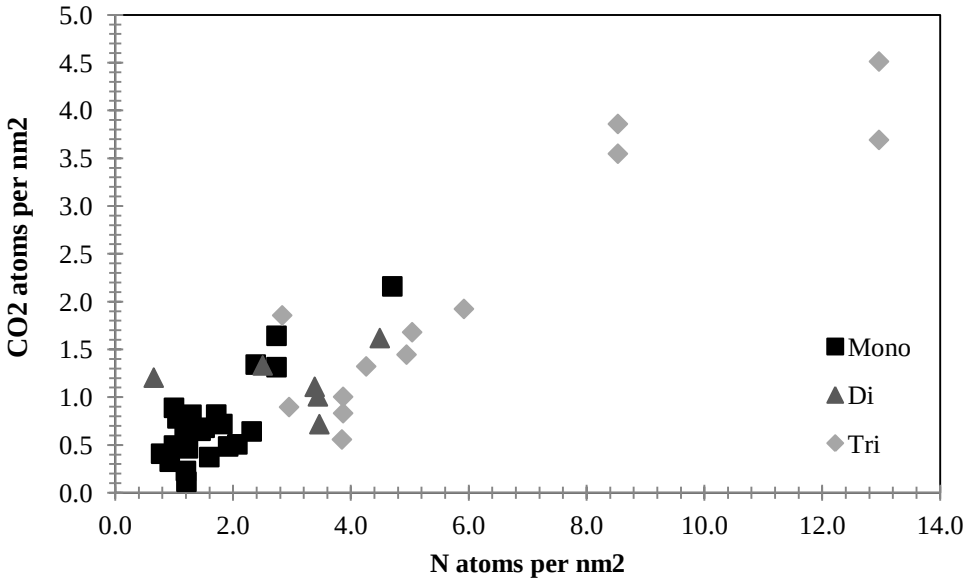

Figure 1.8: Trend of the Amine Density to CO_2 Adsorption Per Unit Area of Multiple Grafted Sorbents.

When grafting with di or tri amines, the tether density becomes less of an issue due to the inherent ability of each tether to form ammonium and carbamate. The construction of these amino-silanes (Figure 1.5) with the ethylenediamine substructures allows them to bend so the zwitterionic species formed can be deprotonated by the inter-neighboring amine (Zheng et al., 2005). Coupled with this inherent property, using the di and tri amino silanes allows one to graft a much higher N content per unit weight of support. Figure 1.9 reveals the benefits using the larger N content amino silanes. Tri-amine, possessing three amine groups per tether, has the greatest performance relative to the di and mono in terms of adsorption capacity as a result of being able to graft more mmol of N per gram of sorbent. For that reason, and also because of this particular chemical's commercial availability, research groups have endeavored to try to optimize the grafting procedure along with exploring more favorable supports (e.g., high silanol

surfaces concentrations, high surface areas) in order to achieve higher performing sorbents.

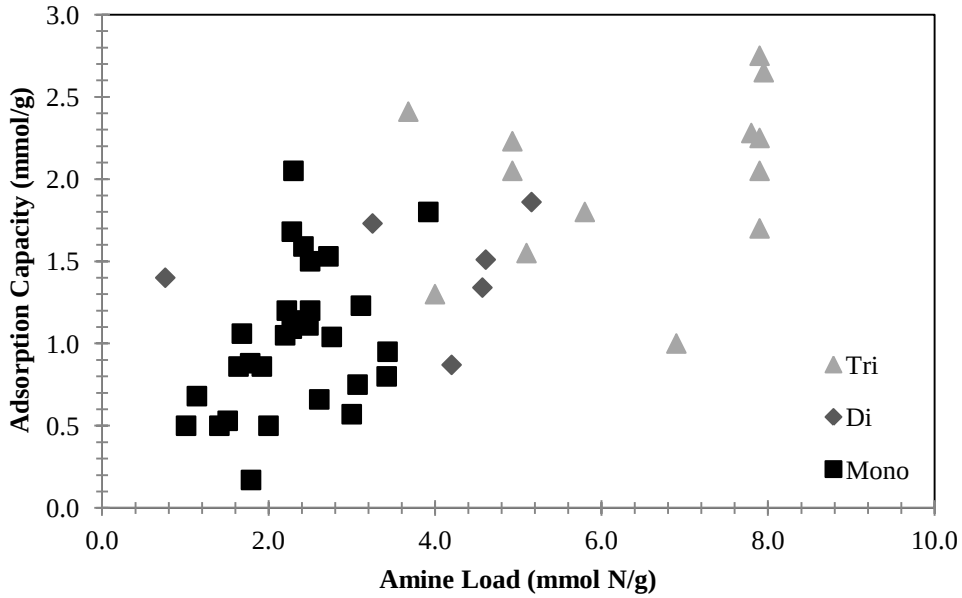

Figure 1.9: Adsorption Capacity of Mono, Di, and Tri-amine Grafted Silica Supports. (All these Sorbents were Tested and Prepared under Similar Conditions)

The common procedure for grafting is an anhydrous method using toluene. Toluene provides a wet free environment and has little influence in the precursors. Other solvents such as ethanol have been used but ethanol has the potential of reversing the grafting procedure (Brinker & Scherer, 1990). For a post modification the main tuning variables are synthesis temperature, silane concentration, grafting time, and silane:silica ratio. The synthesis temperature tends not to play a very significant role as Huang et al., (2013) reveal. They used both toluene and s.c. propane as a solvent finding a slight improvement in performance for the s.c. propane synthesized materials. But for both solvents the temperature affected the adsorption capacity negligibly. Harlick & Sayari, (2007) also confirmed the little influence of temperature for SBA-15 grafted materials.

As for silane concentration and silane:silica ratio, they play a more significant factor. Harlick & Sayari, (2006) revealed that the N content grows quickly from 0 to 2 mL of silane per gram of silica and then tails off with a slow rise after 2 mL/g. Gil et al., (2011) revealed a doubling of the adsorption capacity when the concentration rose by 10 fold. Furthermore, in both of these studies, they show that the when the time of synthesis rises the adsorption capacity as well as N content is further improved. Another variable that can be introduced into the grafting procedure is the addition of water before the grafting procedure. This hydrous method has shown to be promising in improving amine content and adsorption performance (Harlick & Sayari, 2007; Zheng et al., 2005).

Lastly, a special class of grafted materials consists of supports that are amine functionalized by surface polymerization. Similar to grafted sorbents these materials possess amines covalently grafted to the surface but have a much greater potential of attaining higher N content due to the nature of polymerizing the amine monomer from the surface. The method of polymerizing amines from the surface is not new since others have used this method for developing amino polymers on silica substrates for a variety of applications(C. O. Kim, Cho, & Park, 2003; H. Kim, Moon, & Park, 2000; Rosenholm, Duchanoy, & Lindén, 2008; Rosenholm & Linde, 2007; Tsubokawa & Takayama, 2000). One of the first to report the use of this route for CO_2 adsorption applications is Liang, Fadhel, Schneider, & Chaffee, (2008) who prepared a series of SBA-15 bound melamine-based dendrimers. After grafting the SBA-15 with the mono amine AMP, they performed a step-wise polymerization by reacting the primary amine of AMP with cyanuric chloride (Figure 1.5). Then after multiple washings and filtrations, the substrate was placed in a solution of ethylenediamine (EDA, Figure 1.3) to form what they name a generation one

(G1) melamine substrate. Multiple cycles of introducing cynanuric chloride and EDA led them to develop up to a G4 melamine substrate where the pores of the SBA-15 were completely filled with melamine dendrimers. The G3 substrate achieved the best CO_2 adsorption capacity reaching 1.02 mmol/g at 20 ^{o}C with 90% CO_2/Ar. The low capacity was suggested to be due to the low availability of amine binding sites. These step-wise melamine dendrimers lead to a polymer with a low number of primary amines existing mostly at the terminal ends of the polymer. Secondary amines are present at a fair ratio but have a high degree of steric hinderance to form the carbamate and ammonium species for CO_2 capture.

Hicks et al., (2008) prepared a much more effective sorbents by performing an *in situ* polymerization technique using aziridine (Figure 1.5). Similar to Liang, Fadhel, Schneider, & Chaffee, (2008), they grafted AMP onto a SBA-15 support but then in a single step they placed the mono amine grafted SBA-15 into a solution of aziridine where this precursor undergoes spontaneous ring opening polymerization from the surface to form a hyperbranched aminosilica (HAS). Using this method they were able to achieve a HAS with an N content of nearly 10 mmol N/g which achieved an adsorption capacity of 5.6 and 4.2 mmol/g at 25 and 75 ^{o}C (Drese et al., 2009). These sorbents in terms of cyclic stability and adsorption capacity and kinetics is among the best for amine modified materials. Drese et al., (2012) further explored the use of different supports in order to grow larger polymers from the surface for they believed the pore size of SBA-15 restricted further polymer expansion. However, unexpectedly they found that the polymer growth terminated not due to the pore diameter of the support, but due to reasons that involve the reactions mechanisms of the polymer development.

1.4 Research Objectives and Significance

Aerogels sometimes referred to as "frozen smoke" have one of the lowest density, highest thermal insulating, lowest refractive index, and highest surface area per unit volumes of any material. They consist of tangled fractal-like chains of spherical clusters of molecules, each about 3-4 nm in diameter. The chains form a highly porous (95% porosity or greater) solid structure surrounding air filled pores that average about 20 - 40nm. Because of these favorable textural properties, according to the current understanding of solid amine materials, silica aerogels provided a promising support for a CO_2 amine-based sorbent. In the past, aerogels have been investigated as CO_2 capture and sequestration materials by incorporating certain metal oxides such as wollastonite (Santos et al., 2008). Amine modification of aerogels has also been studied, but for other purposes such as drug delivery materials, dissolved metal separations, and for enhancing the mechanical integrity of aerogel's structure (Alnaief & Smirnova, 2010; Capadona et al., 2006; Husing et al., 1999; Im et al., 2000; Katti et al., 2006; Meador et al., 2005). The majority of aerogels utilized however were prepared in the laboratory by the expensive super-critical drying method.

Hydrophobic silica aerogels (called Nanogel) prepared using a proprietary process which circumvents supercritical drying is commercially available in large quantities from Cabot Corporation. The aerogel is in particulate form with particles sizes ranging from 5 μm to 3.5 mm, densities of 40 to 100 kg/m^3, and surface areas of 600 to 800 m^2/g. From a practical application view point it is more attractive to prepare amine modified sorbents on this commercially available particulate aerogel. Therefore the main objective of this

dissertation was to synthesize a novel, high performance CO_2 capture material utilizing a variety of amines and functionalization methods, using the low density aerogel provided by Cabot Corp in order to prepare a potentially viable CO_2 sorbent for commercial use.

In this work, we aimed to synthesize and investigate an amine modified aerogel sorbent with high adsorption capacities, fast adsorption kinetics, and robust cyclic stability. This was executed by a systematic study investigating CO_2 adsorption performance of various types of organic amine polymers and amino silanes in the presence of pure CO_2 and simulated flue gas. Furthermore, different methods for amine functionalization were investigated to improve the physical stability and accessibility of amines within the aerogel pore space for increased adsorption capacity and kinetics. The work accomplished provided further insight into the performance of aerogel as a support for amine modification and the effectiveness of the amine modification methods on amorphous silica materials such as aerogel.

1.5 Structure of the Dissertation

Each chapter in the dissertation presents a method of amine modification of aerogel that was found to yield favorable results compared to other high performing amine based sorbents. Chapter 2 and 3 presents two different methods of wet impregnation. Chapter 2 reveals the performance of TEPA impregnated aerogels using the conventional wet impregnation method and Chapter 3 reveals the performance of a novel TEPA controlled precipitation impregnation method. Chapter 4 addresses the CO_2 adsorption performance of a post-modified amine grafted aerogel using a mono, di, and tri amino silane. Chapter 5 reports the performance of a novel amine functionalized aerogel sorbent using amino silanes in an ALD method. Lastly, Chapter 6 provides a

discussion of recommendations for the future advancement of amine modified aerogels according to their adsorption capacity, kinetics, and stability potential for post combustion CO_2 capture.

CHAPTER 2

SYNTHESIS AND CARBON DIOXIDE SORPTION PROPERTIES OF AMINE IMPREGNATED PARTICULATE SILICA AEROGEL SORBENTS

2.1 Introduction

As described in Chapter 1, there are two primary methods of amine modification under the category of CO_2 amine based adsorbents materials. Wet impregnated materials are those prepared by physically impregnating liquid amines within a porous support. These materials generally retain larger amounts of amine and therefore have larger CO_2 adsorption capacities relative to grafting methods, where the amine is covalently tethered to the silica support surface. Impregnated materials generally achieve higher amine content because the major limiting factor is the amount of pore volume available within the support whereas grafted materials are generally limited by surface area, pore size, and the concentration of surface silanol sites for covalent grafting (Harlick & Sayari, 2006; Knowles et al., 2005; J Wei et al., 2008; Zeleňák et al., 2008).

As mentioned previously, the first to develop an amine impregnated material for CO_2 capture was Xiaochun Xu et al., (2002) utilizing MCM-41 and PEI. The adsorbent achieved a CO_2 capacity of 3.0 mmol/g at 75 ^{o}C under a dry 100% CO_2 feed gas. Many other studies have been conducted since this point where better performing CO_2 adsorbent materials have been synthesized due to the manipulation of a vital variable, the textural properties of support.

Most of the research work for impregnated materials has utilized ordered mesoporous silica materials (e.g. MCM-41, SBA-15, MCM-48) because of their ordered pore structure and tailorable pore properties (Franchi et al., 2005; Heydari-gorji,

Belmabkhout, et al., 2011; Y. Liu et al., 2010, 2011; Son et al., 2008; Xingrui Wang et al., 2011; Jianwen Wei, Liao, Xiao, Zhang, & Shi, 2010; X. Yan, Zhang, Zhang, Yang, et al., 2011; M. B. Yue et al., 2006; Ming Bo Yue et al., 2008). These studies have shown that supports having a larger pore volume and pore diameter give the best adsorption performance (Figure 1.2).

Building on these ideas, Chen et al., (2009) developed a silica monolith with hierarchical pore structure impregnated with PEI and TEPA. The monolith synthesized had a pore volume of 3.2 cm^3/g and pore diameters of 17 and 120 nm, values much larger than conventional molecular sieve supports. The PEI impregnated monolith achieved an adsorption capacity of 4.8 and 3.7 mmol/g with a dry 100% and 5% CO_2 stream at 75 ^oC. The TEPA impregnated monolith achieved an adsorption capacity of 5.9 mmol/g with dry 100% CO_2 at 75 ^oC but had poor adsorption-desorption cyclic stability due to TEPA's higher volatility. Qi et al., (2011) synthesized a novel nanocomposite TEPA impregnated mesoporous silica capsule, achieving adsorption capacities of 6.6 and 5.6 mmol/g with a dry 100% and 10% CO_2 stream at 75 ^oC respectively, as well as 7.9 mmol/g under a humid 10% CO_2 stream, the highest reported adsorption capacity reported for an amine impregnated material. Due to the large pore space and open structural character of these supports, they allowed for high amine loadings and effective amine distributions for CO_2 capture. As a result, the adsorbents were able to achieve significant CO_2 adsorption capacities with excellent adsorption kinetics.

Aerogels, due to their favorable porosities and textural properties as described in Section 1.4, have the potential to be a high performing amine impregnated sorbent. Amine modified aerogels have been prepared by other groups for CO_2 capture but no

other groups have prepared such supported sorbents by the wet impregnation method to our knowledge. The objective of Chapter 2 is to modify aerogel with TEPA and investigate its CO_2 adsorptive performance. The aerogel used is both hydrophobic and hydrophilic Nanogels manufactured by the afore mentioned Cabot Corporation prepared by a proprietary and cost effective ambient drying process.

2.2 Experimental Methods

All chemicals were purchased from Aldrich unless otherwise stated. Methanol (anhydrous, 99.8%), Tetraethylenepentamine (technical grade). Particulate aerogel (MT-1100 Nanogel, particle size of 10 μm respectively) was obtained from Cabot Corp. and is originally hydrophobic in nature. Hydrophilic aerogel, as will be called from hence forth, was prepared by calcining the hydrophobic aerogel in air at 600C^{o} for 8 hours.

2.2.1 Synthesis of Amine Modified Aerogel

The TEPA-aerogel sorbents were prepared using the wet impregnation method (Xiaochun Xu et al., 2002). 70ml of methanol was mixed with a calculated amount of TEPA to obtain a given loading in wt% of amine in the aerogel and mixed vigorously for 10 min. 2.0 g of aerogel were then added to the solution and stirred for an additional 10 min. The slurry was then placed under a vacuum at 25 ^{o}C to dry with stirring until a semi-solid slurry was formed. Stirring was then discontinued and the slurry left under vacuum overnight (24 hour drying period, respectively). Adsorbent samples were then removed and placed in storage for testing. The resulting porosity of the aerogel structure post drying is analogous to xerogels, which are porous solids dried from the prepared sol-gel by solvent evaporation. They have relatively denser structures due to the capillary force induced collapse during the evaporative drying process. Unlike aerogels where the liquid

in the sol-gel is generally replaced by gas through a supercritical solvent extraction method, avoiding capillary forces and maintaining high porosity. However, to avoid confusion of whether aerogels or xerogels were employed, the sample supports will remain named aerogels for the original solid utilized before amine modification is aerogel. Samples were labeled SA-y-x, y indicating hydrophobic (y = O) or hydrophilic (y = I), and x indicating the amount of TEPA immobilized in the aerogel by weight percent.

2.2.2 Sorbent Characterization

Nitrogen adsorption-desorption isotherms were obtained on a Micromeritics ASAP 2020 surface area and porosity analyzer at 77K. Before the nitrogen porosimetry analysis, impregnated samples were activated in an oven at 100 ^{o}C in air at 1 atm for 1 hour. The Micrometrics automated degas application was not used for activation to prevent the vaporization and condensation of TEPA inside the N_2 porosimetry system. This vaporization occurred when degassing under a heated (~100 ^{o}C) vacuum. However, the impregnated samples that were subjected to the mild vacuum (0.01 mm Hg, or 1.333 Pa) prior to nitrogen adsorption porosimetry measurements experienced negligible loss of TEPA for this is performed at room temperature (~20 ^{o}C). This was confirmed by TGA analysis of an 80 wt% TEPA/aerogel sample showing less than 3 wt% weight loss after the vacuum treatment. TEPA has a very low vapor pressure at room temperature (<0.01 mmHg @ 20 ^{o}C). Therefore the vacuum of 0.01 mm Hg (1.333 Pa) resulted in a negligible loss of amino groups. The Brunauer-Emmett-Teller (BET) method and the Barret-Joyner-Halenda (BJH) model of the adsorption isotherm were used to calculate the surface area, the pore size distribution, and pore volume of unmodified aerogel while the

BET surface area, BET pore diameter (4V/A), and the single point pore volume were calculated for the SA-I-x and SA-O-x sorbents. FT-IR spectra of aerogel and amine modified samples were obtained using a Nicolet 4700 spectrometer with the Smart Orbit ATR crystal sampler. Thermogravimetric analyses were conducted with a TA Instruments SDT-Q600 analyzer. Sorbents were equilibrated at 50 ^{o}C and then heated to 500 ^{o}C at a rate of 5 ^{o}C /min in Argon.

2.2.3 Carbon Dioxide Adsorption Analysis

The CO_2 adsorption performance of the sorbents was determined using a Thermo Cahn D-101 electro-microbalance (Figure 2.1). For a typical adsorption analysis, about 10 mg of sample was placed in a stainless steel sample pan and activated at 100 ^{o}C at 1 atm for 30 min under high purity Argon (99.99%) at 100 mL/min to remove unwanted adsorbed species (e.g., H_2O, CO_2, methanol). Sorbents were then cooled to 75 ^{o}C and pure CO_2 (99.99%) or 10% CO_2/Ar was then introduced for 1 hr at 1 atm at a flow rate of 100 mL/min. The CO_2 equilibrium adsorption capacity was determined by the weight gained during the 1 hour adsorption period. For the CO_2 adsorption-desorption cyclic stability test, sorbents were activated by heating to 100 ^{o}C for 30-min under a 100 mL/min Ar flow. After cooling to 75 ^{o}C, 100% CO_2 was introduced for 10 min for adsorption and then the stream was switched to 100% Ar for 20 min at 100 mL/min for desorption.

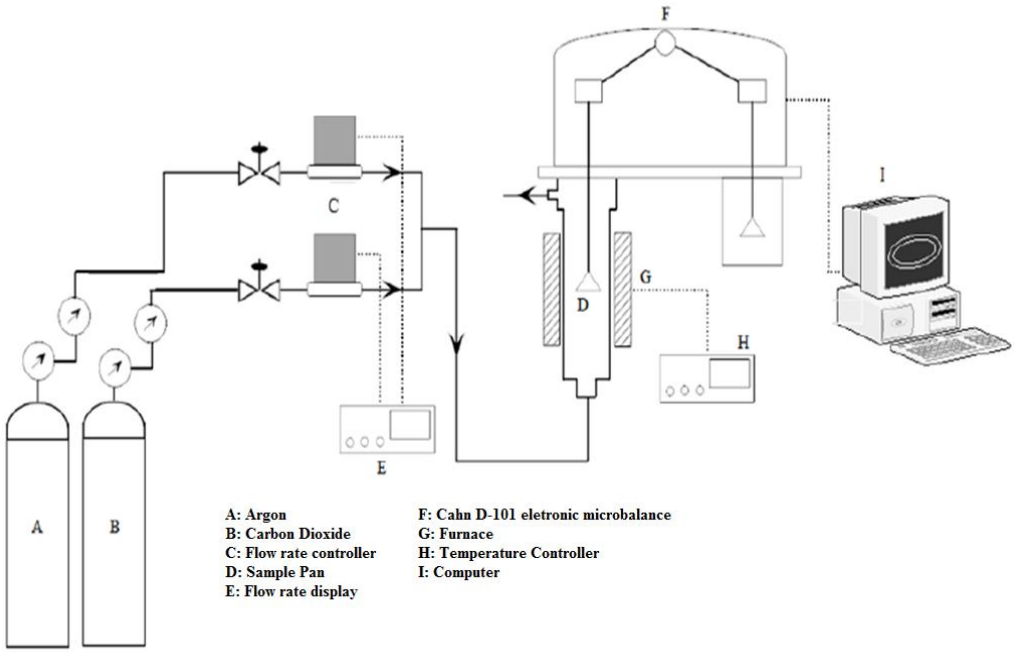

Figure 2.1: Schematic of Experimental Apparatus for Investigating CO_2 Adsorption Performance.

2.3 Results and Discussion

2.3.1 Sorbent Characteristics

Figure 2.2 and 2.3 shows the FT-IR spectra of the hydrophilic and hydrophobic aerogels before and after amine impregnation. The absorption peaks near 1051 and 806cm^{-1} are due to the Si-O-Si vibrations (Llusar, Monros, Roux, Pozzo, & Sanchez, 2003). Regarding the hydrophobic aerogel, peaks located at 2962, 1255, and 842cm^{-1} are a result of the terminal $–CH_3$ groups on silica surface(H. Liu, Sha, Cooper, & Fan, 2009). After amine impregnation of the two aerogel supports, new absorption peaks were observed validating the presence of TEPA inside aerogel supports (Figure 2.2). Bands at 1596, 3280, and 3355 cm^{-1} are attributed to the stretching vibrations of NH_2 and the

peaks seen at 1342, 1455, 2807, 2883, and 2933 cm^{-1} are due to the CH_2 vibrations of TEPA (Qi et al., 2011).

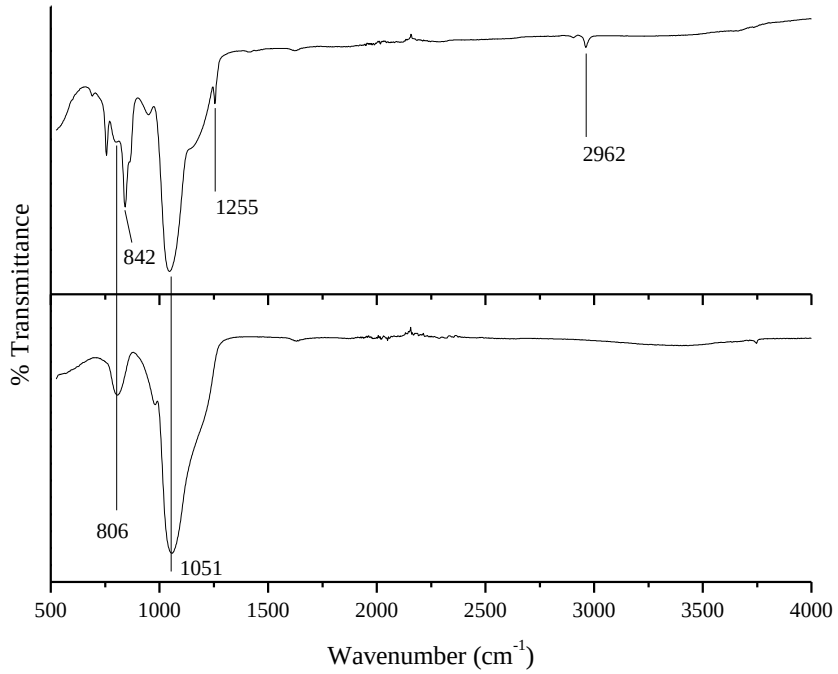

Figure 2.2: FT-IR spectra of Hydrophobic (top) and Hydrophilic (bottom) before Amine Impregnation.

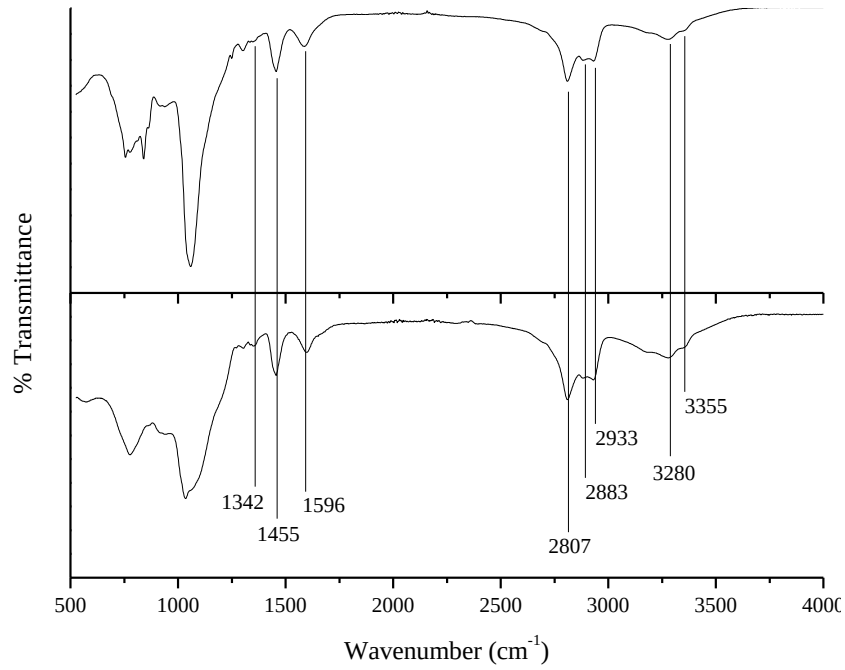

Figure 2.3: FT-IR Spectra of Hydrophobic (top) and Hydrophilic (bottom) after Amine Modification

The N_2 adsorption-desorption isotherms and the pore size distribution of the unmodified hydrophilic (SA-I) and hydrophobic (SA-O) aerogels are shown in Figure 2.4 with Table 2.1 summarizing the textural properties of all samples. The isotherms of the unmodified SA-I and SA-O are type IV with H1 type hysteresis corresponding to the mesoporosity of the aerogel and are similar to those of supercritically dried aerogels (J. H. Lee, Choi, & Kim, 1997; Sing et al., 1985b). The BET surface area of the SA-O aerogel was 673 m^2/g with a BJH pore volume of 3.5 cm^3/g. The pore distribution curve showed a peak at 21 nm. After calcining, the surface area, pore volume, and pore diameter increased to 822 m^2/g, 5.0 cm^3/g, and 42 nm. Supercritically dried unmodified aerogels, when thermally treated at a relatively high temperatures (e.g. greater than 600 ^oC) are known to shrink due to vitrification and sintering (Balkis Ameen, Rajasekar,

Rajasekharan, & Rajasekharan, 2007; Kuchta & Fajnor, 1996). However, the aerogel utilized in this work was functionalized with trimethylchlorosilane during synthesis, giving it its hydrophobicity, and therefore during heat treatment the organic groups tethered to the surface oxidize resulting in greater porosity as reported elsewhere (H. Liu et al., 2009). It has been suggested that the expansion of gas during oxidation causes compression on the aerogel structure, expanding the silica network and increasing its porosity(Kang & Choi, 2000).

Table 2.1: Summary of Nitrogen Adsorption-Desorption Analysis.

Sorbent	Surface Area (m^2/g)	Vp (cm^3/g)[a]	Dp (nm)[b]
SA-I	822	5.0[c]	42[c]
SA-I-40	91	0.18	7.9
SA-I-50	10	0.03	9.9
SA-I-60	2.6	0.01	12
SA-I-70	1.3	-	9.5
SA-I-80	0.74	-	5.7
SA-I-85	0.43	-	5.0
SA-I-90	0.08	-	-
SA-O	673	3.5[c]	21[c]
SA-O-50	0.02	-	-
SA-O-60	0.02	-	-
SA-O-70	0.11	-	-
SA-O-80	0.07	-	-
SA-O-85	0.05	-	-

[a]Single Point Pore Volume

[b]BET Surface Area

[c] Adsorption Isotherm BJH Method Applied

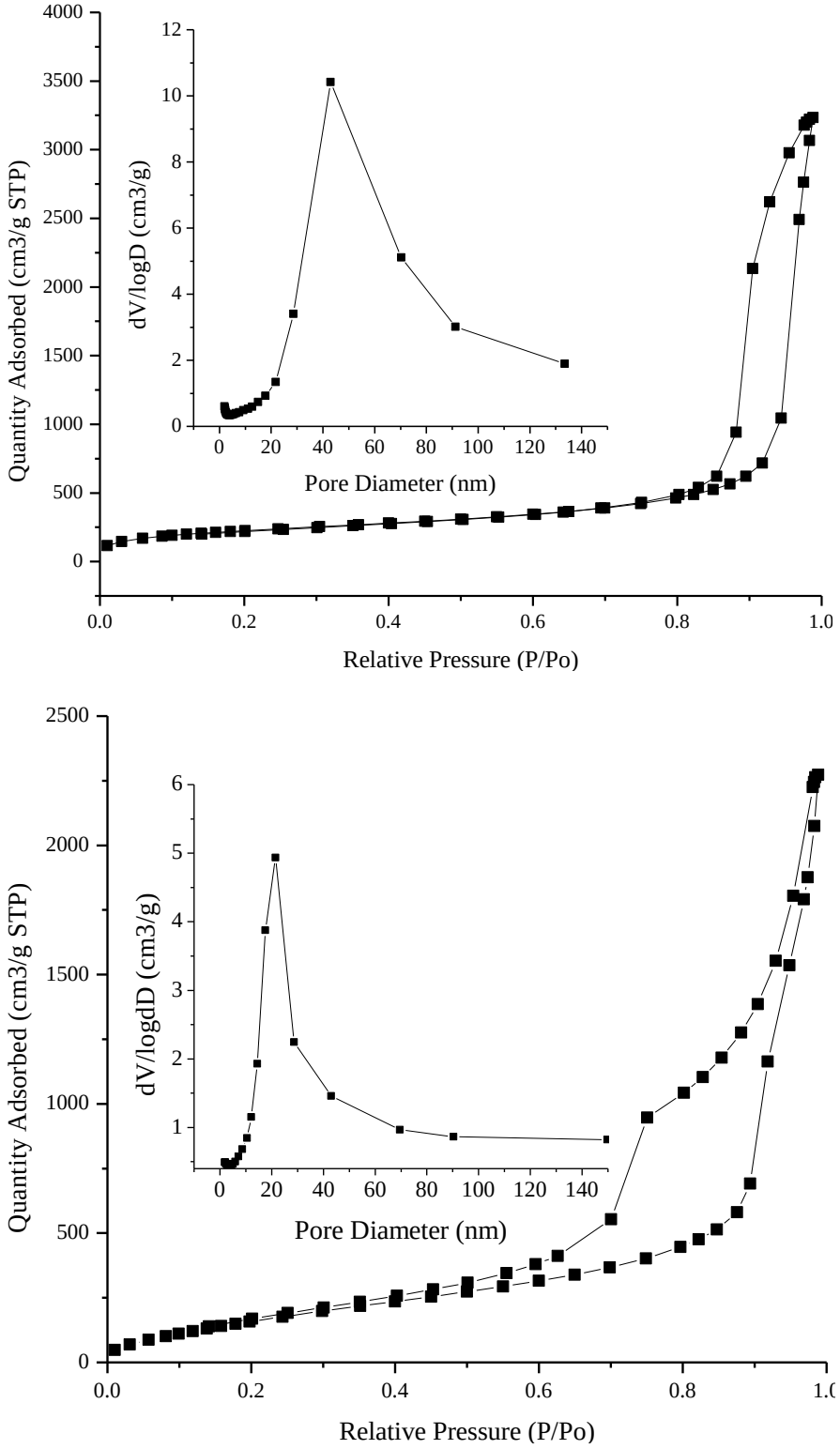

Figure 2.4: Nitrogen Adsorption-Desorption Isotherms of Unmodified SA-I (top) and SA-O (bottom) Aerogels.

After amine impregnation, the surface area and pore volume decrease with increasing amounts of TEPA for both supports due to the amine occupying the pore space of the aerogel(X Xu et al., 2003). Figure 2.5 shows the nitrogen adsorption-desorption isotherms for the SA-I-x sorbents. The SA-I-40 and SA-I-50 samples show some remaining mesoporosity, but with greater amine loadings the isotherms move toward type II suggesting the filling of the pore space. The SA-I-70 through SA-I-90 samples had virtually zero pore volume as a result of the amine filling the pores. As for the SA-O-x samples, (Figure 2.6), there appears to be no remaining mesoporosity in any of the sorbents and all of the SA-O-x samples appear to have completely filled pores. The isotherm for the SA-I-80 sample clearly shows the difference between the hydrophilic and hydrophobic aerogel samples and is included in Figure 2.6 for comparison.

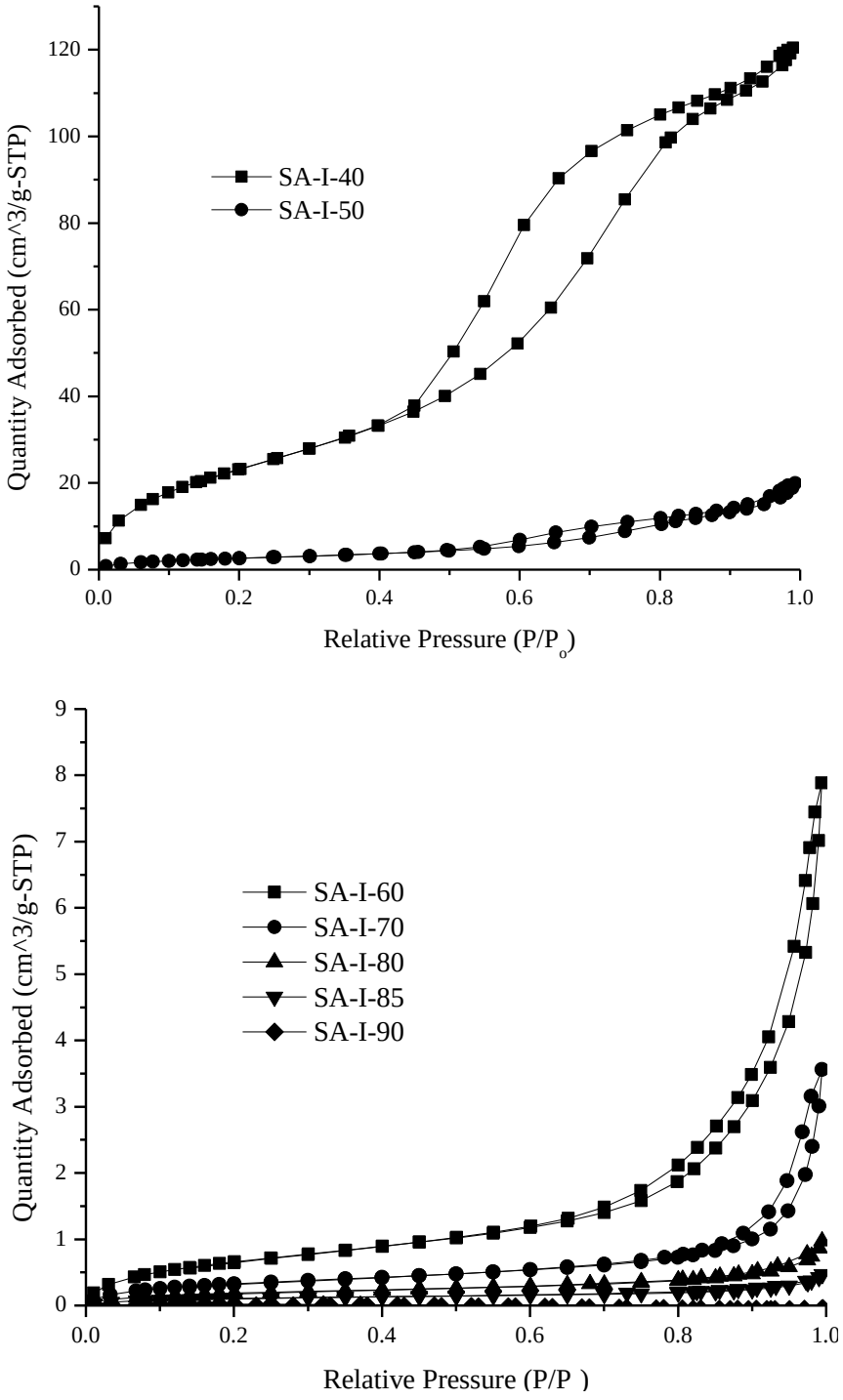

Figure 2.5: Nitrogen Adsorption-Desorption Isotherms of TEPA Impregnated SA-I-x Sorbents.

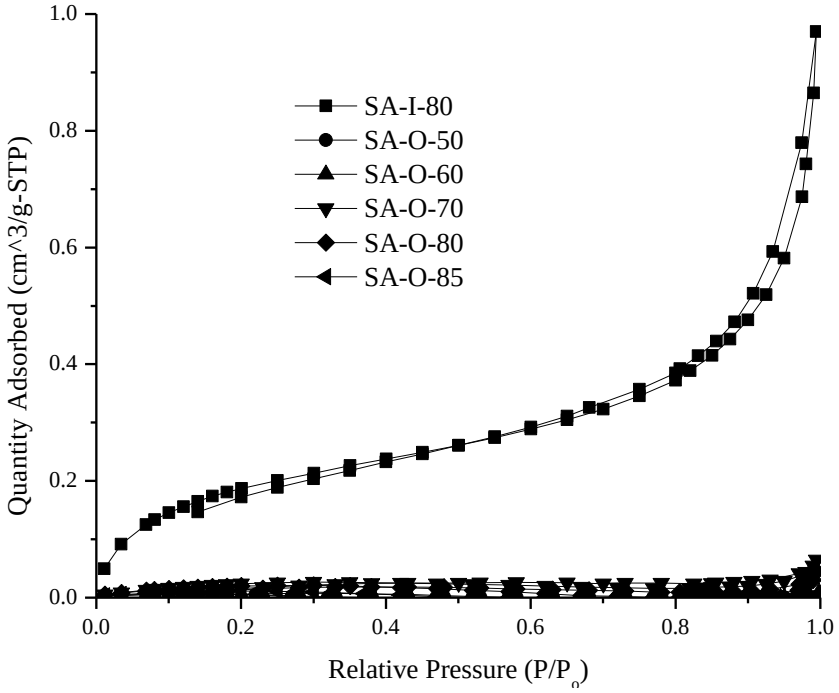

Figure 2.6: Nitrogen Adsorption-Desorption Isotherms of TEPA Impregnated SA-O-x Sorbents.

Theoretically, the maximum amount of TEPA that can be impregnated into the SA-I and SA-O aerogel is about 83 and 77wt% based on TEPA's density of about 1g/cm^3 and pore volumes of 5.0 and 3.5 cm^3/g. There should remain therefore some unoccupied pore space at loadings lower than 83 and 77wt% TEPA for the SA-I-x and SA-O-x sorbents. The near zero pore volumes for the higher loaded SA-I-x sorbents and all of the SA-O-x sorbents observed in Figures 2.5 and 2.6 is likely due to the shrinking of the aerogel supports during drying. Aerogel generally has poor structural integrity and collapses during ambient drying because of the capillary tension imposed on the structure (Baetens, Jelle, & Gustavsen, 2011). During the evaporation of methanol in this case, the aerogel is apparently shrinking until the methanol is removed, leaving a completely

TEPA filled aerogel particle, or until the collapsed particle reaches a stable configuration with the TEPA/methanol solution beginning to recede within the pores of the densified aerogel.

The SA-O-x samples, however, appear to have a greater degree of pore plugging than the SA-I-x samples. Though the pore volume of the unmodified SA-O support is smaller resulting in filled pores at lower relative loadings, there is still no observable mesoporosity seen even for the lowest TEPA loaded sorbent, SA-O-50. These results are most likely due to the hydrophobicity of the surface. The ($-CH_3$) surface groups appear to be contributing toward a greater degree of pore plugging during drying by their molecular interaction with the amine/methanol solution. It may be that the TEPA precipitates out of the solution during the later stages of the drying process and is displaced by the methanol within the pore space of the aerogel particle due to the differences in surface free energies, resulting in amine plugging the pores near the exterior of the aerogel.

To confirm the structure shrinkage of the aerogel upon solvent drying, the pore structure of the aerogel pre-soaked with a solvent (e.g., ethanol without TEPA) followed by the ambient pressure drying was measured. It has a pore volume and surface area respectively of about and 2.1 cm^3/g and 645 m^2/g. Compared to the values of 5.0 cm^3/g and 822 m^2/g for the fresh aerogel (Table 2.1), it is clear that the aerogel structure shrank upon soaking and drying of a solvent. However, the pore volume of the dried aerogel is still much larger than silica xerogel prepared by ambient pressure drying of wet-gel by the sol-gel process (typically in the range of about 0.6-0.8 cm^3/g) (Zeng, Zajac, Clapp, & Rifkin, 1998). This is because xerogel is prepared by drying a wet-gel with a flexible structure not fully condensed. When aerogel is pre-soaked with a solvent followed by

drying in ambient pressure, the aerogel structure is much more rigid than the wet-gel, and therefore more resistant against contraction induced by the capillary pressure as compared to the wet-gel from which xerogel is obtained.

For affirmation of the amount of TEPA impregnated in the SA-I-x and SA-O-x sorbents, TG analyses were conducted and the results are shown in Figure 2.7. All samples show similar mass loss trends within the same temperature ranges. Between the temperatures of 50-100 ^{o}C there was a slight drop in mass (~3%) on all samples which is attributed to pre-adsorbed water, carbon dioxide and possibly residual methanol in the adsorbent material during synthesis. A second weight loss was observed between 150-300 ^{o}C due to the thermal decomposition of TEPA, which has a boiling point of 340 ^{o}C. The decomposition temperature of TEPA is lower than the boiling point in this circumstance, a common observation with impregnated materials (Son et al., 2008; X Xu et al., 2003), which is suggested to be due to the increased volatility of TEPA when its particulate size decreases (Ebner et al., 2011). The amount of TEPA immobilized in the aerogels was calculated from the weight difference from the TGA curve at 100 ^{o}C and 450 ^{o}C shown in Figure 2.7. The TEPA content (in wt% with respect to aerogel weight) is listed in Table 2.1. The TGA data were within 6% of the theoretical amounts calculated, suggesting that little TEPA was lost during synthesis and verifying the validity of the wet impregnation method.

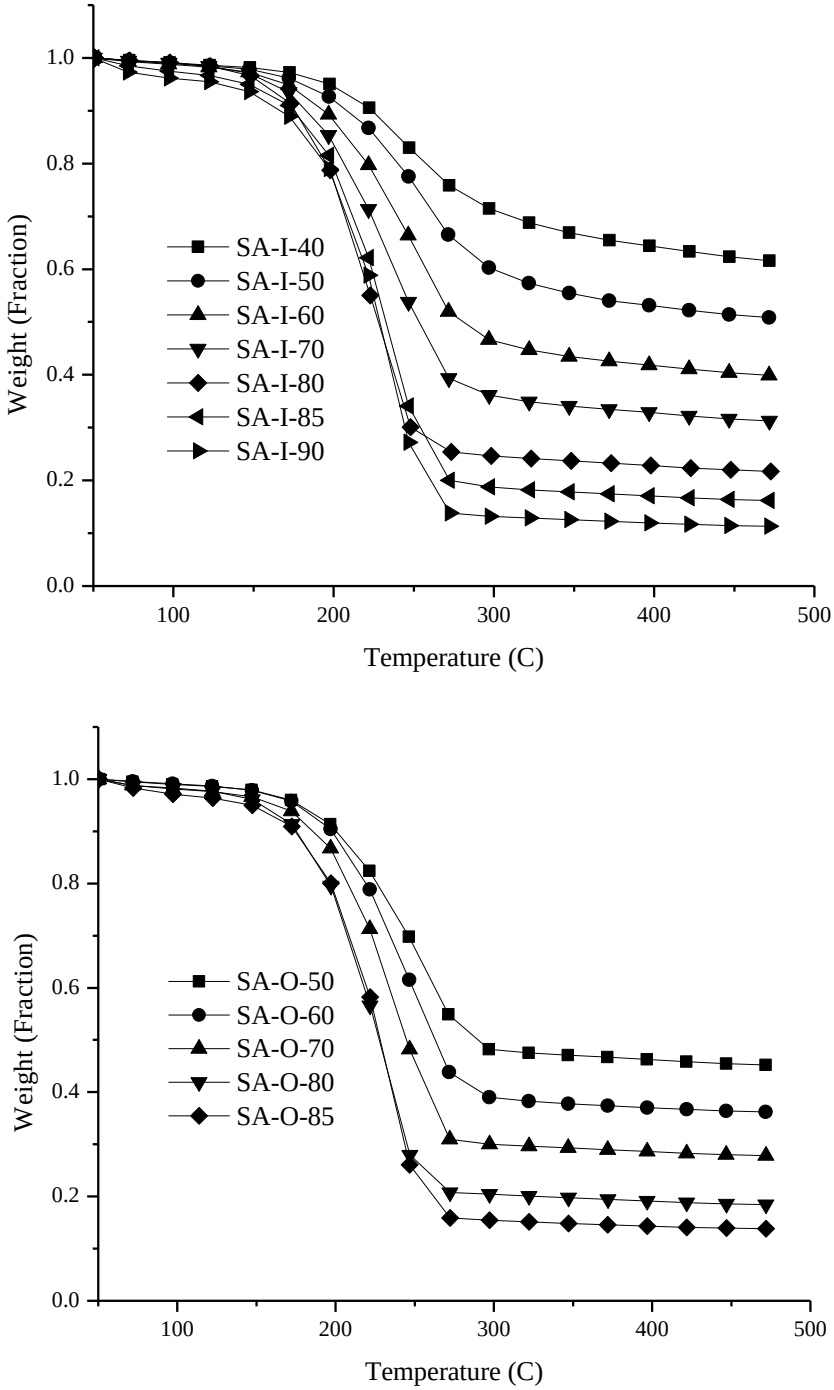

Figure 2.7: TGA Results of SA-I-x (top) and SA-O-x (bottom) Samples (Heating Rate 5 ^{o}C /min from 50 to 500 ^{o}C).

2.3.2 CO_2 Adsorption Performance

Figure 2.8 shows the dynamic CO_2 adsorption capacities for the SA-I-x and SA-O-x samples with 100% CO_2 at 75 ^oC. A temperature of 75 ^oC was chosen for adsorption for these sorbents since 75 ^oC is generally the optimum operating temperature for TEPA impregnated materials (Chen et al., 2009; Y. Liu et al., 2011; Son et al., 2008; Xiaoxing Wang et al., 2012; Xingrui Wang et al., 2011; Xiaochun Xu et al., 2002). Typically, chemisorption is an exothermic process which results in decreased adsorption capacities at higher temperatures. However, for impregnated materials, a diffusional limitation during the CO_2 adsorption process is present that results in the increased adsorption capacities with an increase in temperature. At higher temperatures the amine molecules become more mobile (i.e., less viscous) and therefore allow for greater CO_2 transport through the sorbent, reaching a greater number of amine adsorption sites. Above a certain maximum temperature, however, the adsorption capacity begins to fall due to the thermodynamic limitation becoming the prevalent constraint.

The CO_2 adsorption behavior seen in Figure 2.8 for both the SA-I-x and SA-O-x samples is seen to have a fast first stage adsorption process followed by a slow second stage adsorption progression. This behavior is commonly seen for impregnated sorbents(Chen et al., 2010; Ming Bo Yue et al., 2008). The SA-I-40 sorbent reached 90% of its equilibrium adsorption capacity (considered in this work the adsorption capacity after 1 hour of CO_2 exposure) within the first 5 min. Sorbents SA-I-50 through SA-I-85 reached 90% capacity within the first 10 min of adsorption, the time slightly increasing with increasing TEPA content. However, for SA-I-90, 90% capacity was reached in about 24 min. The longer time to reach 90% capacity with greater amine content is a

consequence of the increasing CO_2 diffusion length, (i.e. the radial distance CO_2 must transport to reach the core of TEPA filled particulate) (Heydari-gorji, Yang, et al., 2011). SA-I-40 has the quickest time due to the lowest diffusion length as a result of the lower amine loading. SA-I-40 virtually reaches the actual thermodynamic equilibrium within the 1 hour period during the first adsorption stage, having a second stage adsorption rate of nearly zero. Sorbents SA-I-50 through SA-I-85 have longer diffusion lengths leading to longer periods of time to reach the thermodynamic equilibrium.

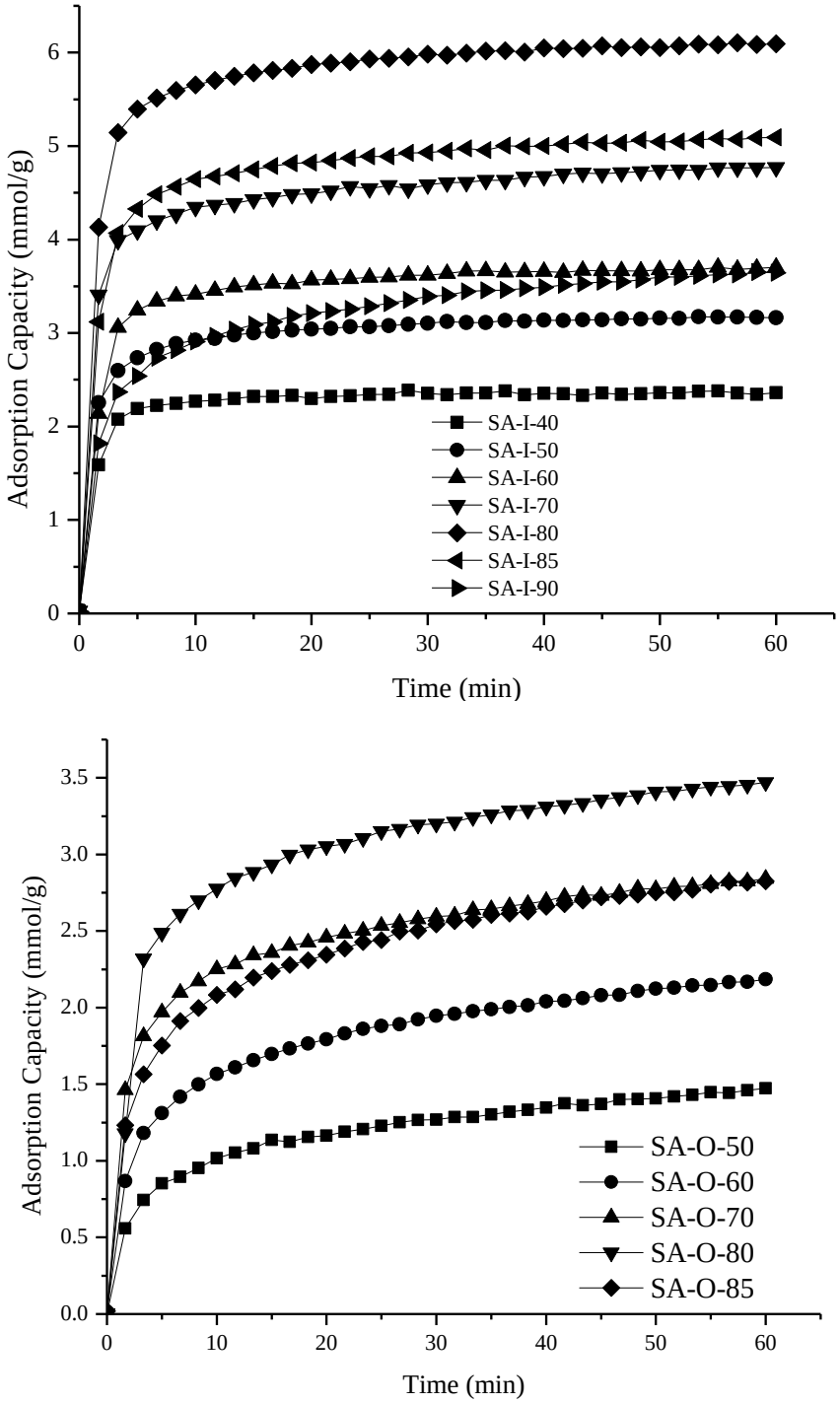

Figure 2.8: Adsorption Performance of Hydrophilic (top) and Hydrophobic (bottom) Sorbents at 75 ^{o}C with 100% CO_2 at 1 atm.

The second stage adsorption rates ranged from 0.003 to 0.008 mmol/g-min for SA-I-50 through SA-I-85, increasing with increasing TEPA content. Subsequently, after pore saturation occurs at amine loadings close to the theoretical maximum the amines begin to layer on the exterior surface of the particles forming large agglomerates (Son et al., 2008; X. Yan, Zhang, Zhang, Qiao, et al., 2011). For SA-I-90, the diffusion length increases substantially leading to a much longer time to reach thermodynamic equilibrium; and the second stage rate for SA-I-90 was as high as 0.013 mmol/g-min.

In regard to the SA-O-x sorbents, the time to reach 90% equilibrium adsorption capacity was fairly constant averaging about 30 min, significantly longer relative to the SA-I-x sorbents. Thus the SA-I support appears to be distributing the TEPA more effectively. As previously discussed in section 2.3.1, the SA-O support seems to encourage a greater degree of pore plugging than SA-I which leads to slower adsorption kinetics**.**

Figure 2.9 shows the equilibrium adsorption capacities as a function of TEPA content for the SA-I-x and SA-O-x sorbents. The SA-I-x samples outperformed the SA-O-x samples at all TEPA loadings achieving a maximum adsorption capacity of 6.1 mmol/g at 80wt% TEPA (SA-I-80). Unmodified SA-I and SA-O aerogels without TEPA showed less than 0.1 wt% weight gain with the switch of the surrounding gas from pure Ar to pure CO_2 stream at 1 atm, confirming negligible adsorption of CO_2 at 1 atm CO_2 pressure by unmodified silica aerogel. This result has also been observed for other silica supports (Meador et al., 2005; Xiaochun Xu et al., 2002; X. Yan, Zhang, Zhang, Qiao, et al., 2011). The highest capacity for the SA-O-x sorbent was 3.5 mmol/g at 80wt% TEPA (SA-O-80). The SA-I-80 and SA-O-80 achieved amine efficiencies (i.e. mol of CO_2/mol

of N) of 0.29 and 0.16 (Figure 2.10), where the theoretical value at the adsorption conditions studied is 0.5 as previously discussed(Caplow, 1968).

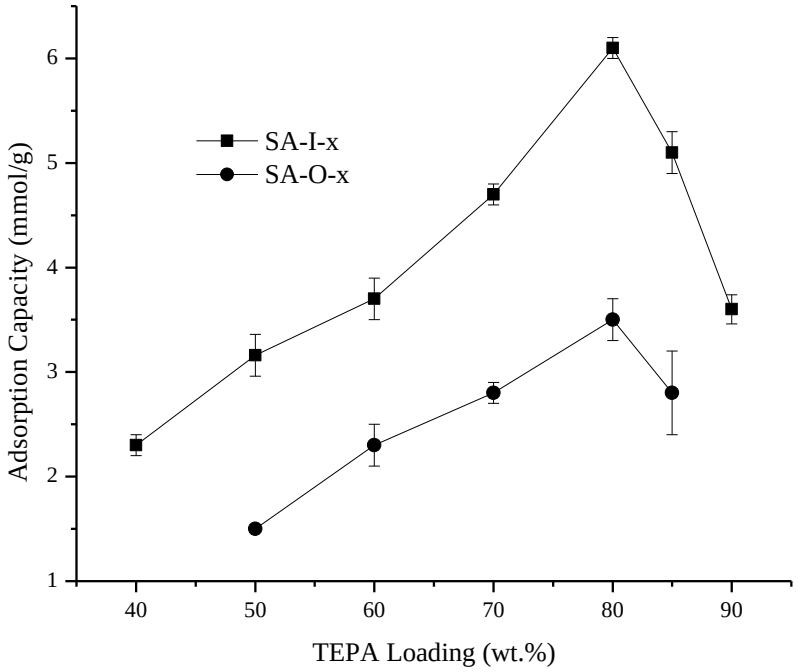

Figure 2.9: CO_2 Adsorption Capacity of SA-I-x and SA-O-x Samples in Relation to Amount of TEPA Immobilized within the Support at 75 ^oC with 100% CO_2 for 1 hour.

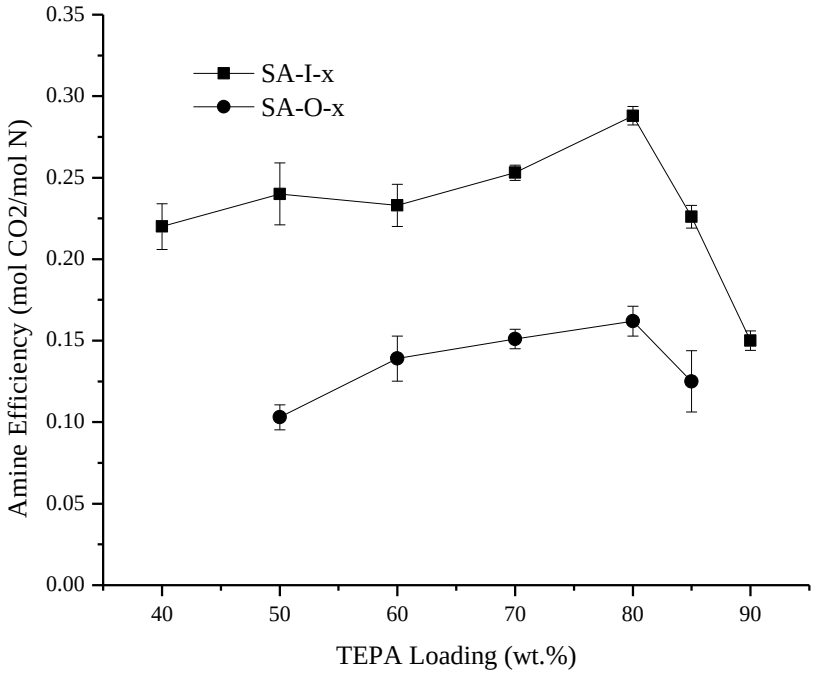

Figure 2.10: Amine Efficiencies of SA-I-x and SA-O-x Samples in Relation to Amount of TEPA Immobilized within Adsorbent.

The optimal adsorption capacity occurs at amine loadings near pore saturation as also seen elsewhere(Choi et al., 2009; Franchi et al., 2005; Qi et al., 2011). Amine loadings near pore saturation allow for the highest amount of N content without excessive agglomeration and CO_2 diffusion resistance, thus optimizing capacity. However, the maximum adsorption capacity could also be a function of particle size, which inherently affects diffusion length (Heydari-gorji, Yang, et al., 2011)**.**

For the SA-I-x sorbents, the adsorption capacity increases non-linearly with rising TEPA content. This is a result of the rising amine efficiency of the sorbent with amine loading. If the amine efficiency remained constant, then theoretically, a linear increase in adsorption capacity would be observed. The increasing amine efficiency is suggested to be due to the increased intermolecular contact between amine molecules as the TEPA

content rises. As previously discussed, two amino groups are required for the chemisorption of CO_2 under dry conditions. At lower relative loadings, the segregation of TEPA along the silica surface is greater and results in less intermolecular interaction between TEPA molecules. Consequently, the amount of CO_2 adsorbed per amino sorption site falls. In regards to the SA-O-x sorbents, the trend exhibits greater linearity and nearly constant amine efficiencies (0.10, 0.14, 0.15, 0.16). This result is most likely due to the different amine distribution because of the hydrophobic surface as mentioned previously.

The SA-I-80 sorbent, which showed the highest CO_2 adsorption capacity, was also tested under low CO_2 partial pressure conditions (10% CO_2/Ar in 1 atm total pressure). Under the low CO_2 partial pressure environment the SA-I-80 sorbent achieved an adsorption capacity of 3.5 mmol/g with an amine efficiency of 0.17. Table 2.2 summarizes the CO_2 adsorption results along with those obtained in other studies for comparison purposes. Note that the CO_2 adsorption capacity of the SA-I-80 sorbent is close to that of the mesoporous capsule (Qi et al., 2011), the impregnated sorbent which reported the highest CO_2 adsorption capacity thus far. The SA-I-80 sample, when examined under low CO_2 partial pressure, also performed competitively when compared to the silica monolith (Chen et al., 2009) and KIT-6 (Y. Liu et al., 2010)sorbent. The exceptional CO_2 adsorption performance of the SA-I-x sorbents compared to other sorbents cited using different supports is ascribed to the large pore volume and pore diameter of aerogel. The large pore volume allows for a high TEPA loading without significant particle agglomeration, mitigating diffusional resistance, while the large pore

diameter provides greater CO_2 transport through the TEPA filled support (Son et al., 2008).

Table 2.2: Summary of CO_2 Adsorption Performance using Aerogel as Compared to Other TEPA Impregnated Sorbent Materials.

Sorbent	Temp. (^oC)	vol% CO_2	TEPA Loading (wt%)	Adsorption Capacity (mmol/g)	amine efficiency (mol CO_2/mol N)	Ref.
SA-I-40	75	100	40	2.3	0.22	--
SA-I-50	75	100	50	3.2	0.24	--
SA-I-60	75	100	60	3.7	0.23	--
SA-I-70	75	100	70	4.7	0.25	--
SA-I-80	75	100	80	6.1	0.29	--
SA-I-80	75	10	80	3.5	0.17	--
SA-I-85	75	100	85	5.1	0.23	--
SA-I-90	75	100	90	3.6	0.15	--
SA-O-50	75	100	50	1.5	0.10	--
SA-O-60	75	100	60	2.3	0.14	--
SA-O-70	75	100	70	2.8	0.15	--
SA-O-80	75	100	80	3.5	0.16	--
SA-O-85	75	100	85	2.8	0.13	--
silica monolith	75	100	65	5.9	0.34	(Chen et al., 2009)
as-prepared MSU-1	75	10	50	3.9	0.29	(Xingrui Wang et al., 2011)
mesoporous capsule	75	100	83	6.6	0.30	(Qi et al., 2011)
as-prepared MCM-41	75	100	60	5.4	0.34	(Ming Bo Yue et al., 2008)
KIT-6	60	10	50	2.9	0.22	(Y. Liu et al., 2010)

In order to have practical industrial application, adsorbents must also demonstrate economical regenerability, stability, and fast adsorption-desorption kinetics over thousands of cycles. Figure 2.11 shows the cyclic performance for the SA-I-80 sorbent. Cyclic tests were performed using a concentration sweep by switching from 100% CO_2

for 10 min of adsorption to 100% Ar for 20 min of desorption. After ten cycles using 100% CO_2, with each adsorption cycle run for 10 minutes, the SA-I-80 adsorption capacity remained nearly constant with a capacity of 5.1 mmol/g. This indicated a decent cyclic stability over 10 cycles though the sorbent loss approximately 5% of its initial mass due to TEPA evaporation. For an industrial setting, a concentration sweep such as steam stripping is suggested to be employed for this sorbent. Other possibilities are temperature swing or pressure swing desorption. However, the sorbents prepared do not look to have the potential to be stable over the large number of cycles required for commercial applications.

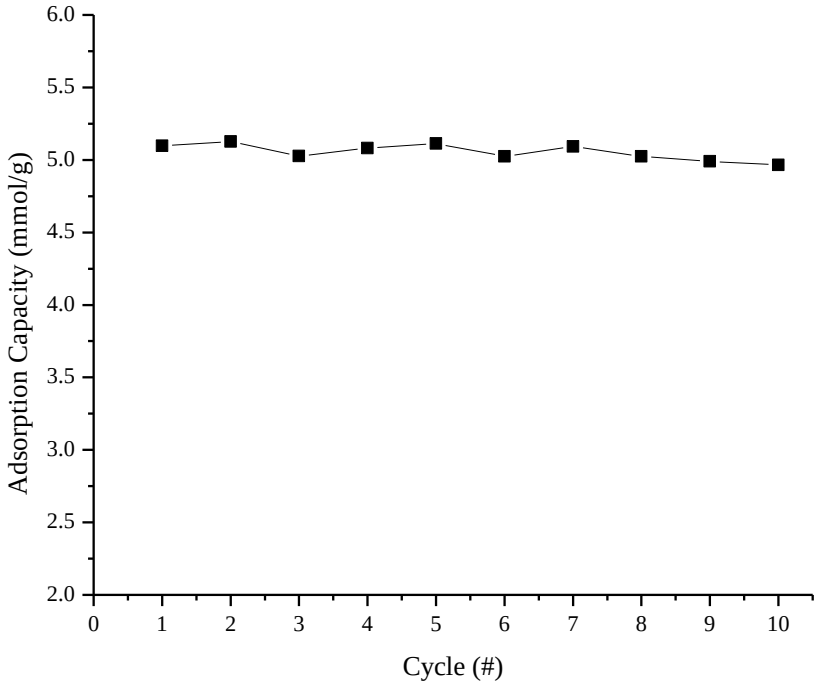

Figure 11: Cyclic Stability of SA-I-80 Sorbent (Adsorption at75 C^o with 100% CO_2 for 10 min; Desorption at75 ^oC with 100% Ar for 20 min).

2.4 Conclusions

Novel wet impregnated amine-based CO_2 sorbent materials were developed by the wet impregnation method using hydrophilic and hydrophobic aerogels (Nanogel obtained from Cabot Corp.) as the support for TEPA. The hydrophilic aerogel sorbents, SA-I-x, outperformed the hydrophobic aerogel sorbents, SA-O-x, presumably due to the difference in TEPA distribution as a result of the difference in hydrophilicity of the support. The surface chemistry of the aerogel appears to influence how TEPA is filling the pores. However, more research is required for a better understanding of the surface chemistry effects on the drying and amine distribution mechanism during synthesis. The SA-I-80 sample achieved an excellent equilibrium CO_2 adsorption capacity of 6.1 and 3.5 mmol/g under a dry 100% and 10% CO_2 stream at 75 ^{o}C. However, the SA-I-80 sample achieved moderate cyclic stability over 10 cycles having an average capacity after 10 minutes of adsorption of 5.1 mmol/g under dry 100% CO_2, making it not an ideal sorbent for industrial use.

CHAPTER 3

RELATIONSHIP OF SYNTHESIS METHOD, AMINE DISTRIBUTION AND CARBON DIOXIDE SORPTION PERFORMANCE OF AMINE IMPREGNATED SILICA AEROGEL SORBENTS

3.1 Introduction

As discussed in Chapter 1, a factor that plays a major role on the adsorption performance of amine impregnated sorbents is the amine distribution within the porous support. The significance of this factor is due to the poor diffusion kinetics of CO_2 through the amine film within the adsorbent. The organic amines predominately used (e.g. PEI) are liquids at room temperature and drastically increase in viscosity upon reacting with CO_2 due to strong carbamate-ammonium hydrogen bonding, resulting in obstructed CO_2 transport (Goodrich et al., 2011; Gutowski & Maginn, 2008; Zhang et al., 2009). The diffusion limitation is readily recognized by the requirement for higher operating temperatures (typically around 75 ^{o}C) during adsorption to reach optimum performance

As explained in Section 1.2, innovations have emerged to improve the amine distribution in impregnated sorbents through the use of template occluded ordered mesoporous silica supports, (Heydari-gorji, Belmabkhout, et al., 2011; B. Li et al., 2011; Xingrui Wang et al., 2011; Jianwen Wei et al., 2010; M. B. Yue et al., 2006; Ming Bo Yue et al., 2008) surfactant-aminopolymer blends,(J. Wang et al., 2012) and short pore length supports(Heydari-gorji, Yang, et al., 2011; Qi et al., 2011). All of these have been shown to improve the CO_2 adsorption performance relative to simply impregnating a pure amino-polymer into the porous support matrix. However, it is still not clearly understood

how the amines are distributed within the pore space of the support upon impregnation, and how synthesis conditions affect their coverage in the support framework. This is a critical insight that needs to be explored in order to design higher performing amine based adsorbents.

Presently, limited work has been done in investigating amino polymer distributions within porous networks for certain methods of amine immobilization. Sanz, Calleja, Arencibia, & Sanz-Pérez, (2012) & (2013) explored the amino polymer distribution of PEI and TEPA impregnated SBA-15 by transmission electron microscopy. The PEI impregnated SBA-15 samples showed heterogeneous distributions of PEI within individual particles, and even some particles containing no PEI. The TEPA impregnated SBA-15 showed relatively homogenous amine coverage within the SBA-15 support. However, the SBA-15 used in this case was grafted with a tri amino silane (Figure 1.5) prior to TEPA impregnation which may influence the amino polymer distribution. This reveals that the surface chemistry and/or molecular weight of the amino polymer could influence polymer distribution. Neimark, Hanson, & Ungert, (1993) investigated the distribution of polybutadiene impregnated in porous silica using fractal analysis. Similar to typical impregnation synthesis, the oligomer was immobilized in the silica by the wet impregnation method but further modified with a cross-linking agent to fixate the polymer position in the pores. They found that the majority of the amine was retained inside the porous silica and was distributed in inclusions randomly throughout the porous network.

In this Chapter, an investigation was performed on the affects of the synthesis route of amine impregnation on the polymer distribution within a porous support. TEPA

impregnated silica aerogel sorbents were prepared by two different methods: a solvent evaporative precipitation method, and the previously reported wet-impregnation method discussed in Chapter 2 (Section 2.2.1). The objective of Chapter 3 is to examine the relationship of synthesis-structure-CO_2 adsorption properties of impregnated sorbents on the silica aerogel supports.

3.2 Experimental Methods

All chemical were purchased from Aldrich unless otherwise stated. These chemicals include methanol (anhydrous, 99.8%), Tetraethylenepentamine (TEPA, technical grade), n-hexane (anhydrous, 95%), sodium periodate ($NaIO_4$, ACS reagent, >99.8%), Ruthenium(IV) oxide hydrate ($RuO_2 \bullet 2H_2O$, powder). Particulate aerogel (MT-1100 Nanogel, particle size of 10 μm) was obtained from Cabot Corp. and is originally hydrophobic in nature. Hydrophilic aerogel was prepared by calcining the hydrophobic aerogel as described in Section 2.2.

3.2.1 Solvent Evaporative Precipitation Method

A saturated TEPA/n-hexane solution was prepared as follows. TEPA (9 mL) was added to 100 mL of n-hexane in a 150 mL Erlenmeyer flask at room temperature. TEPA was chosen as the amino polymer because of its semi-soluble properties in non-polar hexane and high adsorption capacity potential (Y. Liu et al., 2010; Qi et al., 2011; Xingrui Wang et al., 2011; Ming Bo Yue et al., 2008). The mixture was then heated with stirring to a light boil. (~68 ^oC, hexane's boiling temperature). TEPA has a solubility of approximately 7 and 40 mg/mL at 23 ^oC and 68 ^oC, respectively. In a 50 mL Erlenmeyer flask, 1 g of hydrophilic aerogel (MT-1100 Nanogel, previously calcined at 600 ^oC for 8 hrs in atmosphere air) and 20 mL of n-hexane were mixed and heated. The

aerogel/hexane slurry was reduced due to evaporation of n-hexane until a paste developed. The mass ratio of the aerogel/hexane paste reached approximately 1:3. At this point, 5 mL of the TEPA/n-hexane solution at 68 ^{o}C was removed by a glass pipette and added into a 25 mL beaker heated by a second hot plate. This step is required due to the precipitation of the TEPA from the hexane solution inside the pipette. The pipette is at room temperature when withdrawing the 5mL of TEPA/n-hexane solution causing the TEPA to precipitate. Reheating the solution in the heated beaker dissolves the TEPA again into the hexane solution. The beaker with 5 mL of TEPA/n-hexane solution is then added to the aerogel/hexane paste and the contents are then thoroughly mixed and the slurry is reduced (due to n-hexane evaporation) until a paste consistency is reached again. The 5 mL additions of TEPA/n-hexane solution are repeated until a desired total amount of TEPA has been added. Each 5 mL addition contains approximately 200 mg of TEPA. Therefore, as an example, for a 50 wt% TEPA/aerogel sample, 5 additions of 5 mL of TEPA/n-hexane (25 mL total, equivalent to 1 g of TEPA) are required. Once the required amount for a desired loading is added, the slurry is cooled to room temperature and then vacuumed dried at 25 ^{o}C. Samples were labeled P-x, x representing the desired wt.% of TEPA in the prepared sample.

3.2.2 Wet Impregnation Method

TEPA/aerogel sorbents were prepared by the wet impregnation method according to Section 2.2.1. 70 ml of methanol was mixed with a calculated amount of TEPA to obtain a given loading in wt% of amine in the aerogel and mixed vigorously for 10 min. 2 g of hydrophilic aerogel were then added to the solution and stirred for an additional 10 min. The slurry was then placed under a vacuum at 25 ^{o}C to dry with stirring until a semi-

solid slurry was formed. Stirring was then discontinued and the slurry left under vacuum overnight (24 hour drying period). Adsorbent samples were then removed and placed in storage for testing. Samples were labeled W-x, with x representing the desired wt.% of TEPA in the sorbent prepared.

3.2.3 Ruthenium Tetroxide Stain

Some samples prepared by the wet impregnation method and the evaporative precipitation method were stained with ruthenium tetroxide to facilitate transmission electron micrograph contrast for better imaging (Sanz et al., 2012). Ruthenium tetroxide is considered a specific staining compound for amino groups and therefore was chosen to oxidize amine groups on TEPA; the large atomic mass metal facilitated amine detection by TEM (Sawyer, Grubb, & Meyers, 1996). The staining solution was prepared as described by Trent, (1984), i.e., 1 g of $NaIO_4$ was dissolved in 25 mL of deionized water at 25 ^oC and chilled in refrigerator to approximately 0 ^oC and $RuO_2 \bullet 2H_2O$ (150 mg) was added to the chilled $NaIO_4$ solution. The solution turned dark yellow and consisted of 0.5 wt% RuO_4. 10 mg samples were stained by RuO_4 vapor by suspending the sample over RuO_4 solution in a closed container for 10 min.

3.2.4 Sorbent Characterization

Nitrogen adsorption-desorption isotherms were obtained on a Micromeritics ASAP 2020 surface area and porosity analyzer at 77 K. Before the nitrogen porosimetry analysis, samples were activated at 100 ^oC in a 25 inHg vacuum for 1 hour. The Micrometrics automated de-gas application was not used for activation to prevent the vaporization and condensation of TEPA inside the N_2 porosimetry system. The Brunauer-Emmett-Teller (BET) method and the Barret-Joyner-Halenda (BJH) model of the

adsorption isotherm were used to calculate the surface area, the pore size distribution, and pore volume. Transmission electron micrographs were obtained by a JEOL JEM-ARM200F instrument set at 80 kV. Thermogravimetric analyses were conducted with a TA Instruments SDT-Q600 analyzer. Sorbents were equilibrated at 50 ^{o}C and then heated to 500 ^{o}C at a rate of 5 ^{o}C/min in Argon.

3.2.5 Carbon Dioxide Adsorption Analysis

The CO_2 adsorption performance of the sorbents was determined using a Thermo Cahn D-101 electro-microbalance as described in Section 2.2.3. For a typical adsorption analysis, about 10 mg of sample was placed in a stainless steel sample pan and activated at 100 ^{o}C at 1 atm for 30 min under high purity Argon (99.99%) at 100 mL/min to remove unwanted adsorbed species (e.g., H_2O, CO_2, remaining solvent). Sorbents were then cooled to 75 ^{o}C and pure CO_2 (99.99%) was then introduced for 1 hr at 1 atm at a flow rate of 100 mL/min. The CO_2 equilibrium adsorption capacity was determined by the weight gained during the 1 hour adsorption period.

3.3 Results and Discussion

3.3.1 Sorbent Characteristics

Thermogravimetric and rate of mass loss data of the sorbents of different TEPA loadings prepared by the two methods are shown in Figures 3.1 and 3.2. Both the P-x and W-x sorbents showed similar mass loss trends. From 50 to 100 ^{o}C there was an average loss of 4% attributed to the loss of adsorbed H_2O, CO_2, and remaining organic solvent such as methanol or hexane. The weight loss between 150-400 ^{o}C is due to the evaporation of TEPA. The W-x sorbents had a TEPA content close to that desired during the wet impregnation procedure. However, the P-x samples had a TEPA content 5 to 10

wt% less than that desired. During the evaporative precipitation method, specifically the 5 mL transfer step when the TEPA/n-hexane solution precipitates inside pipette, some TEPA is lost due to adsorption of TEPA onto the inside of pipette resulting in lower amounts of TEPA added to the aerogel than desired. Due to differences between the desired and measured TEPA content, figures presenting P-x data and calculations involving TEPA content for the P-x sorbents were evaluated based on the absolute measured weight calculated from TGA data but the value of 'x' remains the desired amount for the P-x samples.

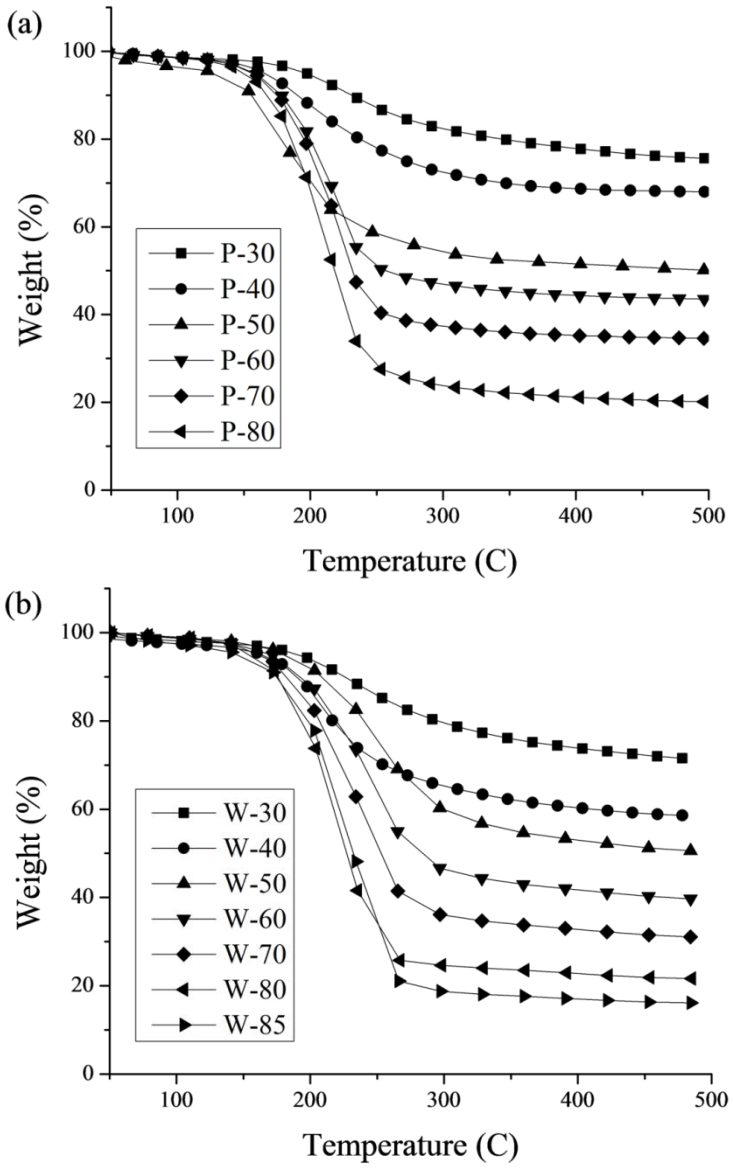

Figure 3.1: Sorbent Mass Loss by TGA prepared by the Evaporative Precipitation Method (a), and the Wet Impregnation Method (b).

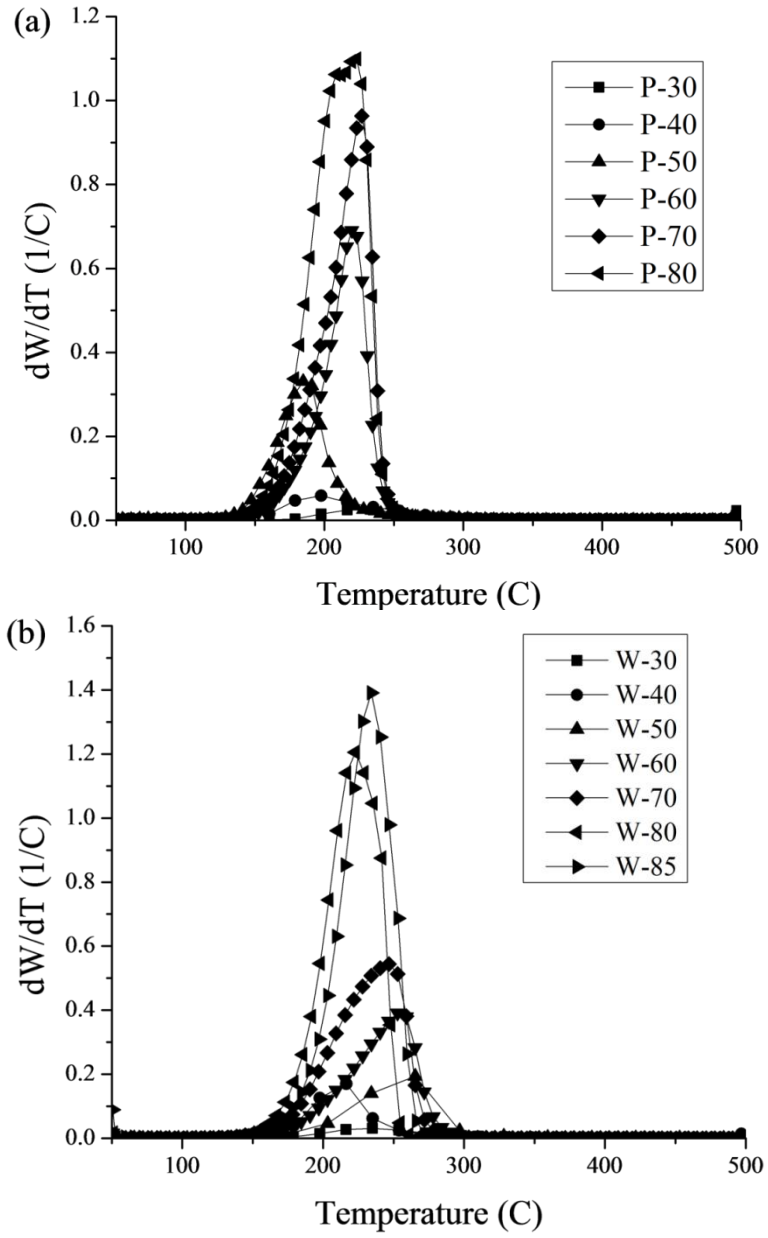

Figure 3.2: Rate of Sorbent Mass Loss prepared by the Evaporative Precipitation Method (a), and the Wet impregnation Method (b).

In Figure 3.2, the peak mass loss rates for the P-x and W-x samples were fairly similar. There are some fluctuations in the temperature where peak loss occurs for the P-x and W-x samples, revealing a rough trend of increasing temperature with decreasing TEPA content. This could possibly be the result of TEPA possessing a slight affinity for

the hydrophilic aerogel surface (Franchi et al., 2005). Also, if the P-x samples actually possessed a nanoscale film layer, the expected temperature for the peak mass loss rate should be depressed relative to the W-x (Lopeandía & Rodríguez-Viejo, 2007; Sun & Simon, 2007). However, there is only a slight temperature depression, roughly 20 ^{o}C, indicating similar amino polymer film scales in both the P-x and W-x samples.

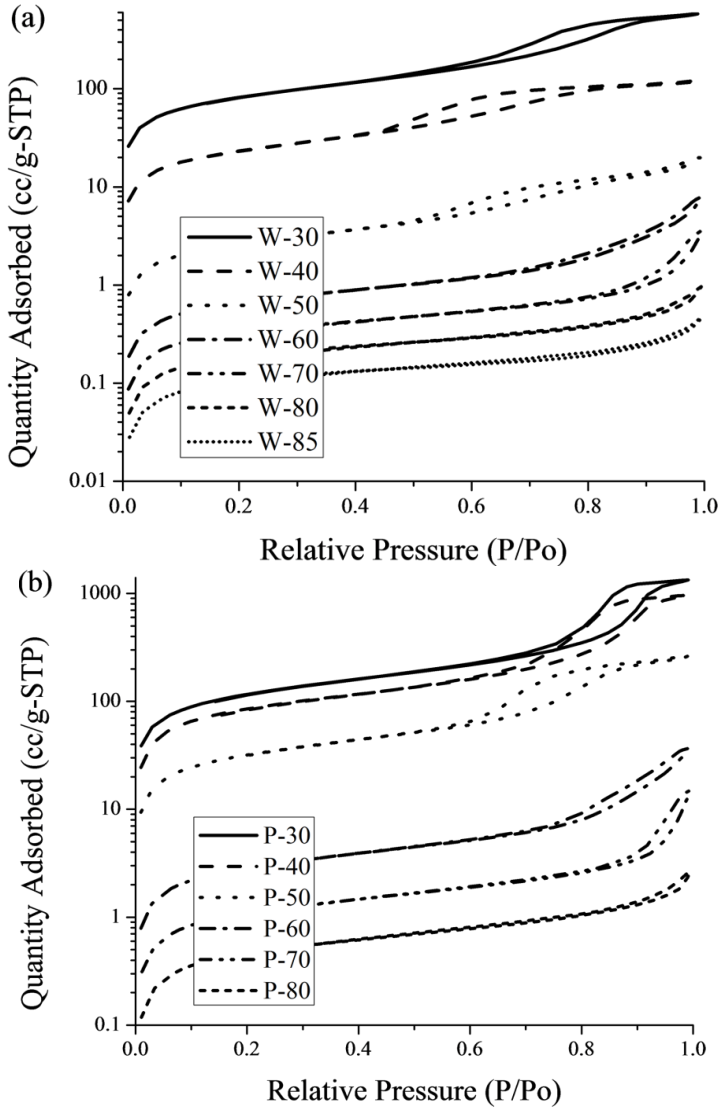

Figure 3.3: Nitrogen Adsorption/Desorption Isotherms of the Samples prepared by the Wet Impregnation Method (a), and the Evaporative Precipitation Method (b).

Figure 3.3 shows the nitrogen adsorption/desorption isotherms for the W-x and P-x sorbents. The isotherms of both P-x and W-x samples show a type IV isotherm with type H_2 hysterisis (Sing et al., 1985a). Between the two methods, the P-x samples, Figure 3.3(b), appear to have a slightly higher porosity than the W-x samples, Figure 3.3(a). The increased porosity is likely the result of the evaporative precipitation synthesis route of amine immobilization that leads to a somewhat better distribution of amine and less pore plugging relative to wet impregnation. Figure 3.4(a) and (b) show the trends of the pore volume and surface area changes relative to the TEPA content. The surface areas and the pore volumes of the P-x and W-x sorbents begin to merge toward zero with increasing TEPA content.

The maximum amount of TEPA able to be retained in the hydrophilic MT-1100 aerogel is ~83 wt% due to its pore volume of 5.0 cm^3/g (Linneen, Pfeffer, & Lin, 2013). Therefore as the amount of TEPA is increased toward this value regardless of the method of impregnation, the remaining porosity will approach zero. However, the P-x samples for TEPA loadings less than 83% show slightly higher surface areas and pore volumes relative to the W-x sorbents which is again attributed to an improved polymer distribution. It is unlikely that TEPA is simply covering the external surface of the particles and the obtained porosity values are a result of interparticle voids. The impregnated aerogels below 80wt% TEPA showed fast adsorption kinetics (Figure 3.7) and are free-flowing powders. If external TEPA film was present, much slower kinetics and agglomerated powders would be observed. Table 3.1 summarizes the nitrogen porosimetry results.

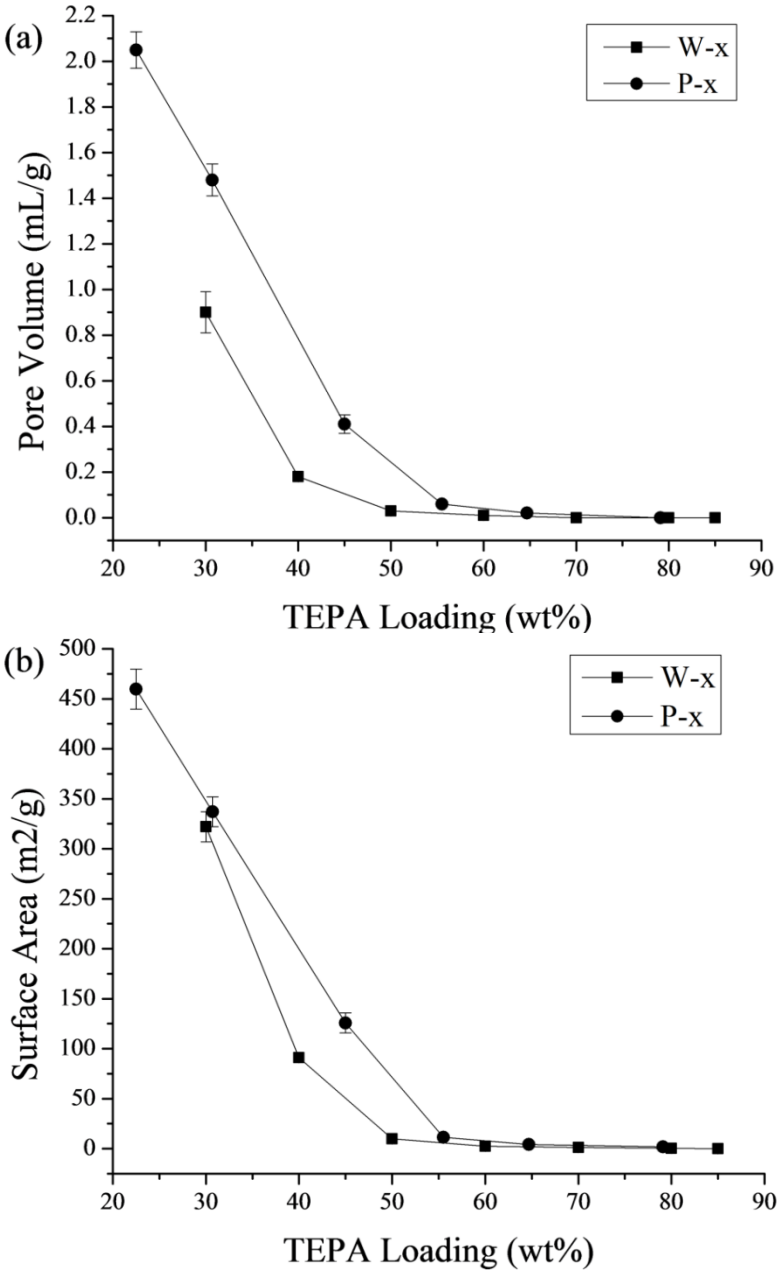

Figure 3.4: Textural Properties of the Sorbents prepared by the Wet Impregnation Method and the Evaporative Precipitation Method as a function of TEPA Loading: (a) Pore Volume, and (b) Surface Area.

Table 3.1. Summary of Nitrogen Porosimetry Analysis of P-x and W-x Samples

Sorbent	TEPA (wt%)	SA (m^2/g)[a]	Vp (cm^3/g)[b]
Aerogel	0	822	5.0
W-30	30	322	0.9
W-40	40	91	0.18
W-50	50	10	0.03
W-60	60	2.6	0.01
W-70	70	1.3	-
W-80	80	0.43	-
W-85	85	0.08	-
P-30	23	459	2.05
P-40	31	337	1.48
P-50	45	125	0.41
P-60	55	11	0.06
P-70	65	4.4	0.02
P-80	79	1.9	-

(-) represents samples with negligible pore volumes due to pore plugging/pore filling.

[a]surface area was calculated using BET method. [b] Pore volumes were calculated based on BJH method

TEM images of unmodified hydrophilic aerogel and unstained P-50 sorbent are shown in Figure 3.5(a)-(b). The unmodified aerogel and the unstained P-50 sorbent had similar contrasts and morphology revealing the spherical silica chain-like network characteristic of aerogel.(Wu, Lin, & Chen, 2012) TEPA in the P-50 sample cannot be clearly seen by the TEM due to the low atomic weight N, C, and H elements in the TEPA molecule. Figure 3.5(c)-(d) and Figure 6 show RuO_4 stained P-50 and W-50 sorbents. The P-50 and W-50 images show fairly similar variations in their TEPA distributions. The P-50 sample shows a more uniform freckle-like coverage in contrast to the W-50 samples showing similar freckle-like coverage but more heterogeneous within the particle. Also some particles in the W-50 sample appear to have no TEPA content present while others showed a clotting of TEPA within the particle framework (Figure 3.6(c)).

These results are similar to the other works mentioned earlier containing heterogeneous distributions and random inclusions (Neimark et al., 1993; Sanz et al., 2012).

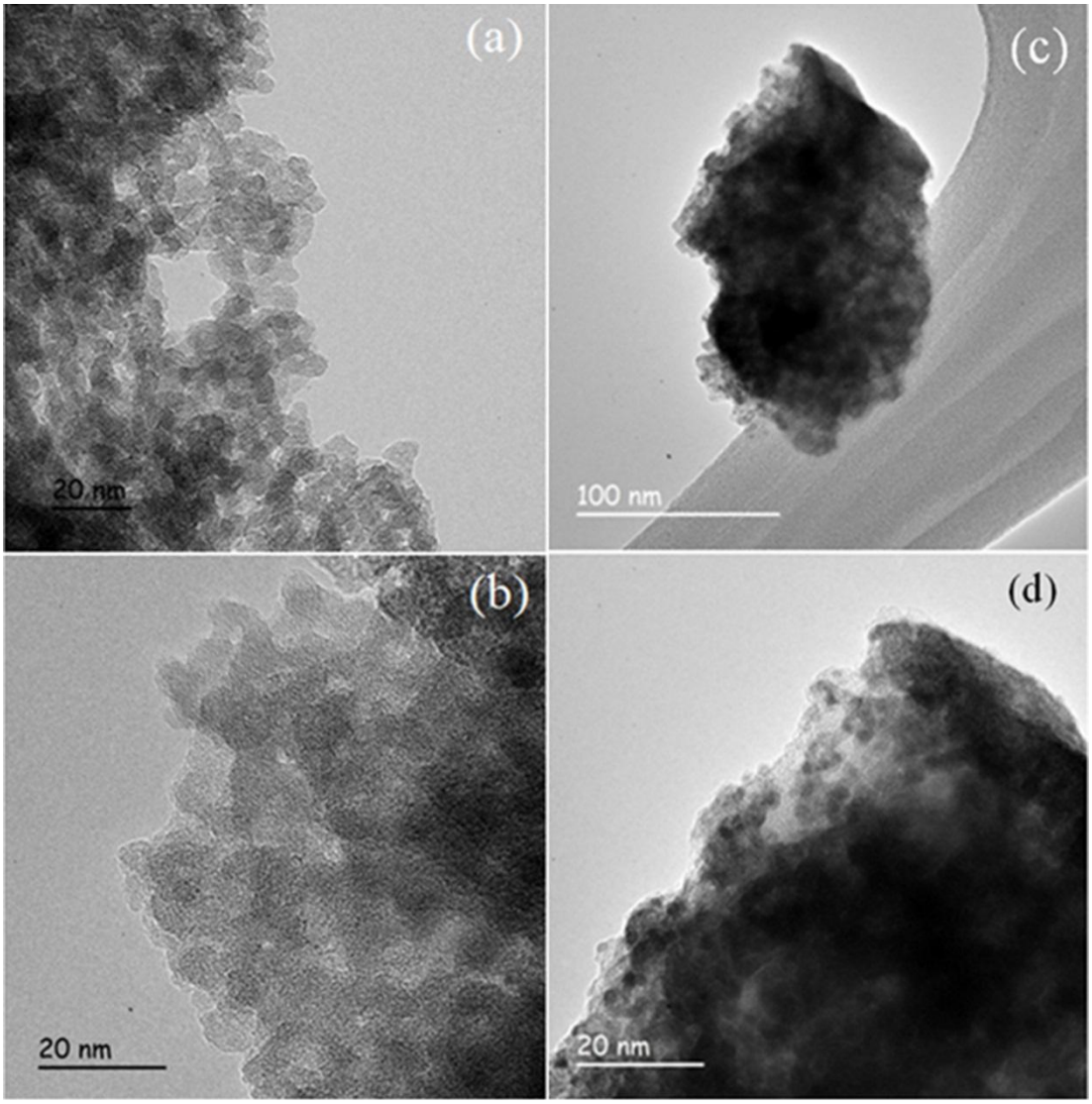

Figure 3.5: TEM Images of (a) Pure Hydrophilic Silica Aerogel, (b) Unstained P-50 Sorbent, (c) RuO_4 Stained P-50 Sorbent, and (d) a Higher Magnification of the Stained P-50 Sorbent.

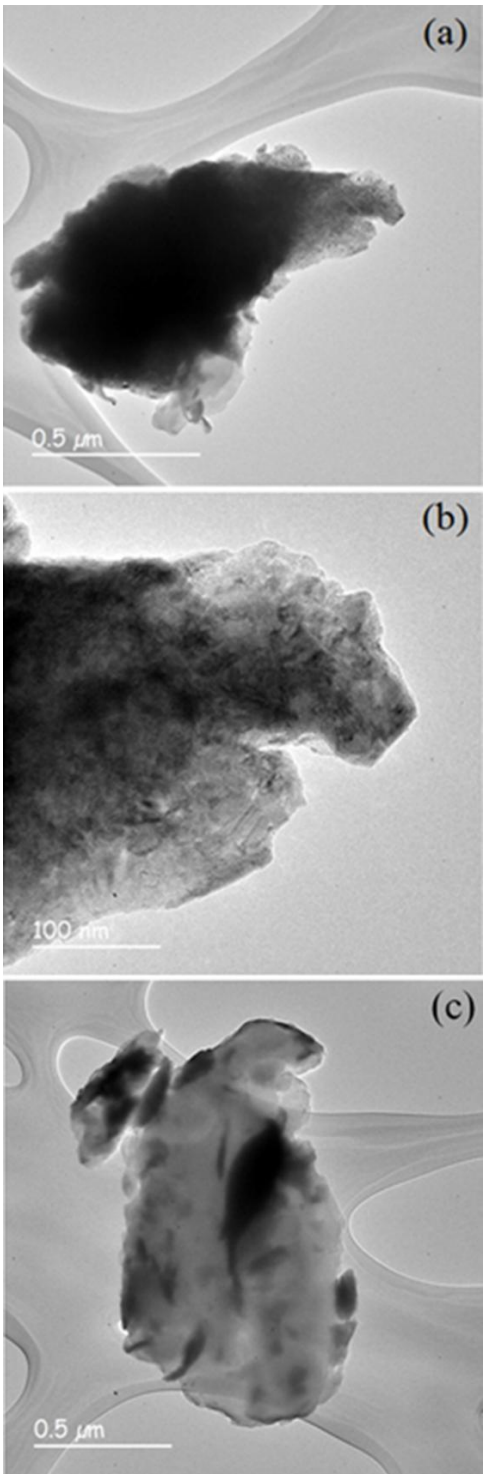

Figure 3.6. TEM Images of (a) RuO_4 Stained W-50 Sorbent, (b) a Higher Magnification of the Stained Sample, and (c) a W-50 Sorbent Particle with little Stained but Clotted TEPA Content.

3.3.2 CO_2 Adsorption Performance

Figure 3.7 shows the CO_2 adsorption uptake curves of the P-x and W-x sorbents. The curves show the typical two stage adsorption kinetics characteristic of impregnated adsorbents (Qi et al., 2011). The first stage, represented by quick initial uptake of CO_2, is due to the reaction of CO_2 with amine binding sites readily available at and near the polymer interface. Following the initial uptake is a slow second stage adsorption rate due to slower mass transport kinetics into deeper areas of the amine film. These effects are more pronounced at higher TEPA loadings as a result of the thicker films present.

Comparing the adsorption kinetics between the two differently prepared sorbents, the P-x samples show somewhat faster adsorption kinetics than W-x sorbents (Figure 3.8). Kinetic rates were measured as the time to reach 90% of the maximum adsorption capacity obtained after 1hr of CO_2 exposure. The small increase in adsorption rate of P-x is the indication of a slight enhancement in amine distribution within the aerogel framework. However, the degree of enhancement is small, near the margin of error, and therefore the P-x and W-x sorbents can be suggested again to have similar amine distribution morphology. In addition, both P-x and W-x samples reveal an increasing adsorption time with increasing TEPA loading, a result of the increased time required for CO_2 to diffuse into thicker amine films to reach the majority of adsorption sites.

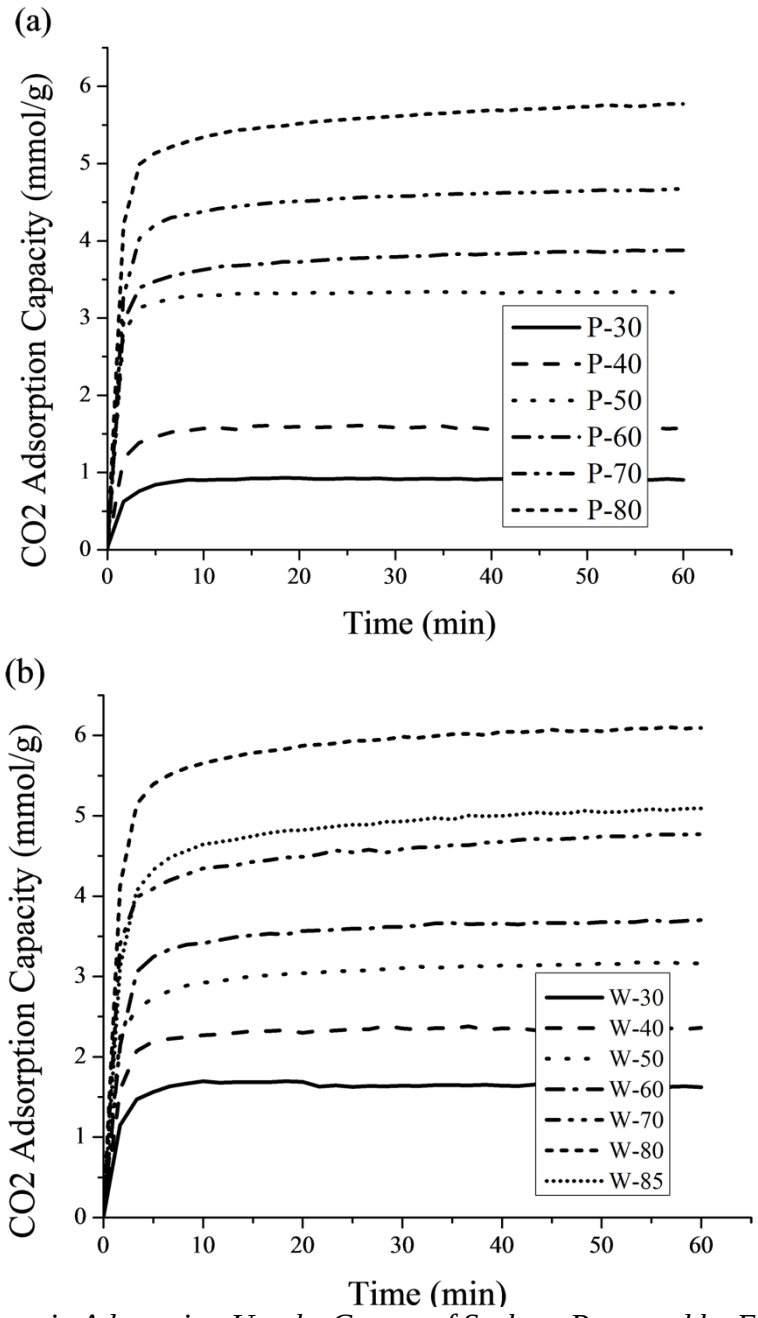

Figure 3.7: Dynamic Adsorption Uptake Curves of Sorbent Prepared by Evaporative Precipitation (a), and Wet Impgrenation (b). Adsorption Conditions: 100%CO_2, 75 ^oC, 1 bar, 100 mL/min.

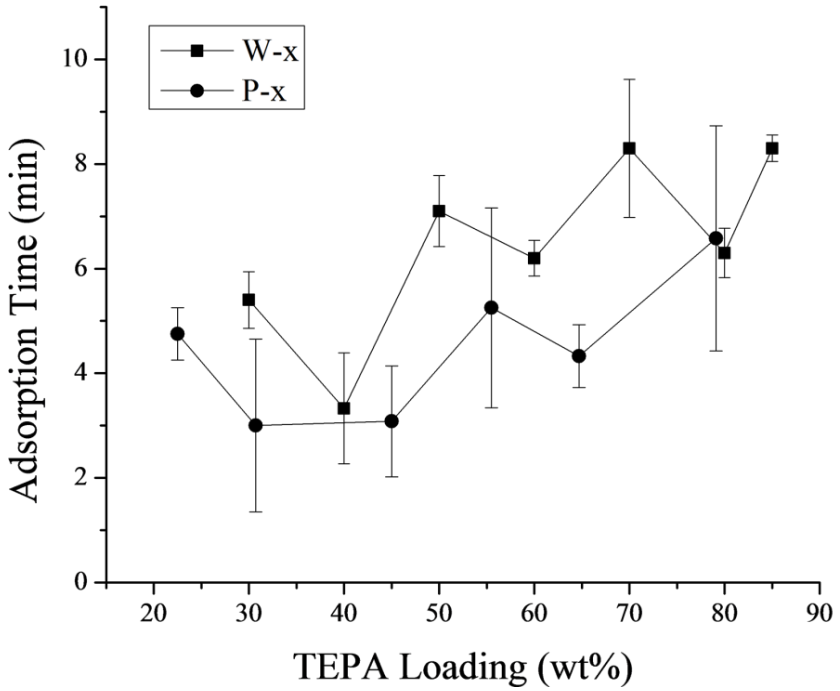

Figure 3.8: Adsorption Kinetics of the W-x and P-x sorbents. Adsorption Time Represents the Time Required to Reach 90% Adsorption Capacity.

Figure 3.9 shows the final adsorption capacities of the P-x and W-x sorbents after 1 hr of CO_2 adsorption. Pure hydrophilic MT-1100 TEPA showed less than 0.1 wt% weight gain in a pure CO_2 stream at 1 atm and therefore adsorption contribution from the silica substrate is negligible (data not shown). The overall trend with higher TEPA content shows increasing CO_2 capacities similar to other studies (S.-H. Liu et al., 2009; Son et al., 2008; Xiaochun Xu et al., 2002; Xiaochun Xu, Song, Miller, & Scaroni, 2005). More amino content within the substrate allows a greater number of amine sites for CO_2 adsorption. However, when aerogel particles are completely filled with amine around 80wt%, the capacity falls because of transport kinetics (Linneen et al., 2013). Comparing the difference in performance between P-x and W-x (Fig. 3.9), P-x shows a small enhancement in adsorption capacities at TEPA loadings less than 80 wt%. In theory they should be the same if an infinite amount time is allotted, but due to the slight improved

distribution of TEPA within the P-x sorbents, somewhat higher capacities are reached in shorter periods of time.

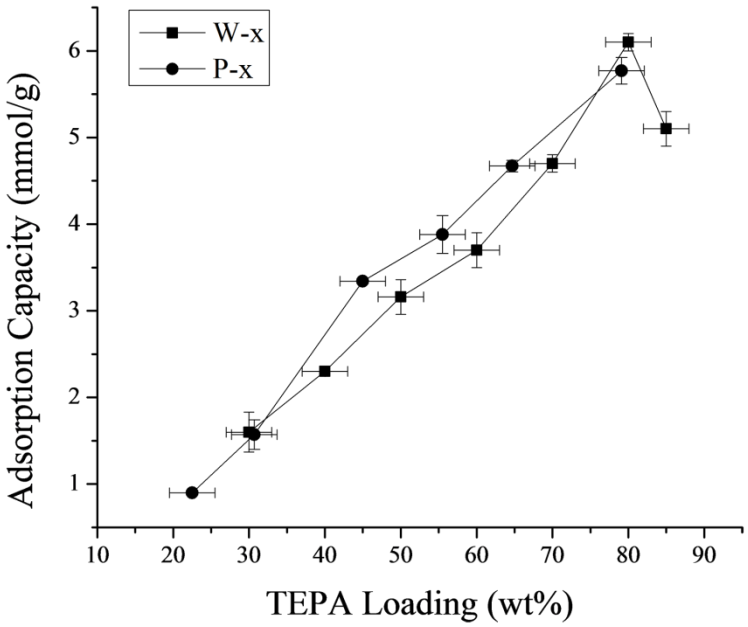

Figure 3.9: Adsorption Capacities of the P-x and W-x Samples Relative to TEPA Content after 1 hr Exposure to 100%CO_2 at 75 ^oC.

When the TEPA content reaches 80 wt%, the capacities and amine efficiencies (Figure 3.10) are nearly equal. At this point the particles are completely filled regardless of the method of amine modification. Furthermore, as a result of the small increase in adsorption capacity of the P-x sorbents, the amine efficiencies of the P-x sorbents are greater than the corresponding W-x samples at loadings less than 80 wt%. However, these improvements are minimal and therefore again it appears that the polymer distributions are nearly equivalent between the two sorbents prepared by different methods. The slight increase in amine efficiency up toward 80 wt% with increasing TEPA content for both the P-x and W-x samples is suggested to be due to the TEPA interaction with the aerogel. The amino polymer at the surface is most likely deactivated

by its affinity with the surface of the support which agrees with the data shown in Figure 3.2. The amine efficiency is maximized at 80 wt% and then begins to fall because once the aerogel pore space is completely filled with TEPA, which is around 80wt%, the TEPA begins to agglomerate outside the aerogel particles resulting in thick amine films making the majority of amine binding sites difficult to reach by CO_2 within the 1 hr adsorption period. Table 3.2 summarizes the CO_2 performance results.

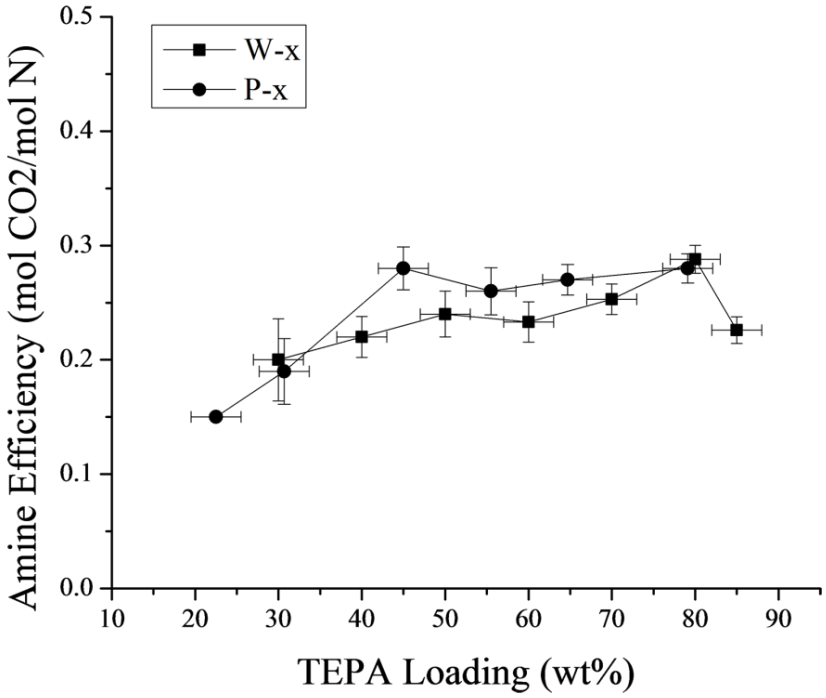

Figure 3.10: Amine Efficiency (mole of CO_2 adsorbed per mole of N) of the P-x and W-x Sorbents as a Function of TEPA Content.

Table 3.2 Summary of CO_2 Adsorption Performance of W-x and P-x Sorbents.

Sorbent	TEPA (wt%)	Kinetics (time to reach 90% capacity, min)	Capacity (mmol/g)	Amine Efficiency (mol CO_2/mol N)	Theo. Max. Adsorp. Capacity[a] (mmol/g)
W-30	30	5.4	1.6	0.20	4.0
W-40	40	3.3	2.3	0.22	5.3
W-50	50	7.1	3.2	0.24	6.6
W-60	60	6.2	3.7	0.23	7.9
W-70	70	8.3	4.7	0.25	9.2
W-80	80	6.3	6.1	0.29	10
W-85	85	8.3	5.1	0.23	11
P-30	23	4.8	0.9	0.15	3.0
P-40	31	3.0	1.6	0.19	4.1
P-50	45	3.1	3.3	0.28	5.9
P-60	55	5.3	3.9	0.26	7.3
P-70	65	4.3	4.7	0.27	8.6
P-80	79	6.6	5.8	0.28	10

[a] *Theoretical Maximum Adsorption Capacity [mmol/g] = (TEPA wt%)/189.3 [TEPA MW]*5 [mol N per mol TEPA]*10*0.5 [stoichiometric ratio possible under dry conditions, 1 mol CO_2 per 2 mol N].*

3.3.3 Distribution of Amine on Aerogel Support

Prior to the data collection and analysis of the P-x and W-x sorbents, it was hypothesized that the evaporative precipitation method would modify aerogel with TEPA as shown by the cartoon in Figure 3.11. The aerogel is first exposed to the saturated TEPA/n-hexane solution, Figure 3.11(a). As n-hexane is evaporated from the aerogel/hexane/TEPA slurry, TEPA will precipitate due to the limited solubility (~40 mg/mL) of TEPA in n-hexane as shown in Figure 3.11(b). The precipitated TEPA will then adsorb onto the hydrophilic aerogel surface (Figure 3.11(c)). With continued cycles of saturated TEPA/n-hexane solution addition and evaporation of n-hexane, the expected

outcome was a TEPA film covering the surface of the chain-like network of aerogel pores. Hydrophilic MT-1100 aerogel has a surface area of approximately 822 m^2/g. If a hypothetical uniform covering existed for a 60 wt% TEPA sorbent, the layer of this thickness would be roughly 2 nm. Such a thin film TEPA coating on the aerogel surface should result in much faster kinetics, higher capacities, and greater amine efficiencies (Heydari-gorji, Yang, et al., 2011; Qi et al., 2011). However, the data showed a near negligible degree of improvement in performance of the samples prepared by the evaporative precipitation compared to the wet impregnation method.

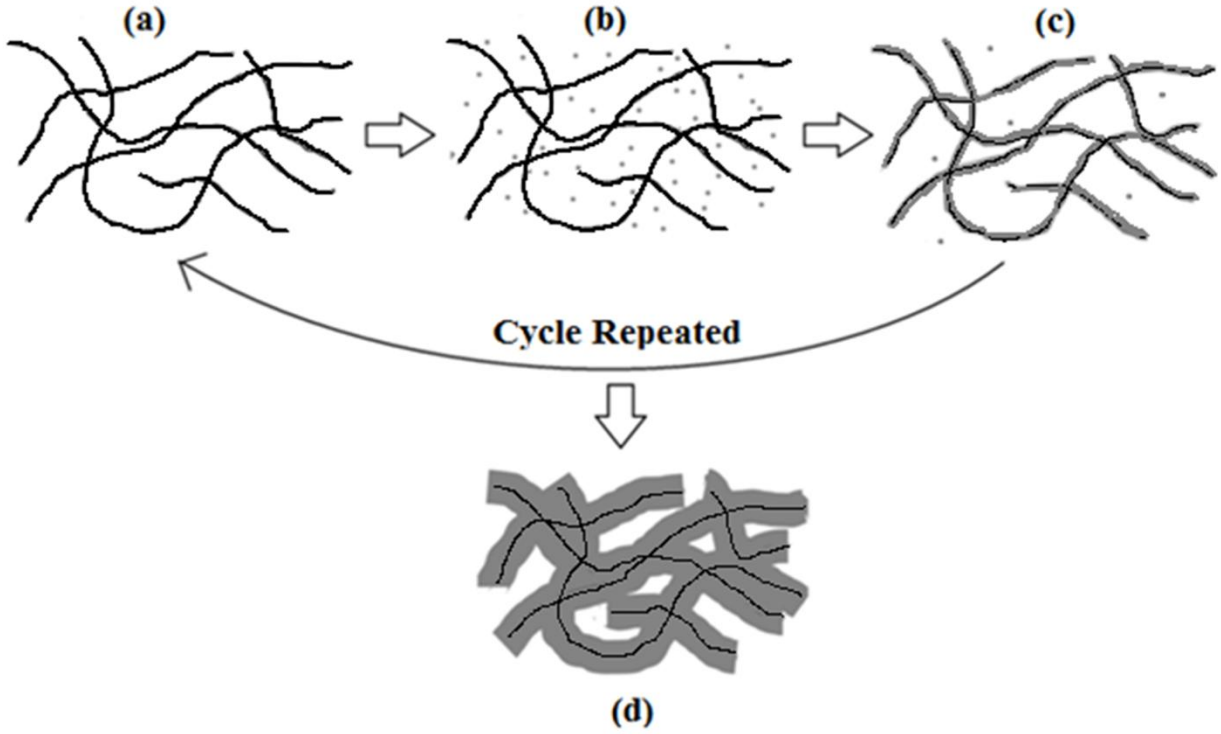

Figure 3.11: Hypothesized Mechanism of the Evaporative Precipitation Method. Aerogel Pore Surfaces are shown in Black, TEPA shown in Gray.

Based on these finding, it appears that the evaporative precipitation method is not effectively distributing the TEPA onto the silica aerogel surface as expected, but rather forming a distribution similar to that prepared by the wet impregnation method. This

suggests that the distribution of TEPA within aerogel is nearly independent of the route of synthesis. A reason for such a result is possibly a free energy thermodynamic limitation. Once the TEPA immerses and adsorbs onto the silica aerogel surface, the TEPA could be consolidating within the aerogel pores to relieve the surface tension, resulting in freckle-like random inclusions and larger film thicknesses as seen in the TEM images. Furthermore, the wettability of TEPA on the silica aerogel surface may be too poor to result in such a thin uniform film coating regardless of the method. Therefore the final morphology of the amine layer is not governed by the method of deposition into the pore space but rather by the thermodynamic stability of the two phase system, i.e., substrate surface chemistry, aminopolymer surface tension, amino polymer structure & chemistry, etc.

3.4 Conclusions

Impregnated TEPA/aerogel-silica sorbents were synthesized by two different methods. Both methods give essentially same amino polymer distributions on the support. These results show that the method of amine modification has little influence on how TEPA is dispersed within the aerogel framework. This suggests that a thermodynamic limitation exists for the liquid/solid two component system. TEPA consolidates within the structure and disperses with an amine distribution that results in the lowest free energy state, independent of how the TEPA was deposited. However, the thermodynamics of this system could change if one were to change the surface chemistry of the support, surface tension of the liquid amino polymer, and/or the morphology of the pore network which could lead to more efficient distributions and therefore enhanced CO_2 adsorption performance.

CHAPTER 4

SYNTHESIS AND CARBON DIOXIDE SORPTION PROPERTIES OF AMINE GRAFTED SILICA AEROGEL SORBENTS

4.1 Introduction

Afore mentioned in Section 1.3, two methods of amine modification are either grafting the amine to the support through a covalent attachment to the surface, or are impregnation within the pore volume and reside by weak physical molecular forces. As seen in Chapter 3 and 4, the latter method of modification possesses competitive adsorption performances with high CO_2 adsorption capacities and fast kinetics (Heydari-gorji, Yang, et al., 2011; Y. Liu et al., 2010; Qi et al., 2011; Xingrui Wang et al., 2011; Ming Bo Yue et al., 2008). Impregnated sorbents however have pore cyclic stability as seen in Figure 1.4 because of amine evaporation due to the absence of any surface anchoring (Heydari-gorji, Belmabkhout, et al., 2011; Qi et al., 2011, 2012; J. Wang et al., 2012; Xingrui Wang et al., 2011).

In regards to grafted (i.e., covalently bonded) amine based sorbents, these materials show considerably greater thermal stability during adsorption and regeneration cycles (Begag et al., 2013; Sayari & Belmabkhout, 2010; Serna-Guerrero, Belmabkhout, & Sayari, 2010a; Serna-guerrero, Belmabkhout, & Sayari, 2011). However, these amine grafted materials generally do not achieve the high adsorption capacities reached by impregnated samples primarily due to the low amount of nitrogen content grafted per unit weight of sorbent (Figure 1.6 & 1.8). The most common and simplistic method of grafting amines to silica surfaces is using alkylamine substituted trialkoxysilanes where the bond is formed by the condensation of the alkoxy groups to surface silanols of the

silica support (Brinker & Scherer, 1990). The alkylamine trialkoxysilanes generally do not carry a large number of amine units (typically 1 to 3 amine units per silane), and therefore making it difficult to achieve a large nitrogen content. In order to counter this dilemma, a number of research groups have attempted to use high surface area silica supports to attain higher nitrogen containing materials for greater CO_2 adsorption capacities (Figure 1.7). Of the plethora of silica supports from ordered mesoporous silica (OMS) to fumed silica being investigated, particulate aerogels show some promising results using both co-condensation and post-gel grafting methods.

Wörmeyer, Alnaief, & Smirnova, (2012) investigated both supercritical fluid dried co-condensed and post-modified aerogels using tetramethylorthosilicate as the main silica precursor and a mono-amine silane. At 0 ^{o}C with pure CO_2, the co-condensation gels obtained a CO_2 adsorption capacity of roughly 1.1 mmol/g and the post-functionalized gels about 1.8 mmol/g. Begag et al., (2013) using a co-condensation method utilizing methyltrimethoxysilane (MTMS) and a aminoalkyltrialkoxysilane as precursors prepared a supercritical fluid dried amine functionalized aerogel and obtained a capacity of approximately 2.4 mmol/g under a humid 15% CO_2/6% O_2/N_2 gas feed at 40 ^{o}C. The sample also showed excellent cyclic stability for over 2000 cycles. Cui, Cheng, Shen, Fan, & Russell, (2011) prepared a supercritical fluid dried mono-amine functionalized aerogel using a post-modification method and reported an adsorption capacity of 1.95 and 6.97 mmol/g with a humidified 15% CO_2 gas feed at 25 ^{o}C. However, the increase in capacity observed for the amine functionalized aerogel under humid conditions seemed overly large, as was the reported capacity of 2.21 mmol/g observed for aerogel without any amine modification.

The above co-condensed or post-modified amine-aerogel sorbents were prepared by a supercritical drying step. However, in this chapter the favorable textural properties of silica aerogels are utilized using the Cabot commercial silica aerogels prepared through ambient drying methods. Therefore, the primary objective of Chapter 4 is to create an amine grafted aerogel based on commercially available dried Cabot aerogels and investigate the CO_2 adsorption properties under a variety of synthesis conditions to reveal their potential as a promising sorbent for CO_2 capture.

4.2 Experimental Methods

All chemicals were purchased from Aldrich unless otherwise stated. Hexane (anhydrous, 99.8%), and toluene (anhydrous, 99.8%). The mono, di, and tri-amine silanes used for grafting are (3-aminopropyl)trimethoxysilane (mono), N-[3-(trimethoxysilyl)propyl]ethylenediamine (di), and N^1-(3-trimethoxysilylpropyl) diethylenetriamine (tri) (see Figure 1.5). Particulate aerogel (MT-1100 Nanogel, particle size of 10 μm respectively) was obtained from Cabot Corp.

4.2.1 Synthesis of Amine Grafted Aerogel

Prior to aerogel modification with amines, the hydrophobic MT-1100 aerogels were heat treated in air in a furnace at 400 ^oC for 8 hrs to oxidize the organic moieties to form surface hydroxyl groups for silane grafting. These aerogels are re-named MT400. The amine anhydrous (dry) grafting was performed by a common functionalization technique but executed in a systematic method for optimization. For dry grafting, a specific amount of MT400 was activated by placing in an oven at 150 ^oC for 2 hrs to remove any adsorbed species, and then placed in a teflon flask with a specified volume of toluene. After mixing for 10 min, a solution of toluene and aminosilane (e.g. tri, di, or

mono-amine silane) was prepared and added to the teflon flask containing the MT400/toluene mixture. The flask was then capped and placed in an oil bath at a designated temperature for 18 hrs. The contents were then filtered and washed with 100 mL of toluene twice and 100 mL of n-hexane once. Filtered samples were then dried in flowing argon at 150 ^{o}C for 2 hrs.

With regard to hydrous (wet) grafting, the method is similar to the approach of Liu et al., (1998). 1.0 g of activated MT400 was placed in a teflon flask with 75 mL of toluene and mixed for 10 min. Then a specific amount of water was added drop-wise to the aerogel/toluene mixture and vigorously stirred for 3 hrs at 80 ^{o}C. A solution composed of 2.0 g of tri-amine and 50 mL of toluene was added into the flask and then placed in an oil bath at a selected temperature for 18 hrs. Only tri-amine was used for the wet grafting experiments since this was the best performing amine under dry conditions. The contents were then filtered, washed, and dried as previously. Samples prepared through the hydrous method are labeled as X/Y where "X" represents the amount of water added in mg/g of silica and "Y" represents the synthesis temperature during grafting in ^{o}C.

4.2.2 Sorbent Characterization

Nitrogen adsorption-desorption isotherms were obtained on a Micromeritics ASAP 2020 surface area and porosity analyzer at 77K for textural characteristics. The Brunauer-Emmett-Teller (BET) method and the Barret-Joyner-Halenda (BJH) model of the adsorption isotherm were used to calculate the surface area, the pore size distribution, and pore volume. CHN elemental analysis was performed on a Perkin Elmer 2400 Elemental Analyzer to obtain the amount of nitrogen mass percentage. Samples were

loaded into capsules in 3-4 mg increments. The combustion temperature set-point was 924 ^{o}C and the reduction temperature was 624 ^{o}C.

4.2.3 Carbon Dioxide Adsorption Analysis

The CO_2 adsorption performance of the sorbents was determined using a Thermo Cahn D-101 electro-microbalance as described in Section 2.2.3. For a typical adsorption analysis, about 10 mg of sample was placed in a stainless steel sample pan and activated at 100 ^{o}C at 1 atm for 30 min under high purity Argon (99.99%) at 100 mL/min to remove unwanted adsorbed species (e.g., H_2O, CO_2, remaining solvent). Sorbents were then cooled to 25 ^{o}C and pure CO_2 (99.99%) was then introduced for 1 hr at 1 atm at a flow rate of 100 mL/min. The CO_2 equilibrium adsorption capacity was determined by the weight gained during the 1 hour adsorption period. Isotherms were obtained using the microbalance with equivalent samples sizes (10 mg) and performed by changing the partial pressure of the CO_2 feed stream in Argon gas. Partial pressures ranged from 0.05 to 1 bar with the total pressure never exceeding 1 bar. The samples were given 1 hour to reach equilibrium at each partial pressure. Cyclic stability tests were performed on a TA Instruments SDT-Q600 analyzer. Sorbents were first activated by heating to 100 ^{o}C at 100mL Argon/min for 30 min and then cooled to 30 ^{o}C. Then the feed gas was switched to a 100% CO_2 gas at 100 mL/min for 15 min for adsorption. Thereafter, the system was heated to 80 ^{o}C for 30 min with 100% Argon. This process was continued for 100 cycles.

4.3 Results and Discussion

4.3.1 Effect of Amino Silane

Initial experiments consisted of a comparative test among the mono, di, and tri-amine silanes. Figure 4.1 shows the CO_2 adsorption capacities of the mono, di, and tri-

amine silane grafted silica aerogels at three adsorption temperatures. The mono, di, and tri-amine aerogel were prepared at 80 ^{o}C, a 2:1 silane to silica weight ratio, and a silane concentration of 16 mg/mL. The highest adsorption capacity was achieved by the tri-amine when the adsorption temperature was 25 ^{o}C. The lowest adsorption capacity was reached with the mono-amino silane at 65 ^{o}C. The increasing capacity trend with decreasing temperature for all the aminosilanes is typical behavior for an exothermic chemisorption process such as the present one (Aziz et al., 2011; Begag et al., 2013). The rising capacity with increasing amount of amine units per silane (i.e. tri>di>mono) is simply due to the increasing amount of nitrogen content grafted as a result of the higher number of amine units, as shown in Figure 4.2. The tri-amine achieves a nitrogen loading of 4.13 mmol N/g whereas the mono-amine reached 1.59 mmol N/g. Since the amine efficiency (mol CO_2/mol N) decreases only slightly for increasing amine units, the tri-amine achieves the highest capacity. The slight decrease in amine efficiency is suggested to be due to steric hindrance of the larger chain molecular structure as the aminosilane is changed from mono to di to tri. The long chain length of the tri-amine silane can possibly block the secondary amine locations on its tether and therefore inhibit access for capture (Hiyoshi et al., 2005).

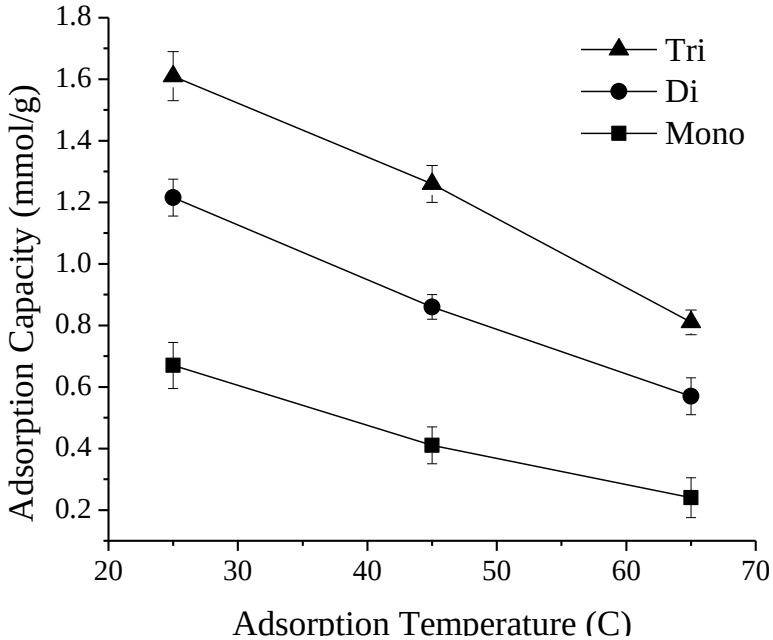

Figure 4.1: Adsorption Capacity of the Mono, Di, and Tri-amine Grafted Aerogel as a Function of Adsorption Temperature (Adsorption Conditions: 25 ^{o}C, 100% CO_2, 1 bar).

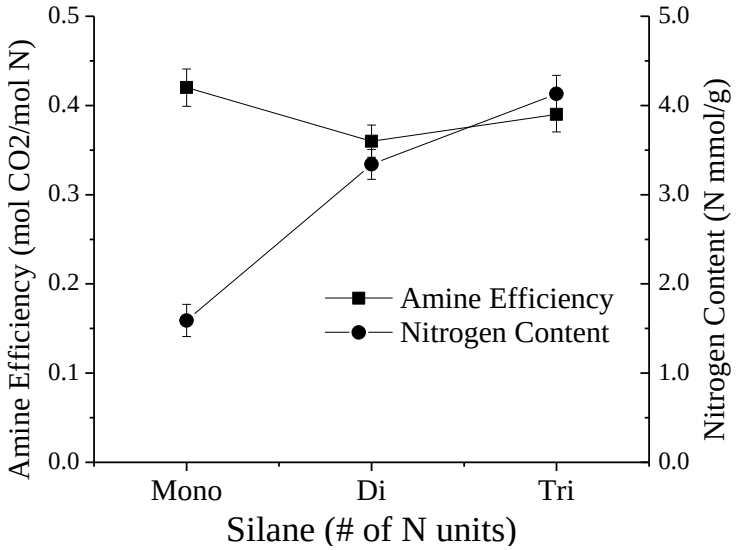

Figure 4.2: The Measured Nitrogen Content and Calculated Amine Efficiencies of Mono, Di, and Tri-amine Grafted Aerogel from the Adsorption Capacity Obtained at 25 ^{o}C.

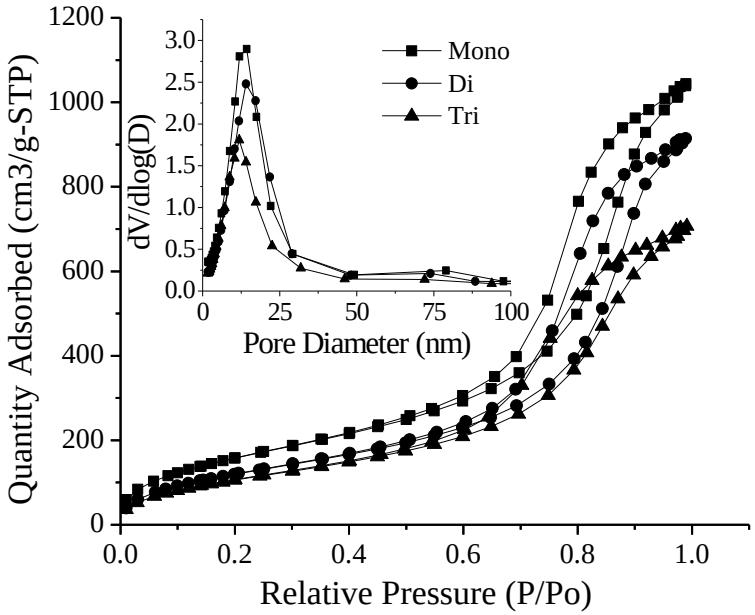

Figure 4.3: Nitrogen Adsorption Isotherms and Pore Size Distributions of the Mono, Di, and Tri-amine Grafted Aerogels.

Figure 4.3 shows the effects of anhydrous (dry) amine grafting on the textural properties of the functionalized aerogel structure. The MT400, after the heat treatment at 400 ^{o}C prior to grafting, has a pore volume of 4.2 cm^3/g, surface area of 767 m^2/g, and a pore diameter of approximately 42.7 nm. After grafting, the mono, di, and tri-amine functionalized aerogels show a much lower pore volume and pore diameter, as summarized in Table 4.1. As shown in Figure 4.3, the pore size distribution maintained a sharp peak while the N_2 adsorption isotherms maintain more of a type IV isotherm like the original type IV with H1 type hysteresis of the unmodified calcined aerogel (Linneen et al., 2013). Such a large decrease in pore volume and surface area is due primarily to the shrinkage of the gels after drying the amine-grafted aerogel. The capillary force coupled with the weak integrity of the aerogel structure, lead to shrinkage during the drying of the gels after the washing step. Furthermore, the increasing alkylamine length

of the silane also appears to decrease the porosity of the final gel as was reported elsewhere (Hiyoshi et al., 2005).

Table 4.1: Summary of Textural and Amine Properties of the Unmodified and Mono, Di, and Tri-amine Grafted Silica Aerogels

Sample	Vp (cm3/g)	SA (m2/g)	Dp (nm)	Grafting Density (tether/nm^2)
MT400	4.2	767	42.7	-
mono	1.62	610	14.3	1.19
di	1.42	471	14.0	1.25
tri	1.10	417	10.5	1.03

4.3.2 Effect of Anhydrous Grafting Conditions

Because the tri-amine performed the best in terms of adsorption capacity, a systematic set of experiments was then carried out using the tri-amine to optimize the adsorption capacity by modifying synthesis variables. Figure 4.4 shows the effect of synthesis temperature ranging from 70 to 110 ^{o}C. The silane concentration and silica to silane mass ratio were held at 16 mg/mL and 2:1. The optimum temperature for dry grafting was found to be 95 ^{o}C with an adsorption capacity of 1.76 mmol of CO_2/g. Though an optimum was reached, the data did not change by a significant amount from the lowest capacity reached at 70 ^{o}C (1.47 mmol/g). The deviation that was observed appears to be primarily due to the amount of nitrogen content grafted which, like the adsorption capacity, follows a similar trend reaching a maximum at 95 ^{o}C as seen in Figure 4.4. This suggests that the temperature of the grafting primarily affects the degree of silylation but to a low degree since the deviation in adsorption capacity was small between temperatures. If, however, the nitrogen loading remained constant under varied temperature conditions while the adsorption capacity continued to show an optimum, it

would suggest that temperature influences the amine orientation and distribution of the silane throughout the silica surface and therefore influences the CO_2 adsorption mechanism. But that was not observed here.

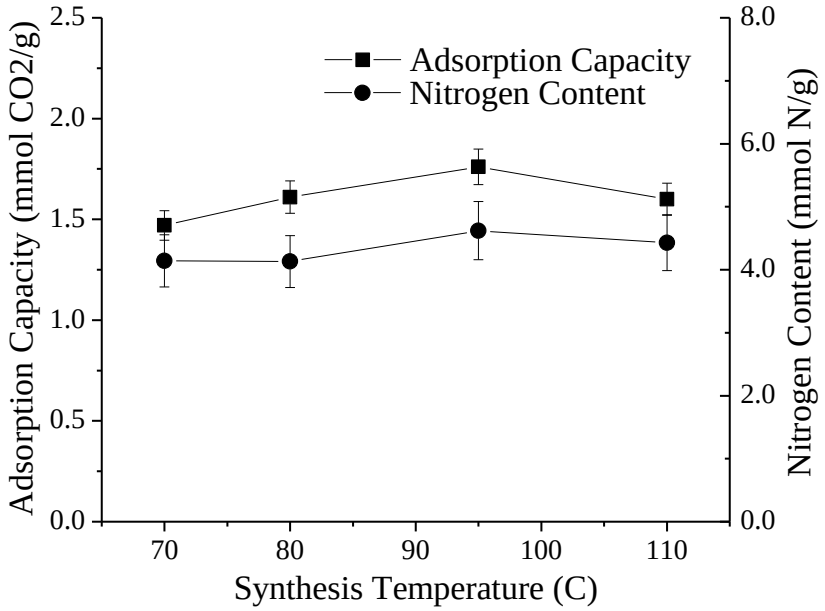

Figure 4.4: Adsorption Capacity and Nitrogen Content of Tri-amine Grafted Aerogel as a Function of Synthesis Temperature. (Adsorption Conditions: 25 ^{o}C, 100% CO_2, 1 bar)

At the optimum grafting temperature of 95 ^{o}C, the silica to silane mass ratio for grafting was varied from 0.5:1 to 4:1, while the concentration of aminosilane solution utilized was held at 16 mg/mL as before. As seen from Figure 4.5, the data reaches a plateau at a ratio of 2:1. Beyond this point it appears the excess amount of silane has little influence on silylation and adsorption capacity. The rise in capacity up to a silica:silane ratio of 2:1 is the result of an excess amount of the silane reagent that stoichiometrically favors a higher grafted product yield. The similar trends in both grafting degree and adsorption capacity again suggest that the enhanced adsorption performance is primarily an effect of the amount of nitrogen content grafted. However, within the ranges tested for

both temperature and mass ratio, the latter appears to affect the degree of grafting more significantly than the synthesis temperature.

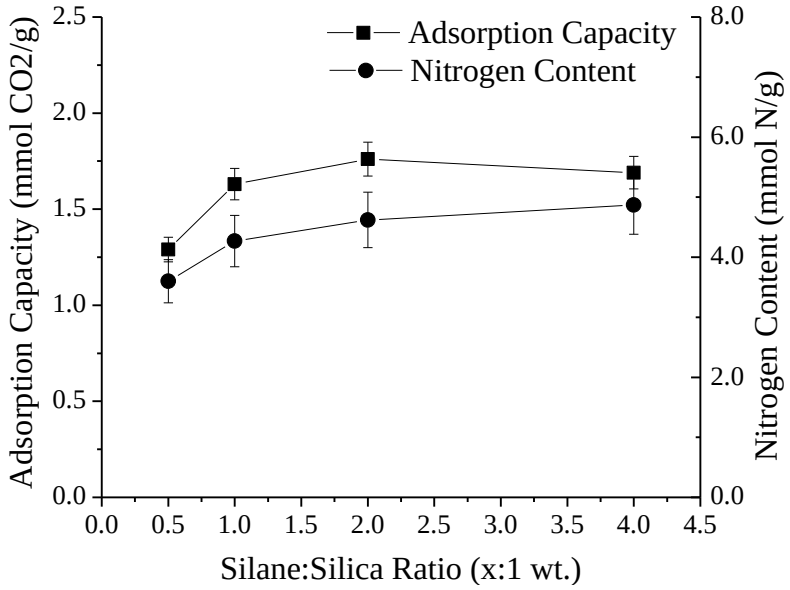

Figure 4.5: Adsorption Capacity and Nitrogen Content of Tri-amine Grafted Aerogel as a Function of Silane:Silica Ratio. (Adsorption Conditions: 25 ^{o}C, 100% CO_2, 1 bar)

To determine the effect of the silane concentration in the toluene solution on the grafting results, the silane concentration was varied from 8 to 27 mg/mL where the synthesis temperature and silane:silica mass ratio were held constant at 95 ^{o}C and 2:1. Figure 4.6 reveals that the silane concentration does not significantly affect the degree of grafting nor the adsorption capacity. It was hypothesized that the higher concentration of silane would lead to a higher degree of grafting due to the greater driving force for the silane to infiltrate the aerogel pore space. Previous studies using other silica supports have shown that functionalization can be affected by pore diameter and therefore the degree of silylation on the silica surface could be a diffusion controlled process (F.-Y. Chang et al., 2009; Harlick & Sayari, 2006; Zeleňák et al., 2008). In this case however, the aerogel's large pore diameter (~40nm) and interconnectivity appears to facilitate the

transport of the silane throughout the entire particle so the grafting process is not diffusionally limited.

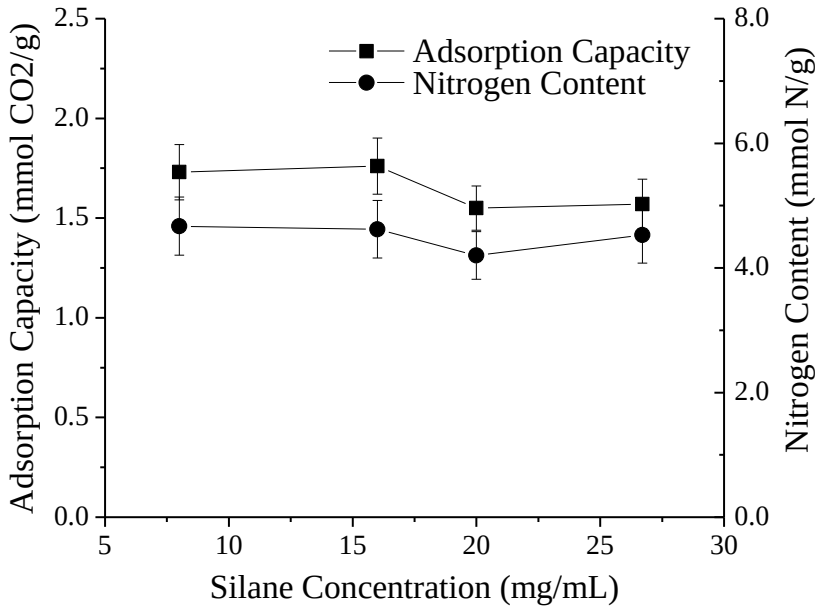

Figure 4.6: Adsorption Capacity and Nitrogen Content of Tri-amine Grafted Aerogel as a Function of Silane Concentration. (Adsorption Conditions: 25 ^{o}C, 100% CO_2, 1 bar).

4.3.3 Effect of Hydrous Grafting Conditions

For dry grafting, the best conditions for functionalization appear to be using the tri-amine with a silane:silica ratio at or above 2:1 and a temperature of 95 ^{o}C. As mentioned above the silane concentration had negligible influence. Therefore for hydrous grafting, the conditions were set at a silane:silica ratio of 2:1 and a silane concentration of 16 mg/mL. In addition to varying the amount of water added, the synthesis temperature was varied due to its clear effect on performance for other mesoporous hydrous grafted materials (Harlick & Sayari, 2007). The idea of grafting silanes in the presence of small amounts of water has been performed on other silica supports (S. Kim et al., 2005; J. Liu et al., 1998; Serna-Guerrero, Belmabkhout, & Sayari, 2010b; Zheng et al., 2005). The

notably higher extent of silylation is suggested to be due to the polymerization of the silane in the presence of water adsorbed on the silica surface due to hydrolysis and condensation reactions of the alkoxy groups occurring concurrently with silane grafting to surface silanol groups.

Figure 4.7 shows the effects of water addition and synthesis temperature on the CO_2 adsorption capacity at 25 ^oC and 100% CO_2. The trends in the data obtained relative to amount of water added are similar to those obtained by Harlick & Sayari, (2007) who prepared a tri-amine functionalized pore-expanded MCM-41 under hydrous conditions. For both cases the synthesis temperature has a much greater effect on adsorption performance for hydrous grafting relative to anhydrous grafting. The presence and amount of water during changes in temperature has a greater influence on hydrolysis and condensation reaction rates relative to conditions where water is absent and therefore can lead to larger fluctuations in functionalization degree (Brinker & Scherer, 1990).

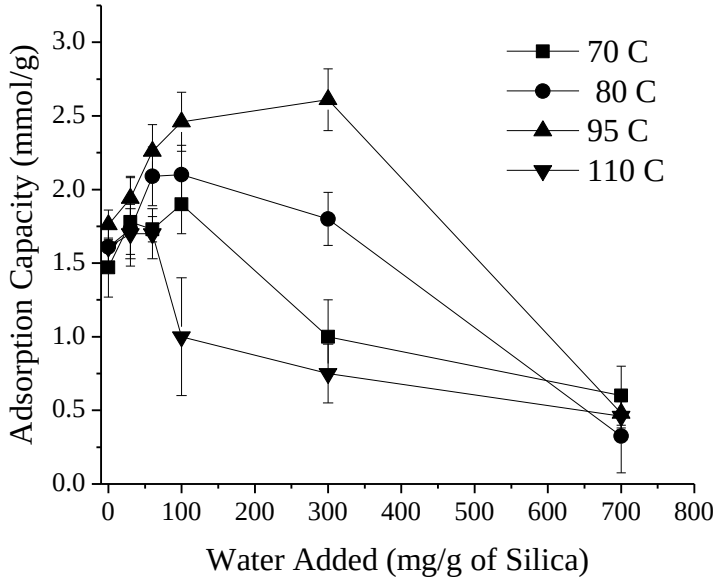

Figure 4.7: Adsorption Capacity of Sorbents Synthesized at Different Temperatures and Various Amount of Water. (Adsorption Conditions: 25 C^o, 100% CO_2, 1 bar).

The 300/95 sample (i.e. prepared with 300 mg water/g of silica and at 95 ^{o}C) achieved the best adsorption capacity of 2.61 mmol/g. Since all other samples (using different amounts of water) synthesized at 95 ^{o}C had higher capacities relative to those prepared at 70, 80, and 110 ^{o}C, it appears that for hydrous grafting the best temperature is 95 ^{o}C, the same as with dry grafting. The reason that the optimum hydrous synthesis temperature is around 95 ^{o}C is most likely due to the silane/water chemistry reaction rates. In the presence of water, a change in temperature is extremely influential on the relative hydrolysis and condensation rates of the silanes(Brinker & Scherer, 1990). It is believed that at a temperature of 95 ^{o}C, the rates of condensation and hydrolysis are such that a polymerized layer inside the aerogel pore space is formed that is the most favorable for CO_2 capture.

There also appears to be an optimum amount of water for each synthesis temperature. Figure 4.8 and 4.9 illustrate a possible cause for such an optimum to exist. As more water is added, the nitrogen content (Figure 4.9) increases and then plateaus to ~7.5 mmol N/g. This behavior is a result of the higher degree of polymerization due to greater amounts water present for hydrolysis and condensation. However, by looking at the changes in surface area and pore volume (Figure 4.8) of the 30/95, 60/95, 100/95, 300/95, and 700/95 samples, increasing water addition dramatically reduces the surface area and pore volume to near negligible values. This suggests that increased addition of water causes a pore plugging effect due to polymerization occurring within the pore space. These pockets or large layers of adsorbed water at the silica surface become localized polymerization points once the silane is introduced, causing an obstruction in the pores and therefore reducing the availability of amine adsorption sites, which reduces

the adsorption capacity. This type of behavior is similar to what has been observed for amine impregnated materials (Linneen et al., 2013; Son et al., 2008; Xiaochun Xu et al., 2002).

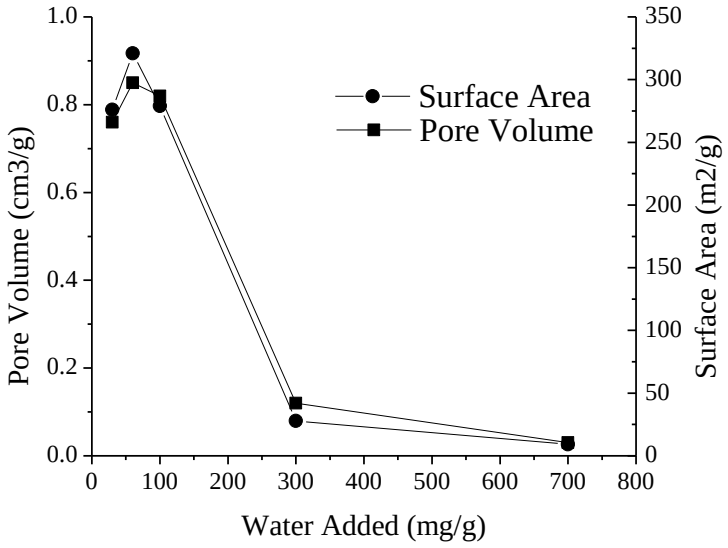

Figure 4.8: The Pore Volume and Surface Area Relative to Amount of Water Added for Tri-amine Grafted Samples Synthesized at 95 ^{o}C

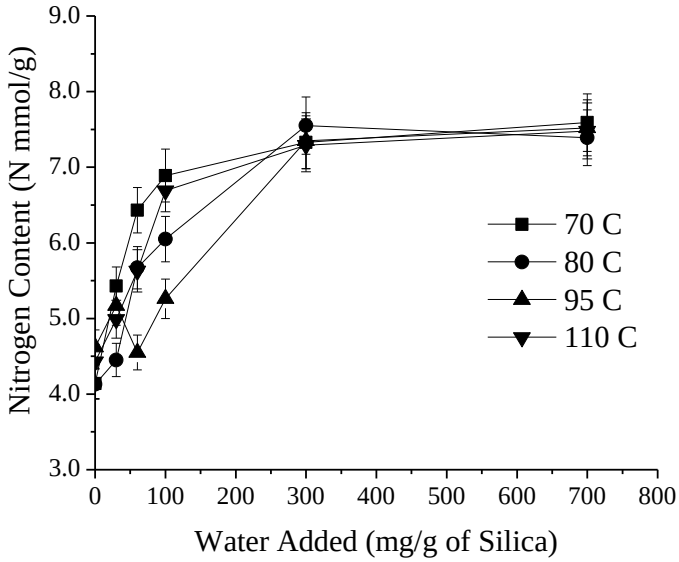

Figure 4.9: The Nitrogen Content of Tri-amine Grafted Samples Synthesized under Hydrous Conditions as a Function of the Amount of Water Addition.

The highest adsorption capacity sample, 300/95, possessed a very low surface area and pore volume of these gels synthesized at 95 ^{o}C. Figure 4.10, illustrating the amine efficiencies as a function of water addition, reveals that the 300/95 sample did not have the highest amine efficiency, but the 60/95 sample reached the highest with a near maximum theoretical stoichiometric amine efficiency of 0.50 mol CO_2/ mol N. Specifically for the 300/95, this indicates the presence of a diffusional limitation possibly due to plugging that is present with amine impregnated samples as mentioned before. However, the reason the 300/95 sample achieved a higher capacity was because it possessed a higher amine content (7.5 mmol N/g) when compared to the 60/95 sample (4.5 mmol N/g). Therefore the 300/95 sample achieved the best balance between N content and a favorable polymerized silane microstructure that facilitates CO_2 transport allowing the majority of amine adsorption sites to be available for binding. Anything above or below this balance between water content and synthesis temperature either results in a low N content or a microstructure that reduces amine availability. The calculated tether densities from the 30/95 to 700/95 increased from 1.15 to 1.88 tethers/nm^2. However this calculation assumes a grafting homogenous layer across the surface of the aerogel whereas, in all probability, polymerization points are occurring creating a large degree of heterogeneity.

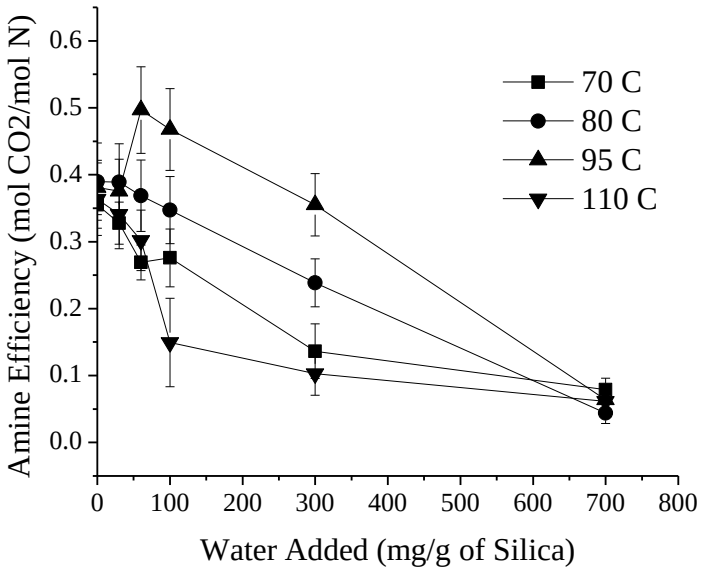

Figure 4.10: The Amine Efficiency of Tri-amine Grafted Samples Synthesized under Hydrous Conditions as a Function of the Amount of Water Addition.

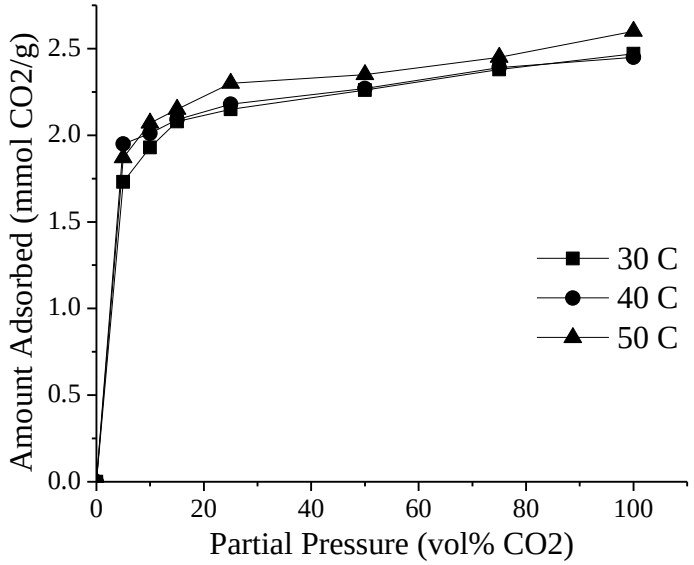

Figure 4.11: CO_2 Adsorption Isotherms of the 300/95 Tri-amine Grafted Aerogel at 30, 40, and 50 ^oC, (Isotherms Done by Binary Mixture of CO_2 and Argon)

Three isotherms at 30, 40, and 50 ^oC were obtained for the 300/95 sample (Figure 4.11) and the data reveals a sharp increase in adsorption with increasing CO_2 partial pressure, which is typical for chemisorbents. At 10% CO_2 the amount adsorbed was 1.93, 2.01, and 2.07 mmol/g at 30, 40, and 50 ^oC. Furthermore, an uncharacteristically slight

increase in adsorption amount with increasing temperature occurs which is not typical for grafted amine materials as seen in Figure 4.1 and by other works (Aziz et al., 2011), but is typical of impregnated materials. Amine impregnated materials commonly possess an optimum operating temperature, about ~75 ^{o}C, which is a result of the balance between the thermodynamic adsorption equilibrium and the diffusion of CO_2 through the impregnated amine polymer. Higher temperatures lead to higher rates of CO_2 transport through the viscous polymer and therefore reaching more amine binding sites, but then adsorption falls due to the thermodynamic equilibrium shift as the temperature is raised. In this case, it further validates the hypothesis that an amine siliceous polymer is developed within the pore space of the aerogel because of water agglomerates within the pore volume causing the observed impregnated-like behavior. Note that if a prolonged amount of time were allowed for true equilibrium to be reached, the 30 ^{o}C isotherm would have shown greater adsorption than the 40 and 50 ^{o}C isotherms since during the 30 ^{o}C experiment the sample still showed a slow rate of adsorption after a few hours (data not shown). But due to the apparent plugging, the 50 ^{o}C sample achieved the highest adsorption within the 1 hour set equilibration period because of the increased diffusion thereby reaching more adsorption sites. Table 4.2 summarizes the best results obtained in this study and compares their performance to other similar grafted silica supports sorbents.

Amine impregnated samples also, due to the absence of any covalent bond to the support, have poor cyclic stability as mentioned earlier. Amine functionalized materials however are much more thermally stable due to the covalent bond present (Sayari & Belmabkhout, 2010; Serna-guerrero et al., 2011). Figure 4.12 and 4.13 show the cyclic

stability of the 300/95 sample and a tetraethylenepentamine (TEPA) impregnated aerogel on an equivalent MT-1100 aerogel support calcined at 400 ^{o}C (Linneen et al., 2013). The loading of TEPA was 70 wt%. The cyclic test for the 300/95 sample was performed by adsorbing 100% CO_2 at 30 ^{o}C for 15 min and regenerating at 80 ^{o}C for 30 min with 100% Argon. The same cyclic procedure was performed for the TEPA impregnated aerogel except that the adsorption temperature was 75 ^{o}C since this was the optimum temperature tested (Linneen et al., 2013). For both samples the working capacity (i.e., the adsorption capacity reached after regeneration) was lower than the capacities given above (see Figure 4.7) due to the shorter time period of adsorption (15 min versus 1 hr) between the two tests. Table 4.2 summarizes the results and other grafted materials prepared by similar liquid phases methods.

Table 4.2 Summary of results compared to other reported amine grafted siliceous supports

Support	Type	Amine (mmol/g)	Ads. Temp. (C)	Ads. Pressure (bar)	CO_2 Conc (mol%)	Dry Ads. Capacity (mmol/g)	Source
Aerogel (dry graft)	Mono	1.59	25	1.0	100	0.67	This work
MCM-48	Mono	2.30	25	1.0	100	2.05	(H. Y. Huang et al., 2003)
AMSA	Mono	2.17	25	1.0	10	1.95	(Cui et al., 2011)
AMSA	Mono	2.17	50	1.0	10	1.19	(Cui et al., 2011)
SBA-15	Mono	3.92	25	0.1	100	1.80	(Hao et al., 2011)
Aerogel	Mono	3.62	0	1.0	100	1.80	(Wörmeyer et al., 2012)
MCM-48	Mono	2.28	25	1.0	100	1.68	(Gil et al., 2011)
Aerogel	Mono	5.00	40	0.15	100	1.80	(Begag et al., 2013)
Aerogel (dry graft)	Di	3.40	25	1.0	100	1.20	This work
HMS	Di	4.57	20	1.0	90	1.34	(Knowles, Delaney, & Chaffee, 2006)
SBA-15	Di	3.25	60	1.0	15	1.73	(F.-Y. Chang et al., 2009)
SBA-15	Di	5.16	45	1.0	100	1.86	(Olea et al., 2013)
Aerogel (dry graft)	Tri	4.13	25	1.0	100	1.64	This Work
Aerogel - 300/95	Tri	7.40	25	1.0	100	2.61	This Work
Boiled SBA-	Tri	5.80	60	1.0	15	1.80	(Hiyoshi et al.,

15							2005)
PE-MCM-41	Tri	7.95	25	1.0	5	2.65	(Harlick & Sayari, 2007)
PE-MCM-41	Tri	7.80	70	1.0	5	2.28	(Serna-Guerrero et al., 2010a)
SBA-15	Tri	5.21	45	1.0	100	1.75	(Calleja, Sanz, Arencibia, & Sanz-Pérez, 2011)
PE-MCM-41	Tri	4.33	50	1.0	100	2.43	(Sayari & Belmabkhout, 2010)
MSF	Tri	4.00	75	1.0	15	1.30	(S.-H. Liu et al., 2009)
SBA-15	Tri	3.68	60	1.0	15	2.41	(F.-Y. Chang et al., 2009)
Silica nanotubes	Tri	4.93	25	1.0	100	2.23	(Ko, Lee, Oh, & Choi, 2013)
PE-MCM-41	Tri	7.90	25	1.0	100	2.75	(Belmabkhout, Heymans, De Weireld, & Sayari, 2011)
Meso. Pore silica	Tri	5.18	25	1.0	100	1.74	(S.-N. Kim et al., 2008)

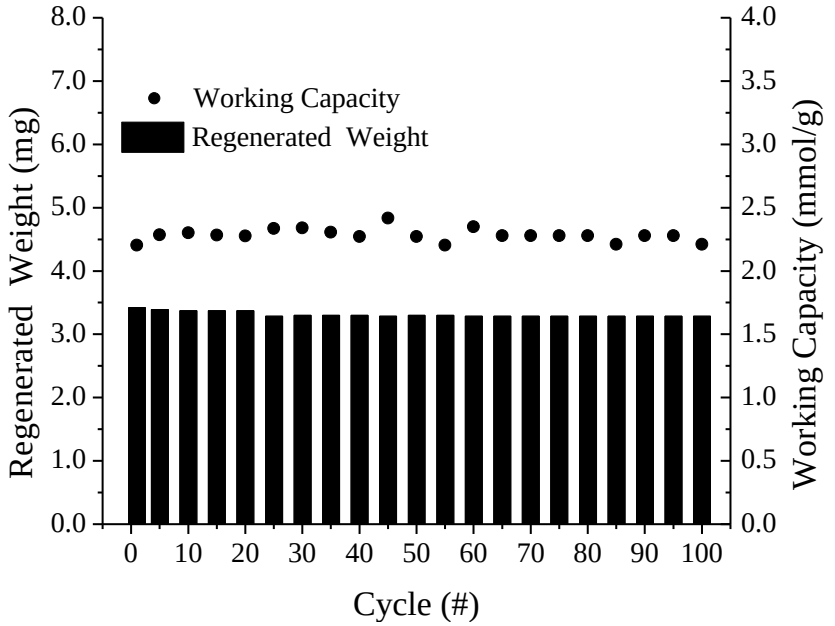

Figure 4.12: Cyclic Working Capacity and Absolute Regenerated Weight of the 300/95 Tri-amine Grafted Aerogel.

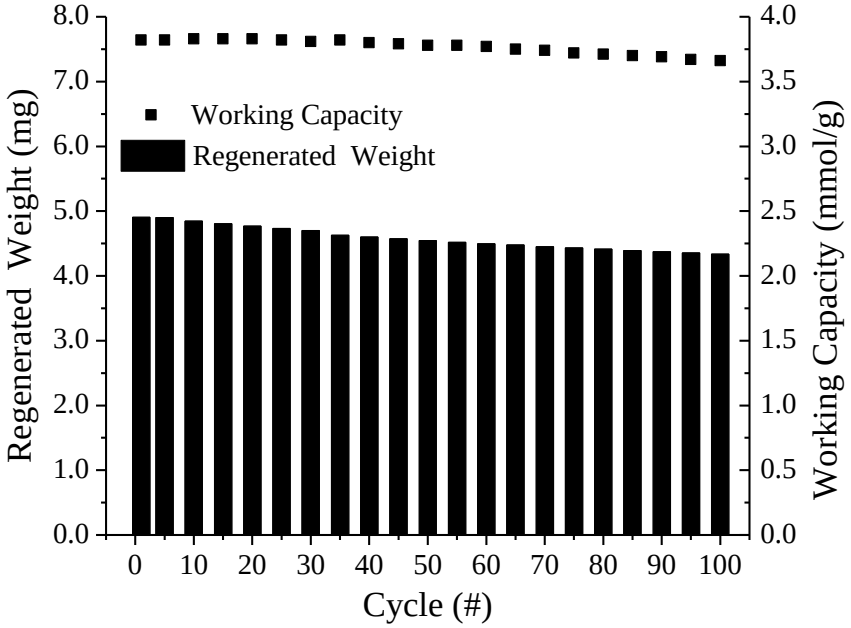

Figure 4.13: Cyclic Working Capacity and Absolute Regenerated Weight of a 70 wt% TEPA Impregnated Aerogel.

As suspected, the impregnated sample decreases in performance with each successive cycle due to TEPA evaporative losses. We believe that the decrease in

performance and loss in weight of the sample is primarily due to evaporative reasons rather than to any degradation route involving CO_2 because temperatures were kept well below 100 ^oC where CO_2 is known to degrade primary amines(Heydari-gorji & Sayari, 2012). The measured weight after each regeneration falls because of loss of amine leading to a decreasing adsorption capacity. The 300/95 sample, on the other hand, remains stable with negligible loss in mass after each regeneration showing a steady adsorption capacity of approximately 2.30 mmol/g. Therefore, though the 300/95 sample appears to show large polymerized aminosilane agglomerates in the structure, these groups appear to be possess enough silane grafted to the surface to be stable under multiple regenerative cycles.

4.4 Conclusions

Mono, di, and tri-amine trialkoxysilanes were grafted to ambient dried particulate aerogels calcined at 400 ^oC. The tri-amine silane performed the best in terms of adsorption capacity due to the greater amount of nitrogen content grafted; the tri-amine was further investigated by changing synthesis variables for both hydrous and anhydrous grafting conditions. For dry conditions the optimum temperature and silane/silica ratio was 95 ^oC and 2:1. The concentration of the silane appeared to have little effect on the grafting degree and adsorption performance. For hydrous grafting, the optimum conditions appeared to be a synthesis temperature again of 95 ^oC and a water addition of 300 mg/g of silica (the 300/95 sample) achieving an adsorption capacity of 2.61 mmol/g with 100% CO_2 at 1 bar and 25 ^oC. Unlike the dry grafting, the adsorption performance as well as the degree of silylation was greatly affected by the grafting temperature. Increasing amounts of water additions were found to have a pore plugging effect similar

to amine impregnated sorbents. It is suggested that with more water added the relative size of adsorbed layers within the aerogel pore space grew and caused localized polymerization points for the silane, leading to decreases in pore volume, surface area, and amine availability for CO_2 adsorption. However, unlike amine impregnated sorbents, the hydrous grafted 300/95 sample showed excellent cyclic stability of 100 regenerative cycles revealing that the siliceous polymer did posses covalent attachment to the surface. Therefore this sorbent looks to have a greater potential for an industrial setting relative to the impregnated sorbents though the adsorption capacities are not competitive relative to other amine grafted materials.

CHAPTER 5

SYNTHESIS OF AMINE MODIFIED PARTICULATE SILICA AEROGELS BY ATOMIC LAYER DEPOSITION

5.1 Introduction

Mentioned in Chapter 1 was a special class of grafted materials prepared by surface polymerization of an amino precursor by a step-wise or *in situ* method. These techniques led to sorbents possessing larger amounts of N content while also possessing greater stability due to anchorage of the amino precursor on the surface where polymerization initiated. Another technique for modifying silica surfaces toward attaining a homogenous layer of organic materials is atomic layer deposition (ALD) of silanes. The deposition of silanes in the vapor phase on silica surfaces has been performed for many years dating back to the 1980's (Buzek & Rathousky, 1981; Jonsson, Olofsson, Malmqvist, & Ronnberg, 1985; Mittal & O'kane, 1976). In regards to ALD of amino silanes on metal oxide substrates, a number of groups have prepared a variety of amino functionalized materials for a number of applications including gas and liquid chromatography, electrochemistry, and biochemical transport (Basiuk & Chuiko, 1990; Haukka, Lakomaa, & Suntola, 1993; Jonsson et al., 1985; Mittal & O'kane, 1976).

Motivations to functionalize substrates by ALD as an alternative to liquid phase grafting are due to the inherent difficulties that are involved when solvents are introduced as a deposition medium. Difficulties include corrosion/structural damage to the substrate surface, non-uniformity of the silane deposited layer, and the poor control of the deposition rate which can be slow in liquid solvents (Mittal & O'kane, 1976). Drying procedures also can become quite laborious to preserve the substrate as can be seen for

the aerogels in Chapter 4 (Wikstrom, Mandenius, & Larsson, 1988). Atomic layer deposition therefore appears to be an efficient method to facilitate grafting for forming a uniform amino silane layer without detrimental effects to the aerogel substrate.

One of the first to graft amino silanes to oxide surfaces using ALD methods is Wikstrom, Mandenius, & Larsson, (1988) who successfully grafted AMP to a porous silica substrate for HPLC applications. They reached a N content of 0.58 mmol N/g at a deposition temperature of 150 ^{o}C leading to a surface tether concentration of 1.7 tethers/nm^2. Juvaste, Iiskola, & Pakkanen, (1999) grafted AMP to silica supports in preparation of catalyst carriers and achieved an N density of 2.0 N/nm^2. A nitrogen content of 1.0 mmol N/g, a density that is found in liquid phase grafting methods (Figure 1.8) but with improved homogeneity was reported in Ek, Iiskola, & Niinisto, (2003).

Ek, Iiskola, & Niinisto, (2003) conducted a thorough study of AMP grafting using trifunctional, bifunctional, and monofunctional AMP (i.e., they varied the number of alkoxy ligands available for surface grafting) on silica pretreated from 200 to 800 ^{o}C to reveal the effects on silanol density to grafting degree. They found that the lower heat treatment (i.e., 200 ^{o}C) led to the greatest N density for all types of AMP as a result of there being a greater presence of silanol functional groups for silane anchoring. However this relationship was not linear and suggested that the degree of grafting is not dependent on the total silanol content but more on the isolated silanol concentration, i.e., silanol's with no other neighboring silanols susceptible to hydrogen bonding. Furthermore, the functionality of the silane (e.g., mono, bi, tri) had a small impact on the grafting degree where the N density difference between the tri and mono-functional was only 0.2 N/nm^2 confirming the dependency of exclusively isolated silanols.

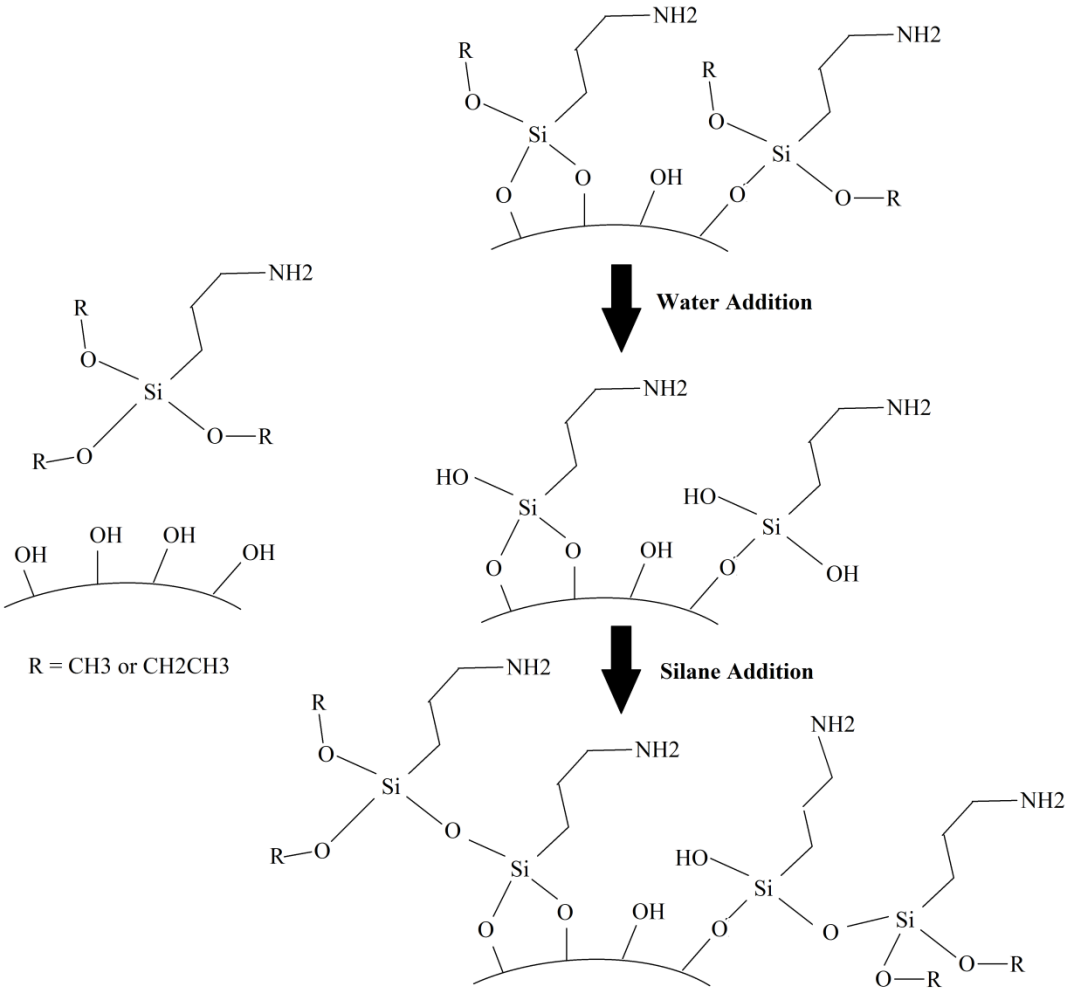

Figure 5.1: Illustration of the Cyclic ALD Process with Silane and Water Introductions.

Ek, Iiskola, & Niinisto, (2004), in order to increase amine density on a porous substrate surface, applied a step-wise growth method similar to those mentioned in Chapter 1 by sequentially reacting AMP and water after initial ALD of silane to the surface (Figure 5.1). During this procedure the alkoxy functional groups of AMP that did not anchor to the surface silanols deposited onto the surface during the first ALD are hydrolyzed during the water introduction. Then another ALD step of amino silanes is performed that condenses onto the previously hydrolyzed silanes. This process is continued until the step-wise reactions are terminated. They were able to achieve five

cycles of ALD reaching a N density of 3.0 N/nm^2. Ek et al., (2004) went further and repeated this procedure suing AEAPS, a di amino silane (Figure 1.5), and achieved an amine density of 5.5 N/nm^2, values significant enough to be a potentially good CO_2 adsorbent.

Therefore in Chapter 5, the objective is to apply the step-wise ALD method on hydrophilic particulate silica aerogels from Cabot Corp. The surface of the aerogel will undergo a series of sequential reactions with amino silanes and water to form a high amine density surface in order to be utilized as a CO_2 adsorbent, which to our knowledge would be the first amino silane ALD modified aerogel for CO_2 capture applications found in literature.

5.2 Experimental Methods

All chemicals were purchased from Aldrich unless otherwise stated. The mono-amine silane used for grafting are (3-aminopropyl)trimethoxysilane) (see Figure5.1). Particulate aerogel (MT-1100 Nanogel, particle size of 10 μm) was obtained from Cabot Corp.

5.2.1 Atomic Layer Deposition

The schematic of the ALD apparatus is shown in Figure 5.2. The aerogel was thermally pretreated at 400 ^oC for 8 hrs in air designated MT-400. Approximately 30 mg of MT-400 was placed in the sample pan and activated in two sequential steps. First the reactor chamber was heated to 150 ^oC with a purge flow of Argon at 100 mL/min for 30 min. Then holding this temperature the reactor chamber was vacuumed to less than 5 mbar and held for 30 min.

First silylation of the mono silane occurred right after activation. Before introduction of the silane reagent the vessel was completely purged with Argon and then

vacuumed to less than 5 mbar. This procedure was repeated for the water containing vessel. The temperature of the silane vessel was held at 130 ^{o}C and the heating tape (see (9) in Figure 5.2) was held at 150 ^{o}C to prevent condensation. With the reactor chamber at 5 mbar and 150 ^{o}C, the silane vessel valve was opened and allowed to react for 24 hrs. Once complete and the vessel valve shut the reactor chamber was purged with Ar for 30 min and then vacuumed for 30 min to rid the system of silane vapor. Water was then introduced by opening the valve of the water vessel. The vessel temperature was 25 ^{o}C and the time for reaction was maintained at 3 hrs. After water introduction the reactor chamber was purged and vacuumed as explained previously after silylation. The repeated introduction of silane and then water was repeated for a number of cycles. Samples were named G1, G2, and G3 where G1 is the first silylation step of the surface, and G2 and G3 are the second and third introduction of silane after water treatment.

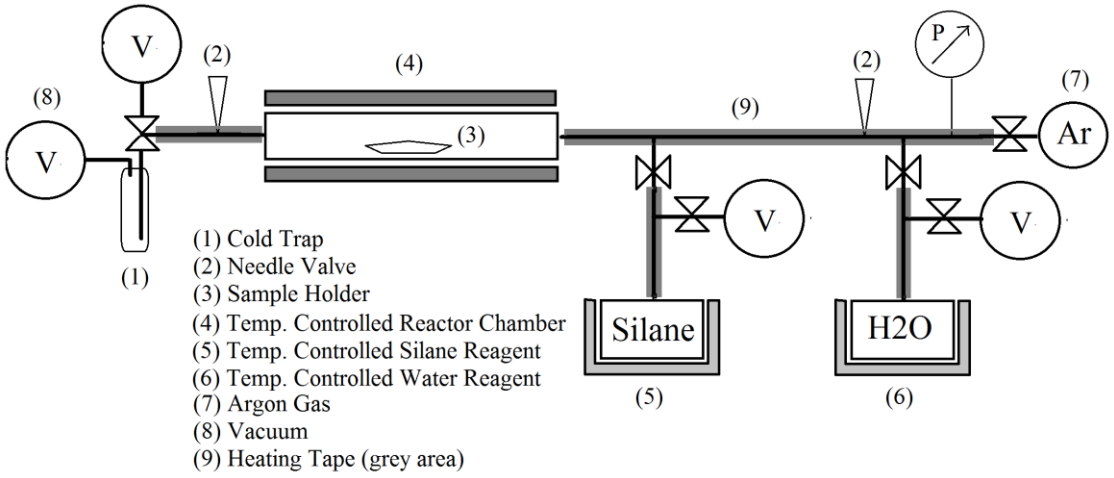

Figure 5.2: Schematic of ALD Apparatus for Silane Gas Phase Grafting.

5.2.2 Sorbent Characterization

Nitrogen adsorption-desorption isotherms were obtained on a Micromeritics ASAP 2020 surface area and porosity analyzer at 77K for textural characteristics. The Brunauer-

Emmett-Teller (BET) method and the Barret-Joyner-Halenda (BJH) model of the adsorption isotherm were used to calculate the surface area, the pore size distribution, and pore volume. CHN elemental analysis was performed on a Perkin Elmer 2400 Elemental Analyzer to obtain the amount of nitrogen mass percentage. Samples were loaded into capsules in 3-4 mg increments. The combustion temperature set-point was 924 ^{o}C and the reduction temperature was 624 ^{o}C.

5.2.3 Carbon Dioxide Adsorption Analysis

The CO_2 adsorption performance of the sorbents was determined using a Thermo Cahn D-101 electro-microbalance as described in Section 2.2.3. For a typical adsorption analysis, about 10 mg of sample was placed in a stainless steel sample pan and activated at 100 ^{o}C at 1 atm for 30 min under high purity Argon (99.99%) at 100 mL/min to remove unwanted adsorbed species (e.g., H_2O, CO_2, remaining solvent). Sorbents were then cooled to 25 ^{o}C and pure CO_2 (99.99%) was then introduced for 1 hr at 1 atm at a flow rate of 100 mL/min. The CO_2 equilibrium adsorption capacity was determined by the weight gained during the 1 hour adsorption period.

5.3 Results and Discussion

5.3.1 Sorbent Characteristics

After calcining the Cabot aerogel at 400 ^{o}C, the surface area, pore volume, and pore diameter was 767 m^2/g, 4.2 cm^3/g, and 42 nm (Section 4.3). After the first, second, and third ALD cycles, the textural properties progressively drop as shown in Figure 5.3 and 5.4. The nitrogen adsorption isotherms in Figure 5.3 show a type IV isotherm with type II hysteresis very close to that of the unmodified calcined aerogel in Chapter 1. This indicates very little change to the mesostructure of the aerogel during the grafting

procedure. Figure 5.4 shows the progressive drop in surface area and pore volume with each sequential cycle as a resulting of the building layer of amino silane on the silica surface. However, even after the third cycle G3 maintains a very high porosity of 3.9 cm^3/g, indicating the possibility of successfully growing a greater number of layers with more cycles of ALD. Figure 5.1 illustrates the process of the silane/water ALD cycles and pictorially reveals how the layers are building. The amino silane first condenses on the surface to available silanol groups forming a Si-O-Si bond with an alcohol byproduct. Then during water vapor introduction the alkoxy groups of the previously attached silanes are hydrolyzed. Once again during the next wave of silane introduction the amino silanes will condense to the recently hydrolyzed silanes. Continuation of this process will create layers of silanes onto the silica surface until the majority of alkoxy groups have been terminated and therefore making further hydrolization steps trivial.

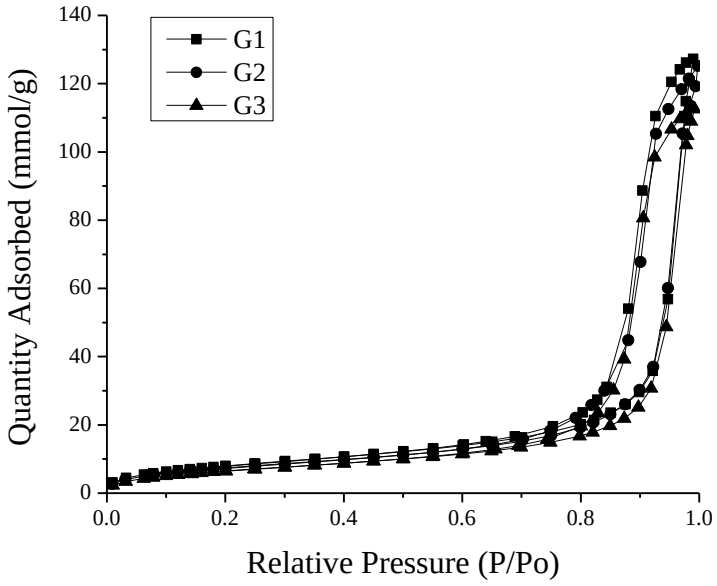

Figure 5.3: Nitrogen Adsorption Isotherms of the ALD Modified Aerogels After One (G1), Two (G2), and Three (G3) ALD Cycles of Mono Amino Silane.

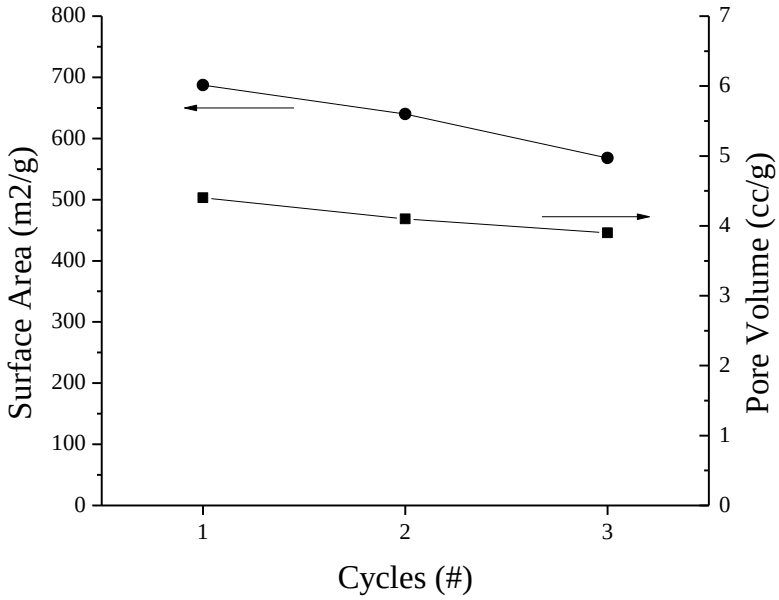

Figure 5.4: Surface Area and Pore Volume of ALD Modified Gels of One (G1), Two (G2), and Three (G3) ALD Cycles of Mono Amine Silane.

5.3.2 CO_2 Adsorption Performance

Figure 5.5 shows the dynamic adsorption performance of the ALD samples under 100% CO_2 at 25 ^{o}C and 1 bar. G1 achieved an adsorption capacity of 0.67 mmol/g and after each successive cycle the adsorption capacity increases by approximately 30% from the G1 sample to G3 with a capacity of 1.2 mmol/g. Furthermore the kinetics of the adsorption indicates that the amine binding sites are readily available. In less than 5 min G1, G2, and G3 reached 95% of their maximum adsorption capacity with very little tailing revealing that the layer of amines grafted to the surface do not obstruct any CO_2 transport mechanisms to the amine binding locations. Figure 5.6 shows the amount of nitrogen content grafted and the amine efficiency with each cycle. The amount of amine grafted steadily rises from 1.8 to 2.7 mmol N/g, values very similar to those grafting mono amine silanes in the anhydrous liquid phase conditions (Figure 1.6), indicating that

this method is quite efficient for grafting silanes. The amine efficiencies of the ALD samples are also comparable to those liquid phase grafted samples reaching an amine efficiency of 0.44, which is also very close to the theoretical stoichiometric maximum for this CO_2-amine chemistry (Chapter 1). Note also that the amine efficiency is increasing with increasing number of cycles. The greater number of cycles is believed to yield a layer of silanes where the amino groups are in much closer proximity to other amines and thus creating a higher amine density adsorption environment More mono amines therefore have more neighboring available nitrogens to form the carbamate and ammonium species for CO_2 capture. Table 5.1 summarizes the data of the ALD samples. As a comparison, the results of Ek, Iiskola, Niinisto, et al., (2003) are included in Table 5.1. They were able to achieve a higher amine density due to the higher isolated silanol content for silica gel (2.1 OH/nm^2) relative to calcined aerogels (1.7 OH/nm^2) but aerogel achieved a higher amine content due to its higher surface area.

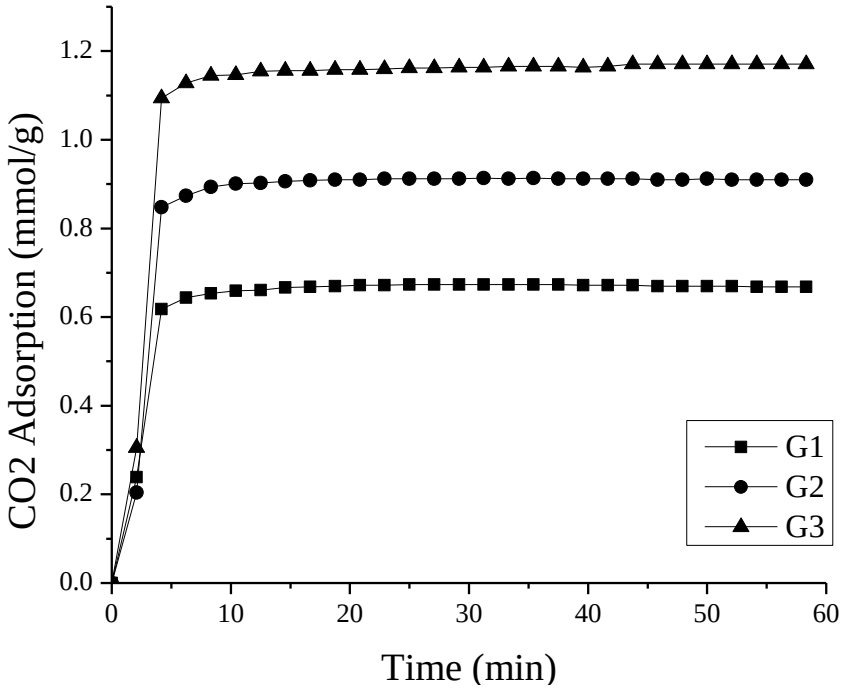

Figure 5.5: Adsorption Uptake Curves of the ALD Samples (Adsorption: 100% CO_2, 25 ^oC, 1bar).

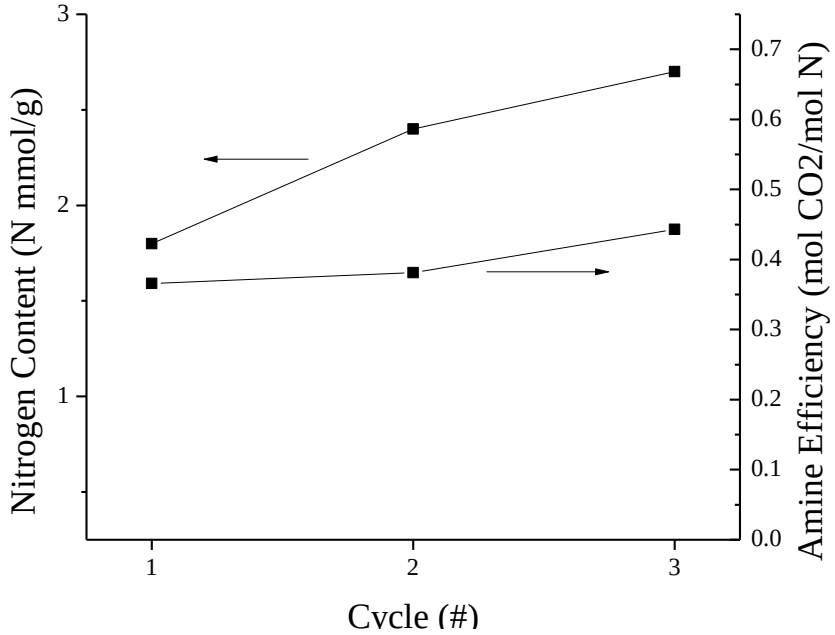

Figure 5.6: Amine Efficiencies of the Amino Silane ALD Samples.

Table 5.1: Summary of data of the mono amine ALD aerogels.

Cycle	SA (m^2/g)	Vp (cm^3/g)	Adsorption Capacity (mmol/g)	N content (mmol N/g)	Amine Efficiency (mol CO_2/mol N)	Amine density (amines/ nm^2)	Ref.
1	687	4.4	0.67	1.8	0.37	1.3	This work
2	640	4.1	0.9	2.4	0.38	1.8	This work
3	568	3.9	1.2	2.7	0.44	2.0	This work
3	244	1.0	-	1.3	-	2.7	(Ek, Iiskola, Niinisto, et al., 2003)
5	234	0.9	-	1.5		3.0	(Ek, Iiskola, Niinisto, et al., 2003)

5.4 Conclusions

Amine modified aerogels were synthesized by a atomic layer deposition (ALD) method using mono amine silane precursors. Aerogel was exposed to the amine silane vapor and then sequentially introduced to water vapor to hydrolyze the non condensed alkoxy groups to provide more grafting sites (silanols) in successive cycles. One, two, and three cycles were performed and the CO_2 adsorption performance was tested. The aerogels subjected to ALD showed adequate adsorption capacities and kinetics and were comparable to liquid phase amine grafted aerogels and were still able to retain the mesoporosity of the aerogel unlike the shrinkage occurring as shown in Chapter 4. The amine efficiency of the material increased with increasing cyclic ALD runs. The more cycles of ALD led to a higher N content as well as a greater amine density so the amines can more effectively bind CO_2.

CHAPTER 6

SUMMARY AND RECOMMENDATIONS

6.1 Summary

The research presented in this dissertation focused on the use of commercially available particulate silica aerogel as a support for amine modification that could be utilized as a post-combustion CO_2 adsorbent. Of the amine modification techniques discussed in Chapter 1, the wet impregnation method, amine grafting through liquid phase silane chemistry, and ALD of silanes were investigated in order to prepare a high performing and stable CO_2 sorbent.

Chapter 2 discussed the performance of the hydrophobic and hydrophilic TEPA impregnated aerogels. The hydrophilic aerogels were prepared by calcining the hydrophobic Cabot Nanogel to oxidize the surface organic groups. A number of TEPA loadings were prepared and the CO_2 adsorption performance was studied. The hydrophilic aerogel performed much better than the hydrophobic aerogel in both adsorption capacity and adsorption kinetics reaching an adsorption capacity of 6.1 mmol/g at 75 ^{o}C with 100% CO_2. It was suggested that the hydrophilicity of the surface created a more efficient distribution of the TEPA during the impregnation process. The poor distribution of the TEPA was further supported by the nitrogen porosimetry results where the TEPA impregnated hydrophilic samples possessed a greater porosity and surface area than the hydrophobic analogues. The cyclic stability of the hydrophilic samples over many cycles however was not adequate for a commercial user. Over the first 10 cycles the sorbent had a fairly steady capacity of 5.1 mmol/g with some loss in mass due to TEPA evaporation.

In Chapter 3, a new method of amine modification, a controlled evaporative precipitation route, was performed. This new technique was expected to improve the TEPA distribution relative to the common wet impregnation method discussed in Chapter 2 and therefore enhance the CO_2 adsorption performance of the sorbent. This technique involved precipitating TEPA from n-hexane while immersed in an aerogel/n-hexane slurry in order deposit the TEPA onto the silica to develop a uniform thin film of amine on the surface. The performance of these newly modified sorbents were only slightly improved from their wet impregnated counterparts. Their porosities, surface areas, adsorption kinetics, and CO_2 capacities were similar. TEM images of the samples were also similar with both showing a high degree of heterogeneity. These results revealed that for physical modification methods, the way in which the amine polymer is imbued into mesoporous supports makes little difference in the way in which the amines will be distributed. Therefore the method of introducing the polymer inside the pore space is not significant; but rather the distribution of amines is governed by the thermodynamic free energy of this two phase system. The polymer surface tension and the surface energy of the support, i.e., the surface chemistry of the surface, will determine the morphology of the liquid polymer, from thin films to large consolidated inclusions.

In Chapter 4 the performance of a grafted amine aerogel sorbent was investigated. The amine grafting was done by reacting amino silanes (Figure 1.5) to the surface of the hydrophilic aerogel supports. The silanol groups on the surface of the silica bond to the alkoxy ligands of the silanes to form a strong Si-O-Si bond. Of the amino silanes tested, the tri-amine silane performed the best simply due to the greater number of amines present per silane, resulting in a higher amine content. Unlike impregnation methods,

there are considerably more variables involved in silane grafting techniques, and therefore in order to achieve the best possible amine grafted aerogel the variables that were optimized were the synthesis temperature, silane concentration, and silica:silane ratio. Of these variables it appeared that the synthesis temperature had the greatest impact due to the sensitivity of condensation rates of the alkoxy moieties of the silane precursors. Furthermore hydrous grafting was conducted due to its capability to increase the degree of amine modification. Since in the anhydrous grafting procedures, the synthesis temperature had the biggest influence, only the synthesis temperature was varied for the hydrous grafting. The performance of the hydrous grafted sorbents was much superior to the anhydrous analogues due to water acting as another hydroxyl source rather than just the silanols on the surface. These results led to much greater nitrogen contents and increased CO_2 adsorption capacities. Moreover, the cyclic stability was much superior to the wet impregnated TEPA sorbents due to the strong covalent bonds attached to the surface. However these materials do not possess adequate CO_2 adsorption capacities required for an industrial application.

The final objective of this study was the synthesis and CO_2 adsorption performance of amine modified materials through ALD methods. Liquid phase grafting presented in Chapter 4 requires the addition of water to reach adequate adsorption capacities. The addition of water however creates a large degree of heterogeneity and obstruction of CO_2 transport. A more homogenous layer of amines distributed across the surface would allow for a much more efficient sorbent. In Chapter 5 a mono amine silane was vaporized and deposited onto the silica surface of the calcined Cabot aerogels using an ALD reactor apparatus. Furthermore, in order to build multiple layers and create a greater amine

density and N content, a cyclic sequential treatment between the amino silane and water was executed. The highest performing ALD sorbent was that prepared after three ALD cycles achieving an adsorption capacity of 1.2 mmol/g. These materials showed very little microstructural changes, large amine efficiencies and very favorable kinetics indicating a greater degree of homogeneity and good amine densities.

6.2 Recommendations

Based on the experimental and theoretical studies presented in this dissertation, the following recommendations are suggested for future work.

6.2.1 Increasing ALD Cycles and Other Silanes

The ALD method presented in Chapter 5 showed some of the best potential for a post combustion capture CO_2 sorbent. However, an increase in the CO_2 adsorption capacity is necessary. Three ALD cycles were insufficient in obtaining an amine modified aerogel with a large N content and therefore resulted in a relatively low adsorption capacity. As discussed in Chapter 1 the working capacity for a viable CO_2 sorbent is approximately 3 mmol/g in order to be competitive with absorption technologies. Therefore I would suggest that future work would be aimed toward synthesizing aerogels with a larger number of ALD cycles. As seen in the work of Ek, Iiskola, Niinisto, et al., (2003) using a porous silica support similar to fumed silica, the largest number of water/silane ALD cycles was about 5. The amount of N content began to plateau after 5 cycles and any more ALD steps would be trivial. However the unique microstructure and porosity of aerogel could lead to a greater ability for more layers to be deposited. Cabot also provides a larger particle size aerogel that can be easily fluidized. Therefore a more effective method for production of amine modified aerogels can be

achieved by using a fluidized ALD reactor using the larger particle size particulate aerogels.

Furthermore, in order to increase the amine content, di and tri amino silanes could be implemented. Mono amine is commonly utilized due its lower boiling point relative to the di and tri and therefore with the mono amine silane, a higher vapor pressure of silane can be obtained in order to achieve sufficient grafting. Di and tri amino silanes can be deposited onto silica surfaces but with higher temperatures needed to obtain larger partial pressure of silane in the reactor. It is possible that the amino silane can self polymerize if temperatures are too high (~200 ^{o}C), therefore in order to counter the lower vapor pressure it is suggested that longer times of grafting or even catalysts such as triethylamine be implemented to achieve the desired degree of grafting.

6.2.2 Aziridine in situ Polymerization

As discussed in Chapter 1, another way to obtain a sufficient amount of covalently bounded amine on a silica support such as the silica aerogel presented in this study is to apply an *in situ* polymerization technique. As performed by Drese et al., (2009) on SBA-15, the precursor aziridine (Figure 1.5) can be polymerized from the surface of silica either through pre-grafted amines or by the pre-existing silanol groups. The result is a highly branched amino polymer anchored to the surface. With aerogel's high porosity and surface area, it is an excellent candidate for this method of modification. However, careful precautions need to be implemented since aziridine (a.k.a. ethyleneimine) is an extremely toxic compound that is unstable, highly flammable, and a known carcinogen.

REFERENCES

Adewole, J. K., Ahmad, a. L., Ismail, S., & Leo, C. P. (2013). Current challenges in membrane separation of CO2 from natural gas: A review. *International Journal of Greenhouse Gas Control*, *17*, 46–65. doi:10.1016/j.ijggc.2013.04.012

Alnaief, M., & Smirnova, I. (2010). Effect of surface functionalization of silica aerogel on their adsorptive and release properties. *Journal of Non-Crystalline Solids*, *356*(33-34), 1644–1649. doi:10.1016/j.jnoncrysol.2010.06.027

Aquino, C. C., Richner, G., Chee Kimling, M., Chen, D., Puxty, G., Feron, P. H. M., & Caruso, R. a. (2013). Amine-Functionalized Titania-based Porous Structures for Carbon Dioxide Postcombustion Capture. *The Journal of Physical Chemistry C*, *117*(19), 9747–9757. doi:10.1021/jp312118e

Araki, S., Doi, H., Sano, Y., Tanaka, S., & Miyake, Y. (2009). Preparation and CO(2) adsorption properties of aminopropyl-functionalized mesoporous silica microspheres. *Journal of Colloid and Interface Science*, *339*(2), 382–9. doi:10.1016/j.jcis.2009.07.024

Aziz, B., Hedin, N., & Bacsik, Z. (2012). Quantification of chemisorption and physisorption of carbon dioxide on porous silica modified by propylamines: Effect of amine density. *Microporous and Mesoporous Materials*, *159*, 42–49. doi:10.1016/j.micromeso.2012.04.007

Aziz, B., Zhao, G., & Hedin, N. (2011, April 5). Carbon dioxide sorbents with propylamine groups-silica functionalized with a fractional factorial design approach. *Langmuir : The ACS Journal of Surfaces and Colloids*. doi:10.1021/la104629m

Baetens, R., Jelle, B. P., & Gustavsen, A. (2011). Aerogel insulation for building applications : A state-of-the-art review. *Energy & Buildings*, *43*(4), 761–769. doi:10.1016/j.enbuild.2010.12.012

Bai, S., Liu, J., Gao, J., Yang, Q., & Li, C. (2012). Hydrolysis controlled synthesis of amine-functionalized hollow ethane–silica nanospheres as adsorbents for CO2 capture. *Microporous and Mesoporous Materials*, *151*, 474–480. doi:10.1016/j.micromeso.2011.09.014

Balkis Ameen, K., Rajasekar, K., Rajasekharan, T., & Rajasekharan, M. V. (2007). The effect of heat-treatment on the physico-chemical properties of silica aerogel prepared by sub-critical drying technique. *Journal of Sol-Gel Science and Technology*, *45*(1), 9–15. doi:10.1007/s10971-007-1630-y

Barbosa, M. N., Araujo, A. S., Galvão, L. P. F. C., Silva, E. F. B., Santos, A. G. D., Luz, G. E., & Fernandes, V. J. (2011). Carbon dioxide adsorption over DIPA

functionalized MCM-41 and SBA-15 molecular sieves. *Journal of Thermal Analysis and Calorimetry*, *106*(3), 779–782. doi:10.1007/s10973-011-1398-8

Basiuk, V. A., & Chuiko, A. A. (1990). Gas-Phase Synthesis, Properties, and Some Applications of Acylamide Stationary Phase for Phases for High-Performance Liquid Chromatography. *Journal of Chromatography*, *521*.

Begag, R., Krutka, H., Dong, W., Mihalcik, D., Rhine, W., Gould, G., … Nahass, P. (2013). Superhydrophobic amine functionalized aerogels as sorbents for CO capture.pdf. *Greenhouse Gases Science and Technology*, *3*, 30–39.

Belmabkhout, Y., Heymans, N., De Weireld, G., & Sayari, A. (2011). Simultaneous Adsorption of H 2 S and CO 2 on Triamine-Grafted Pore-Expanded Mesoporous MCM-41 Silica. *Energy & Fuels*, *25*(3), 1310–1315. doi:10.1021/ef1015704

Bosch, P., Berstein, L., Canziani, O., Chen, Z., Christ, R., Davidson, O., … Yohe, G. (2007). *Climate Change 2007 : Synthesis Report*. *Change* (pp. 26–73). Valencia, Spain.

Bradshaw, J., Chen, Z., Garg, A., Gomez, D., Rogner, H.-H., Simbeck, D., & Williams, R. (2005). *IPCC Special Report on Carbon Dioxide Capture and Storage* (pp. 76–104).

Brinker, C. J., & Scherer, G. (1990). *Sol-Gel Science: The Physics and Chemistry of Sol-gel Processing* (1st ed.). Academic Press, Inc.

Buzek, F., & Rathousky, J. (1981). Stoichiometry and Kinetics of the Reaction of Silica with Organosilicon Compounds. *Journal of Colloid and Interface Science*, *79*(1).

Calleja, G., Sanz, R., Arencibia, a., & Sanz-Pérez, E. S. (2011). Influence of Drying Conditions on Amine-Functionalized SBA-15 as Adsorbent of CO2. *Topics in Catalysis*, *54*(1-4), 135–145. doi:10.1007/s11244-011-9652-7

Capadona, L. a., Meador, M. A. B., Alunni, A., Fabrizio, E. F., Vassilaras, P., & Leventis, N. (2006). Flexible, low-density polymer crosslinked silica aerogels. *Polymer*, *47*(16), 5754–5761. doi:10.1016/j.polymer.2006.05.073

Caplow, M. (1968). Kinetics of Carbamate Formation and Breakdown’. *Journal of the American Chemical Society*, *90*, 6795–6803.

Chang, A. C., Chuang, S. S. C., Gray, M. L., & Soong, Y. (2003). In-Situ Infrared Study of CO2 Adsorption on SBA-15 Grafted with γ-(Aminopropyl)triethoxysilane. *Energy & Fuels*, *17*, 468–473.

Chang, F.-Y., Chao, K.-J., Cheng, H.-H., & Tan, C.-S. (2009). Adsorption of CO2 onto amine-grafted mesoporous silicas. *Separation and Purification Technology*, *70*(1), 87–95. doi:10.1016/j.seppur.2009.08.016

Chen, C., Son, W.-J., You, K.-S., Ahn, J.-W., & Ahn, W.-S. (2010). Carbon dioxide capture using amine-impregnated HMS having textural mesoporosity. *Chemical Engineering Journal*, *161*(1-2), 46–52. doi:10.1016/j.cej.2010.04.019

Chen, C., Yang, S.-T., Ahn, W.-S., & Ryoo, R. (2009). Amine-impregnated silica monolith with a hierarchical pore structure: enhancement of CO2 capture capacity. *Chemical Communications*, 3627–9. doi:10.1039/b905589d

Choi, S., Drese, J. H., & Jones, C. W. (2009). Adsorbent Materials for Carbon Dioxide Capture from Large Anthropogenic Point Sources. *Chemical Communications*, *2*, 796 – 854. doi:10.1002/cssc.200900036

Conway, W., Wang, X., Fernandes, D., Burns, R., Lawrance, G., Puxty, G., & Maeder, M. (2012). Toward rational design of amine solutions for PCC applications: the kinetics of the reaction of CO2(aq) with cyclic and secondary amines in aqueous solution. *Environmental Science & Technology*, *46*(13), 7422–9. doi:10.1021/es300541t

Conway, W., Wang, X., Fernandes, D., Burns, R., Lawrance, G., Puxty, G., & Maeder, M. (2013). Toward the understanding of chemical absorption processes for post-combustion capture of carbon dioxide: electronic and steric considerations from the kinetics of reactions of CO2(aq) with sterically hindered amines. *Environmental Science & Technology*, *47*(2), 1163–9. doi:10.1021/es3025885

Cui, S., Cheng, W., Shen, X., Fan, M., & Russell, T. (2011). Mesoporous amine-modified SiO 2 aerogel : a potential CO 2 sorbent. *Energy & Environmental Science*, *4*, 2070–2074. doi:10.1039/c0ee00442a

Danckwerts, P. V. (1979). THE REACTION OF CO2 WITH ETHANOLAMINES. *CHemical Engineering Science*, *34*, 443–446.

Demessence, A., D'Alessandro, D. M., Foo, M. L., & Long, J. R. (2009). Strong CO2 binding in a water-stable, triazolate-bridged metal-organic framework functionalized with ethylenediamine. *Journal of the American Chemical Society*, *131*(25), 8784–6. doi:10.1021/ja903411w

Diffenbaugh, N. S., & Field, C. B. (2013). Changes in ecologically critical terrestrial climate conditions. *Science (New York, N.Y.)*, *341*(6145), 486–92. doi:10.1126/science.1237123

Donaldson, T. L., & Nguyen, Y. N. (1980). Carbon Dioxide Reaction Kinetics and Transport in Aqueous Amine Membranes. *Industrial & Engineering Chemistry Fundamentals*, *19*(3), 260–266. doi:10.1021/i160075a005

Drage, T. C., Snape, C. E., Stevens, L. a., Wood, J., Wang, J., Cooper, A. I., … Irons, R. (2012). Materials challenges for the development of solid sorbents for post-combustion carbon capture. *Journal of Materials Chemistry*, *22*(7), 2815. doi:10.1039/c2jm12592g

Drese, J. H., Choi, S., Didas, S. A., Bollini, P., Gray, M. L., & Jones, C. W. (2012). Effect of support structure on CO 2 adsorption properties of pore-expanded hyperbranched aminosilicas. *Microporous and Mesoporous Materials*, *151*, 231–240. doi:10.1016/j.micromeso.2011.10.031

Drese, J. H., Choi, S., Lively, R. P., Koros, W. J., Fauth, D. J., Gray, M. L., & Jones, C. W. (2009). Synthesis-€ "Structure-€ "Property Relationships for Hyperbranched Aminosilica CO2 Adsorbents. *Advanced Functional Materials*, *19*(23), 3821–3832. doi:10.1002/adfm.200901461

Du, N., Park, H. B., Dal-Cin, M. M., & Guiver, M. D. (2012). Advances in high permeability polymeric membrane materials for CO2 separations. *Energy & Environmental Science*, *5*(6), 7306. doi:10.1039/c1ee02668b

Ebner, A. D., Gray, M. L., Chisholm, N. G., Black, Q. T., Mumford, D. D., Nicholson, M. A., & Ritter, J. A. (2011). Suitability of a Solid Amine Sorbent for CO 2 Capture by Pressure Swing Adsorption. *Industrial & Engineering Chemistry Research*, *50*, 5634–5641.

Ek, S., Iiskola, E. I., & Niinisto, L. (2003). Gas-Phase Deposition of Aminopropylalkoxysilanes on Porous Silica, (13), 3461–3471.

Ek, S., Iiskola, E. I., & Niinisto, L. (2004). Atomic Layer Deposition of Amino-Functionalized Silica Surfaces Using N - (2-Aminoethyl) -3-aminopropyltrimethoxysilane as a Silylating Agent, 9650–9655.

Ek, S., Iiskola, E. I., Niinisto, L., Vaittinen, J., Pakkanen, T. T., Einstein, A. A., & Cedex, F.-V. (2003). Atomic Layer Deposition of a High-Density Aminopropylsiloxane Network on Silica through Sequential Reactions of γ -Aminopropyltrialkoxysilanes and Water, (11), 10601–10609.

Favre, E. (2011). Membrane processes and postcombustion carbon dioxide capture : Challenges and prospects. *Chemical Engineering Journal*, *171*(3), 782–793. doi:10.1016/j.cej.2011.01.010

Fernandes, D., Conway, W., Burns, R., Lawrance, G., Maeder, M., & Puxty, G. (2012). Investigations of primary and secondary amine carbamate stability by 1H NMR

spectroscopy for post combustion capture of carbon dioxide. *The Journal of Chemical Thermodynamics*, *54*, 183–191. doi:10.1016/j.jct.2012.03.030

Franchi, R. S., Harlick, P. J. E., & Sayari, A. (2005). Applications of Pore-Expanded Mesoporous Silica. 2. Development of a High-Capacity, Water-Tolerant Adsorbent for CO 2. *Industrial & Engineering Chemistry Research*, *44*(21), 8007–8013. doi:10.1021/ie0504194

Gil, M., Tiscornia, I., de la Iglesia, Ó., Mallada, R., & Santamaría, J. (2011). Monoamine-grafted MCM-48: An efficient material for CO2 removal at low partial pressures. *Chemical Engineering Journal*, *175*, 291–297. doi:10.1016/j.cej.2011.09.107

Goeppert, A., Meth, S., Prakash, G. K. S., & Olah, G. A. (2010). Nanostructured silica as a support for regenerable high-capacity organoamine-based CO2 sorbents. *Energy & Environmental Science*, *3*(12), 1949–1960. doi:10.1039/c0ee00136h

Goodrich, B. F., de la Fuente, J. C., Gurkan, B. E., Zadigian, D. J., Price, E. a., Huang, Y., & Brennecke, J. F. (2011). Experimental Measurements of Amine-Functionalized Anion-Tethered Ionic Liquids with Carbon Dioxide. *Industrial & Engineering Chemistry Research*, *50*(1), 111–118. doi:10.1021/ie101688a

Gray, M., Champagne, K., Fauth, D., Baltrus, J., & Pennline, H. (2008). Performance of immobilized tertiary amine solid sorbents for the capture of carbon dioxide. *International Journal of Greenhouse Gas Control*, *2*(1), 3–8. doi:10.1016/S1750-5836(07)00088-6

Gray, M. L., Soong, Y., Champagne, K. J., Pennline, H., Baltrus, J. P., Stevens Jr., R. W., … Filburn, T. (2005). Improved immobilized carbon dioxide capture sorbents. *Fuel Processing Technology*, *86*(14-15), 1449–1455. doi:10.1016/j.fuproc.2005.01.005

Gui, M. M., Yap, Y. X., Chai, S.-P., & Mohamed, A. R. (2013). Multi-walled carbon nanotubes modified with (3-aminopropyl)triethoxysilane for effective carbon dioxide adsorption. *International Journal of Greenhouse Gas Control*, *14*, 65–73. doi:10.1016/j.ijggc.2013.01.004

Gutowski, K. E., & Maginn, E. J. (2008). Amine-functionalized task-specific ionic liquids: a mechanistic explanation for the dramatic increase in viscosity upon complexation with CO2 from molecular simulation. *Journal of the American Chemical Society*, *130*(44), 14690–704. doi:10.1021/ja804654b

Hao, S., Chang, H., Xiao, Q., Zhong, Y., & Zhu, W. (2011). One-Pot Synthesis and CO 2 Adsorption Properties of Ordered Mesoporous SBA-15 Materials Functionalized with APTMS. *Journal of Physical Chemistry*, *115*, 12873–12882.

Hao, S., Zhang, J., Zhong, Y., & Zhu, W. (2012). Selective adsorption of CO2 on amino-functionalized silica spheres with centrosymmetric radial mesopores and high amino loading. *Adsorption*, *18*(5-6), 423–430. doi:10.1007/s10450-012-9428-9

Harlick, P. J. E., & Sayari, A. (2006). Applications of Pore-Expanded Mesoporous Silicas. 3. Triamine Silane Grafting for Enhanced CO 2 Adsorption. *Industrial & Engineering Chemistry Research*, *45*(9), 3248–3255. doi:10.1021/ie051286p

Harlick, P. J. E., & Sayari, A. (2007). Applications of Pore-Expanded Mesoporous Silica. 5. Triamine Grafted Material with Exceptional CO 2 Dynamic and Equilibrium Adsorption Performance. *Industrial & Engineering Chemistry Research*, *46*(2), 446–458. doi:10.1021/ie060774+

Hart, A., & Gnanendran, N. (2009). Cryogenic CO2 capture in natural gas. *Energy Procedia*, *1*(1), 697–706. doi:10.1016/j.egypro.2009.01.092

Haukka, S., Lakomaa, E.-L., & Suntola, T. (1993). Analytical and chemical techniques in the study of surface species in atomic layer epitaxy. *Thin Solid Films*, *225*(1-2), 280–283. doi:10.1016/0040-6090(93)90170-T

He, L., Fan, M., Dutcher, B., Cui, S., Shen, X., Kong, Y., … McCurdy, P. (2012). Dynamic separation of ultradilute CO2 with a nanoporous amine-based sorbent. *Chemical Engineering Journal*, *189-190*, 13–23. doi:10.1016/j.cej.2012.02.013

Heydari-gorji, A., Belmabkhout, Y., & Sayari, A. (2011). Polyethylenimine-Impregnated Mesoporous Silica : Effect of Amine Loading and Surface Alkyl Chains on CO 2 Adsorption. *Langmuir*, *27*, 12411–12416.

Heydari-Gorji, A., & Sayari, A. (2011). CO2 capture on polyethylenimine-impregnated hydrophobic mesoporous silica: Experimental and kinetic modeling. *Chemical Engineering Journal*, *173*(1), 72–79. doi:10.1016/j.cej.2011.07.038

Heydari-gorji, A., & Sayari, A. (2012). Thermal , Oxidative , and CO 2 -Induced Degradation of Supported Polyethylenimine Adsorbents. *Industrial & Engineering Chemistry Research*, *51*, 6887–6894.

Heydari-gorji, A., Yang, Y., & Sayari, A. (2011). Effect of the Pore Length on CO2 Adsorption over Amine-Modified Mesoporous Silicas. *Energy & Fuels*, *25*, 4206–4210.

Hicks, J. C., Drese, J. H., Fauth, D. J., Gray, M. L., Qi, G., & Jones, C. W. (2008). Designing adsorbents for CO2 capture from flue gas-hyperbranched aminosilicas capable of capturing CO2 reversibly. *Journal of the American Chemical Society*, *130*(10), 2902–3. doi:10.1021/ja077795v

Hiyoshi, N., Yogo, K., & Yashima, T. (2005). Adsorption characteristics of carbon dioxide on organically functionalized SBA-15. *Microporous and Mesoporous Materials*, *84*, 357–365. doi:10.1016/j.micromeso.2005.06.010

Hoegh-Guldberg, O., Mumby, P. J., Hooten, a J., Steneck, R. S., Greenfield, P., Gomez, E., … Hatziolos, M. E. (2007). Coral reefs under rapid climate change and ocean acidification. *Science (New York, N.Y.)*, *318*(5857), 1737–42. doi:10.1126/science.1152509

Hofmann, D. J., Butler, J. H., & Tans, P. P. (2009). A new look at atmospheric carbon dioxide. *Atmospheric Environment*, *43*(12), 2084–2086. doi:10.1016/j.atmosenv.2008.12.028

Huang, C.-H., Klinthong, W., & Tan, C.-S. (2013). SBA-15 grafted with 3-aminopropyl triethoxysilane in supercritical propane for CO2 capture. *The Journal of Supercritical Fluids*, *77*, 117–126. doi:10.1016/j.supflu.2013.02.028

Huang, H. Y., Yang, R. T., Chinn, D., & Munson, C. L. (2003). Amine-Grafted MCM-48 and Silica Xerogel as Superior Sorbents for Acidic Gas Removal from Natural Gas. *Industrial & Engineering Chemistry Research*, *42*(12), 2427–2433. doi:10.1021/ie020440u

Hughes, T. P., Baird, a H., Bellwood, D. R., Card, M., Connolly, S. R., Folke, C., … Roughgarden, J. (2003). Climate change, human impacts, and the resilience of coral reefs. *Science (New York, N.Y.)*, *301*(5635), 929–33. doi:10.1126/science.1085046

Husing, N., Schubert, U., Mezei, R., Fratzl, P., Riegel, B., Kiefer, W., … Mader, W. (1999). Formation and Structure of Gel Networks from Si(OEth)4/(MeO)3Si(CH2)3NR’2 Mixtures (NR'2 = NH2 or NHCH2CH2NH2). *Chemistry of Materials*, *11*, 451–457.

Im, H.-J., Yang, Y., Allain, L. R., Barnes, C. E., Dai, S., & Xue, Z. (2000). Funtionalized Sol−Gels for Selective Copper(II) Separation. *Environmental Science & Technology*, *34*(11), 2209–2214. doi:10.1021/es9911014

Jonsson, U., Olofsson, G., Malmqvist, M., & Ronnberg, I. (1985). Chemical Vapour Deposition of Silanes. *Thin Solid Films*, *124*, 117–123.

Jorgensen, E., & Faurholt, C. (1954). Reactions between Carbon Dioxide and Amino Alcohols. II. Triethanolamine. *Acta Chemica Scandinavica*, *8*, 1141–1144.

Juvaste, H., Iiskola, E. I., & Pakkanen, T. T. (1999). Preparation of new modified catalyst carriers. *Journal of Molecular Catalysis A: Chemical*, *150*(1-2), 1–9. doi:10.1016/S1381-1169(99)00200-9

Kang, S., & Choi, S. (2000). Synthesis of low-density silica gel at ambient pressure : Effect of heat treatment, *5*, 4971–4976.

Kanniche, M., Gros-Bonnivard, R., Jaud, P., Valle-Marcos, J., Amann, J.-M., & Bouallou, C. (2010). Pre-combustion, post-combustion and oxy-combustion in thermal power plant for CO2 capture. *Applied Thermal Engineering*, *30*(1), 53–62. doi:10.1016/j.applthermaleng.2009.05.005

Katti, A., Shimpi, N., Roy, S., Lu, H., Fabrizio, E. F., Dass, A., … Leventis, N. (2006). Chemical, Physical, and Mechanical Characterization of Isocyanate Cross-linked Amine-Modified Silica Aerogels. *Chemistry of Materials*, *18*(2), 285–296. doi:10.1021/cm0513841

Kim, C. O., Cho, S. J., & Park, J. W. (2003). Hyperbranching polymerization of aziridine on silica solid substrates leading to a surface of highly dense reactive amine groups. *Journal of Colloid and Interface Science*, *260*(2), 374–378. doi:10.1016/S0021-9797(03)00039-0

Kim, H., Moon, J., & Park, J. (2000). A Hyperbranched Poly(ethyleneimine) Grown on Surfaces. *Journal of Colloid and Interface Science*, *227*(1), 247–249. doi:10.1006/jcis.2000.6861

Kim, S., Ida, J., Guliants, V. V, & Lin, J. Y. S. (2005). Tailoring pore properties of MCM-48 silica for selective adsorption of CO2. *The Journal of Physical Chemistry. B*, *109*(13), 6287–93. doi:10.1021/jp045634x

Kim, S.-N., Son, W.-J., Choi, J.-S., & Ahn, W.-S. (2008). CO2 adsorption using amine-functionalized mesoporous silica prepared via anionic surfactant-mediated synthesis. *Microporous and Mesoporous Materials*, *115*(3), 497–503. doi:10.1016/j.micromeso.2008.02.025

Klinthong, W., Chao, K., & Tan, C. (2013). CO 2 Capture by As-Synthesized Amine-Functionalized MCM-41 Prepared through Direct Synthesis under Basic Condition.

Knowles, G. P., Delaney, S. W., & Chaffee, A. L. (2006). Diethylenetriamine [propyl (silyl)] -Functionalized (DT) Mesoporous Silicas as CO 2 Adsorbents. *Society*, *45*, 2626–2633.

Knowles, G. P., Graham, J. V., Delaney, S. W., & Chaffee, A. L. (2005). Aminopropyl-functionalized mesoporous silicas as CO2 adsorbents. *Fuel Processing Technology*, *86*(14-15), 1435–1448. doi:10.1016/j.fuproc.2005.01.014

Ko, Y. G., Lee, H. J., Oh, H. C., & Choi, U. S. (2013). Amines immobilized double-walled silica nanotubes for CO2 capture. *Journal of Hazardous Materials*, *250-251*, 53–60. doi:10.1016/j.jhazmat.2013.01.035

Ko, Y. G., Shin, S. S., & Choi, U. S. (2011). Primary, secondary, and tertiary amines for CO2 capture: designing for mesoporous CO2 adsorbents. *Journal of Colloid and Interface Science*, *361*(2), 594–602. doi:10.1016/j.jcis.2011.03.045

Kuchta, L., & Fajnor, V. S. (1996). About the synthesis and thermal stability of SiO2-aerogel. *Journal of Thermal Analysis*, *46*, 515.

Kumar, V., Labhsetwar, N., Meshram, S., & Rayalu, S. (2011). Functionalized Fly Ash Based Alumino-Silicates for Capture of Carbon Dioxide. *Energy & Fuels*, *25*(10), 4854–4861. doi:10.1021/ef201212h

Kuwahara, Y., Kang, D.-Y., Copeland, J. R., Bollini, P., Sievers, C., Kamegawa, T., … Jones, C. W. (2012). Enhanced CO(2) Adsorption over Polymeric Amines Supported on Heteroatom-Incorporated SBA-15 Silica: Impact of Heteroatom Type and Loading on Sorbent Structure and Adsorption Performance. *Chemistry (Weinheim an Der Bergstrasse, Germany)*, (class 1), 16649–16664. doi:10.1002/chem.201203144

Kuwahara, Y., Kang, D.-Y., Copeland, J. R., Brunelli, N. a, Didas, S. a, Bollini, P., … Jones, C. W. (2012). Dramatic enhancement of CO2 uptake by poly(ethyleneimine) using zirconosilicate supports. *Journal of the American Chemical Society*, *134*(26), 10757–60. doi:10.1021/ja303136e

Leal, O. (1995). Reversible adsorption of carbon dioxide on amine surface-bonded silica gel. *Inorganica Chimica Acta*, *240*(1-2), 183–189. doi:10.1016/0020-1693(95)04534-1

Lee, D.-H., Choi, W.-J., Moon, S.-J., Ha, S.-H., Kim, I.-G., & Oh, K.-J. (2008). Characteristics of absorption and regeneration of carbon dioxide in aqueous 2-amino-2-methyl-1-propanol/ammonia solutions. *Korean Journal of Chemical Engineering*, *25*(2), 279–284. doi:10.1007/s11814-008-0049-7

Lee, J. H., Choi, S. Y., & Kim, C. E. (1997). The effects of initial sol parameters on the microstructure and optical transparency of TiO 2 — SiO 2 binary aerogels. *Journal of Materials Science*, *32*, 3577–3585.

Lee, S., Filburn, T. P., Gray, M., Park, J., & Song, H. (2008). Screening Test of Solid Amine Sorbents for CO 2 Capture. *Cycle*, 7419–7423.

Li, B., Jiang, B., Fauth, D. J., Gray, M. L., Pennline, H. W., & Richards, G. A. (2011). Innovative nano-layered solid sorbents for CO2 capture. *Chemical Communications*, *47*(6), 1719–1721. doi:10.1039/c0cc03817b

Li, W., Bollini, P., Didas, S. a, Choi, S., Drese, J. H., & Jones, C. W. (2010). Structural changes of silica mesocellular foam supported amine-functionalized CO2 adsorbents

upon exposure to steam. *ACS Applied Materials & Interfaces*, *2*(11), 3363–72. doi:10.1021/am100786z

Liang, Z., Fadhel, B., Schneider, C. J., & Chaffee, A. L. (2008). Stepwise growth of melamine-based dendrimers into mesopores and their CO2 adsorption properties. *Microporous and Mesoporous Materials*, *111*(1-3), 536–543. doi:10.1016/j.micromeso.2007.08.030

Linneen, N., Pfeffer, R., & Lin, Y. S. (2013). CO2 capture using particulate silica aerogel immobilized with tetraethylenepentamine. *Microporous and Mesoporous Materials*, *176*, 123–131. doi:10.1016/j.micromeso.2013.02.052

Liu, H., Sha, W., Cooper, A. T., & Fan, M. (2009). Preparation and characterization of a novel silica aerogel as adsorbent for toxic organic compounds. *Colloids and Surfaces A: Physicochemical and Engineering Aspects*, *347*, 38–44. doi:10.1016/j.colsurfa.2008.11.033

Liu, J., Feng, X., Fryxell, G. E., Wang, L.-Q., Kim, A. Y., & Gong, M. (1998). Hybrid Mesoporous Materials with Functionalized Monolayers. *Advanced Materials*, *10*(2), 161–165. doi:10.1002/(SICI)1521-4095(199801)10:2<161::AID-ADMA161>3.0.CO;2-Q

Liu, S.-H., Wu, C.-H., Lee, H.-K., & Liu, S.-B. (2009). Highly Stable Amine-modified Mesoporous Silica Materials for Efficient CO2 Capture. *Topics in Catalysis*, *53*(3-4), 210–217. doi:10.1007/s11244-009-9413-z

Liu, Y., Shi, J., Chen, J., Ye, Q., Pan, H., Shao, Z., & Shi, Y. (2010). Dynamic performance of CO2 adsorption with tetraethylenepentamine-loaded KIT-6. *Microporous and Mesoporous Materials*, *134*(1-3), 16–21. doi:10.1016/j.micromeso.2010.05.002

Liu, Y., Ye, Q., Shen, M., Shi, J., Chen, J., Pan, H., & Shi, Y. (2011). Carbon dioxide capture by functionalized solid amine sorbents with simulated flue gas conditions. *Environmental Science & Technology*, *45*(13), 5710–5716. doi:10.1021/es200619j

Llusar, M., Monros, G., Roux, C., Pozzo, J. L., & Sanchez, C. (2003). One-pot synthesis of phenyl- and amine-functionalized silica fibers through the use of anthracenic and phenazinic organogelators. *Journal of Materials Chemistry*, *13*(10), 2505. doi:10.1039/b304479n

Loganathan, S., Tikmani, M., & Ghoshal, A. K. (2013). Novel pore-expanded MCM-41 for CO2 capture: synthesis and characterization. *Langmuir : The ACS Journal of Surfaces and Colloids*, *29*(10), 3491–9. doi:10.1021/la400109j

Lopeandía, a. F., & Rodríguez-Viejo, J. (2007). Size-dependent melting and supercooling of Ge nanoparticles embedded in a SiO2 thin film. *Thermochimica Acta*, *461*(1-2), 82–87. doi:10.1016/j.tca.2007.04.010

Mahajani, V. V, & Joshi, J. B. (1988). Review Kinetics of reactions between dioxide and alkanolamines. *Gas Separation and Purification*, *2*, 50–64.

Meador, M. A. B., Fabrizio, E. F., Ilhan, F., Dass, A., Zhang, G., Vassilaras, P., … Leventis, N. (2005). Cross-linking Amine-Modified Silica Aerogels with Epoxies. Mechanically Strong Lightweight Porous Materials. *Chemistry of Materials*, *17*, 1085–1098.

Mello, M. R., Phanon, D., Silveira, G. Q., Llewellyn, P. L., & Ronconi, C. M. (2011). Amine-modified MCM-41 mesoporous silica for carbon dioxide capture. *Microporous and Mesoporous Materials*, *143*(1), 174–179. doi:10.1016/j.micromeso.2011.02.022

Meth, S., Goeppert, A., Prakash, G. K. S., & Olah, G. A. (2012). Silica Nanoparticles as Supports for Regenerable CO 2 Sorbents.

Mittal, K. L., & O'kane, D. F. (1976). Vapor Deposited Silanes and other Coupling Agents. *The Journal of Adhesion*, *8*(1), 93–97. doi:10.1080/00218467608075073

Montanari, T., & Busca, G. (2008). On the mechanism of adsorption and separation of CO2 on LTA zeolites: An IR investigation. *Vibrational Spectroscopy*, *46*(1), 45–51. doi:10.1016/j.vibspec.2007.09.001

Neimark, A. V, Hanson, J. M., & Ungert, K. K. (1993). Fractal Analysis of the Distribution of High-Viscosity Fluids in Porous Supports. *Journal of Physical Chemistry*, *97*(22), 6011–6015.

Nik, O. G., Nohair, B., & Kaliaguine, S. (2011). Aminosilanes grafting on FAU/EMT zeolite: Effect on CO2 adsorptive properties. *Microporous and Mesoporous Materials*, *143*(1), 221–229. doi:10.1016/j.micromeso.2011.03.002

Notz, R. J., Tönnies, I., McCann, N., Scheffknecht, G., & Hasse, H. (2011). CO2 Capture for Fossil Fuel-Fired Power Plants. *Chemical Engineering & Technology*, *34*(2), 163–172. doi:10.1002/ceat.201000491

Olea, a., Sanz-Pérez, E. S., Arencibia, a., Sanz, R., & Calleja, G. (2013). Amino-functionalized pore-expanded SBA-15 for CO2 adsorption. *Adsorption*, *19*(2-4), 589–600. doi:10.1007/s10450-013-9482-y

Plaza, M. G., Pevida, C., Arias, B., Fermoso, J., Arenillas, a., Rubiera, F., & Pis, J. J. (2008). Application of thermogravimetric analysis to the evaluation of aminated solid sorbents for CO2 capture. *Journal of Thermal Analysis and Calorimetry*, *92*(2), 601–606. doi:10.1007/s10973-007-8493-x

Puxty, G., Rowland, R., Allport, A., Yang, Q. I., Bown, M., Burns, R., … Attalla, M. (2009). Carbon Dioxide Postcombustion Capture : A Novel Screening Study of the Carbon Dioxide Absorption Performance of 76 Amines. *Environmental Science & Technology*, *43*(16), 6427–6433.

Qi, G., Fu, L., Choi, B. H., & Giannelis, E. P. (2012). Efficient CO2 sorbents based on silica foam with ultra-large mesopores. *Energy & Environmental Science*, *5*(6), 7368. doi:10.1039/c2ee21394j

Qi, G., Wang, Y., Estevez, L., Duan, X., Anako, N., Park, A.-H. A., … Giannelis, E. P. (2011). High efficiency nanocomposite sorbents for CO2 capture based on amine-functionalized mesoporous capsules. *Energy & Environmental Science*, *4*(2), 444. doi:10.1039/c0ee00213e

Rezaei, F., Lively, R. P., Labreche, Y., Chen, G., Fan, Y., Koros, W. J., & Jones, C. W. (2013). Aminosilane-grafted polymer/silica hollow fiber adsorbents for CO_2 capture from flue gas. *ACS Applied Materials & Interfaces*, *5*(9), 3921–31. doi:10.1021/am400636c

Rochelle, G. T. (2009). Amine scrubbing for CO2 capture. *Science (New York, N.Y.)*, *325*(5948), 1652–4. doi:10.1126/science.1176731

Rosenholm, J. M., Duchanoy, A., & Lindén, M. (2008). Hyperbranching Surface Polymerization as a Tool for Preferential Functionalization of the Outer Surface of Mesoporous Silica †. *Chemistry of Materials*, *20*(3), 1126–1133. doi:10.1021/cm7021328

Rosenholm, J. M., & Linde, M. (2007). Wet-Chemical Analysis of Surface Concentration of Accessible Groups on Different Amino-Functionalized Mesoporous SBA-15 Silicas, (6), 5023–5034.

Santos, A., Ajbary, M., Kherbeche, A., Piñero, M., Rosa-Fox, N., & Esquivias, L. (2008). Fast CO2 sequestration by aerogel composites. *Journal of Sol-Gel Science and Technology*, *45*(3), 291–297. doi:10.1007/s10971-007-1672-1

Sanz, R., Calleja, G., Arencibia, A., & Sanz-Pérez, E. S. (2012). Amino functionalized mesostructured SBA-15 silica for CO2 capture: Exploring the relation between the adsorption capacity and the distribution of amino groups by TEM. *Microporous and Mesoporous Materials*, *158*, 309–317. doi:10.1016/j.micromeso.2012.03.053

Sanz, R., Calleja, G., Arencibia, A., & Sanz-Pérez, E. S. (2013). Development of high efficiency adsorbents for CO2 capture based on a double-functionalization method of grafting and impregnation. *Journal of Materials Chemistry A*, *1*(6), 1956. doi:10.1039/c2ta01343f

Sartori, G., & Savage, D. W. (1983). Sterically hindered amines for carbon dioxide removal from gases. *Industrial & Engineering Chemistry Fundamentals*, *22*, 239–249.

Savage, D. W., Sartori, G., & Astarita, G. (1984). Amines as rate promoters for carbon dioxide hydrolysis. *Faraday Discussions of the Chemical Society*, *77*, 17. doi:10.1039/dc9847700017

Sawyer, L. C., Grubb, D. T., & Meyers, G. F. (1996). *Polymer Microscopy* (3rd ed.). London: Chapmand & Hall.

Sayari, A., & Belmabkhout, Y. (2010). Stabilization of amine-containing CO(2) adsorbents: dramatic effect of water vapor. *Journal of the American Chemical Society*, *132*(18), 6312–4. doi:10.1021/ja1013773

Serna-Guerrero, R., Belmabkhout, Y., & Sayari, A. (2010a). Influence of regeneration conditions on the cyclic performance of amine-grafted mesoporous silica for CO2 capture: An experimental and statistical study. *Chemical Engineering Science*, *65*(14), 4166–4172. doi:10.1016/j.ces.2010.04.029

Serna-Guerrero, R., Belmabkhout, Y., & Sayari, A. (2010b). Triamine-grafted pore-expanded mesoporous silica for CO2 capture: Effect of moisture and adsorbent regeneration strategies. *Adsorption*, *16*(6), 567–575. doi:10.1007/s10450-010-9253-y

Serna-guerrero, R., Belmabkhout, Y., & Sayari, A. (2011). Adsorption of CO 2 - containing gas mixtures over amine-bearing pore-expanded MCM-41 silica : application for CO 2 separation. *Adsorption*, *17*, 395–401. doi:10.1007/s10450-011-9348-0

Sie, S. L. W. H. W. (2012). Tetraethylenepentamine-modified mesoporous adsorbents for CO 2 capture : effects of preparation methods, 431–437. doi:10.1007/s10450-012-9429-8

Sing, K. S. W., Everett, D. H., Haul, R. A. W., Moscou, L., Pierotti, R. A., Rouquerol, J., & Siemieniewska, T. (1985a). REPORTING PHYSISORPTION DATA FOR GAS / SOLID SYSTEMS with Special Reference to the Determination of Surface Area and Porosity. *Pure and Applied Chemistry*, *57*(4), 603–619.

Sing, K. S. W., Everett, D. H., Haul, R. A. W., Moscou, L., Pierotti, R. A., Rouquerol, J., & Siemieniewska, T. (1985b). Reporting physisorption data for gas/solid systems

with special reference to the determination of surface area and porosity (Recommendations 1984). *Pure and Applied Chemistry*, *57*(4), 603–619. doi:10.1351/pac198557040603

Son, W.-J., Choi, J.-S., & Ahn, W.-S. (2008). Adsorptive removal of carbon dioxide using polyethyleneimine-loaded mesoporous silica materials. *Microporous and Mesoporous Materials*, *113*(1-3), 31–40. doi:10.1016/j.micromeso.2007.10.049

Subagyono, D. J. N., Liang, Z., Knowles, G. P., & Chaffee, A. L. (2011). Amine modified mesocellular siliceous foam (MCF) as a sorbent for CO2. *Chemical Engineering Research and Design*, *89*(9), 1647–1657. doi:10.1016/j.cherd.2011.02.019

Subagyono, D. J. N., Liang, Z., Knowles, G. P., Webley, P. a., & Chaffee, A. L. (2011). PEI modified mesocellular siliceous foam: A novel sorbent for CO2. *Energy Procedia*, *4*, 839–843. doi:10.1016/j.egypro.2011.01.127

Sun, J., & Simon, S. L. (2007). The melting behavior of aluminum nanoparticles. *Thermochimica Acta*, *463*(1-2), 32–40. doi:10.1016/j.tca.2007.07.007

Tanthana, J., & Chuang, S. S. C. (2010). In situ infrared study of the role of PEG in stabilizing silica-supported amines for CO(2) capture. *ChemSusChem*, *3*(8), 957–64. doi:10.1002/cssc.201000090

Trent, J. S. (1984). Ruthenium tetraoxide staining of polymers: new preparative methods for electron microscopy. *American Chemical Society*, 2930–2931.

Tsubokawa, N., & Takayama, T. (2000). Surface modification of chitosan powder by grafting of "dendrimer-like" hyperbranched polymer onto the surface. *Reactive and Functional Polymers*, *43*(3), 341–350. doi:10.1016/S1381-5148(99)00065-6

Vaidya, P. D., & Kenig, E. Y. (2007). CO2-Alkanolamine Reaction Kinetics: A Review of Recent Studies. *Chemical Engineering & Technology*, *30*(11), 1467–1474. doi:10.1002/ceat.200700268

Versteeg, G. F., Van Dijck, A. J., & Van Swaaij, W. P. M. (1996a). ON THE KINETICS BETWEEN CO AND ALKANOLAMINES BOTH IN AQUEOUS AND NON-AQUEOUS SOLUTIONS. AN OVERVIEW. *Chemical Engineering*, *144*(1), 113–158.

Versteeg, G. F., Van Dijck, L. a. J., & Van Swaaij, W. P. M. (1996b). on the Kinetics Between Co 2 and Alkanolamines Both in Aqueous and Non-Aqueous Solutions. an Overview. *Chemical Engineering Communications*, *144*(1), 113–158. doi:10.1080/00986449608936450

Wang, J., Long, D., Zhou, H., Chen, Q., Liu, X., & Ling, L. (2012). Surfactant promoted solid amine sorbents for CO2 capture. *Energy & Environmental Science*, *5*(2), 5742. doi:10.1039/c2ee02272a

Wang, L., & Yang, R. T. (2011). Increasing Selective CO 2 Adsorption on Amine-Grafted SBA-15 by Increasing Silanol Density, 21264–21272.

Wang, M., Lawal, a., Stephenson, P., Sidders, J., & Ramshaw, C. (2011). Post-combustion CO2 capture with chemical absorption: A state-of-the-art review. *Chemical Engineering Research and Design*, *89*(9), 1609–1624. doi:10.1016/j.cherd.2010.11.005

Wang, Q., Luo, J., Zhong, Z., & Borgna, A. (2011). CO2 capture by solid adsorbents and their applications: current status and new trends. *Energy & Environmental Science*, *4*(1), 42. doi:10.1039/c0ee00064g

Wang, X., Li, H., Liu, H., & Hou, X. (2011). AS-synthesized mesoporous silica MSU-1 modified with tetraethylenepentamine for CO2 adsorption. *Microporous and Mesoporous Materials*, *142*(2-3), 564–569. doi:10.1016/j.micromeso.2010.12.047

Wang, X., Ma, X., Schwartz, V., Clark, J. C., Overbury, S. H., Zhao, S., … Song, C. (2012). A solid molecular basket sorbent for CO 2 capture from gas streams with low CO 2 concentration under ambient conditions. *Physical Chemistry Chemical Physics*, *14*, 1485–1492. doi:10.1039/c1cp23366a

Wei, J., Liao, L., Xiao, Y., Zhang, P., & Shi, Y. (2010). Capture of carbon dioxide by amine-impregnated as-synthesized MCM-41. *Journal of Environmental Sciences*, *22*(10), 1558–1563. doi:10.1016/S1001-0742(09)60289-8

Wei, J., Shi, J., Pan, H., Zhao, W., Ye, Q., & Shi, Y. (2008). Adsorption of carbon dioxide on organically functionalized SBA-16. *Microporous and Mesoporous Materials*, *116*(1-3), 394–399. doi:10.1016/j.micromeso.2008.04.028

Wikstrom, P., Mandenius, C. F., & Larsson, P.-O. (1988). Gas Phase Silylation, A Rapid Method for Preparation of High-performance Liquid Chromatography Supports. *Journal of Chromatography*, *455*, 105–117.

Wörmeyer, K., Alnaief, M., & Smirnova, I. (2012). Amino functionalised Silica-Aerogels for CO2-adsorption at low partial pressure. *Adsorption*, *18*(3-4), 163–171. doi:10.1007/s10450-012-9390-6

Wu, C.-M., Lin, S.-Y., & Chen, H.-L. (2012). Structure of a monolithic silica aerogel prepared from a short-chain ionic liquid. *Microporous and Mesoporous Materials*, *156*, 189–195. doi:10.1016/j.micromeso.2012.02.039

Xu, X., Song, C., Andresen, J. M., Miller, B. G., & Scaroni, A. W. (2002). Novel Polyethylenimine-Modified Mesoporous Molecular Sieve of MCM-41 Type as High-Capacity Adsorbent for CO 2 Capture. *Energy & Fuels*, *16*(6), 1463–1469. doi:10.1021/ef020058u

Xu, X., Song, C., Andresen, J. M., Miller, B. G., & Scaroni, A. W. (2003). Preparation and characterization of novel CO2 "molecular basket" adsorbents based on polymer-modified mesoporous molecular sieve MCM-41. *Microporous and Mesoporous Materials*, *62*(1-2), 29–45. doi:10.1016/S1387-1811(03)00388-3

Xu, X., Song, C., Miller, B. G., & Scaroni, A. W. (2005). Adsorption separation of carbon dioxide from flue gas of natural gas-fired boiler by a novel nanoporous "molecular basket" adsorbent. *Fuel Processing Technology*, *86*(14-15), 1457–1472. doi:10.1016/j.fuproc.2005.01.002

Xue, Q., Wu, D., Zhou, Y., & Zhou, L. (2012). Improvement of amine-modification with piperazine for the adsorption of CO2. *Applied Surface Science*, *258*(8), 3859–3863. doi:10.1016/j.apsusc.2011.12.046

Yan, W., Tang, J., Bian, Z., Hu, J., & Liu, H. (2012). Carbon Dioxide Capture by Amine-Impregnated Mesocellular-Foam-Containing Template. *Industrial & Engineering Chemistry Research*, *51*(9), 3653–3662. doi:10.1021/ie202093h

Yan, X., Zhang, L., Zhang, Y., Qiao, K., Yan, Z., & Komarneni, S. (2011). Amine-modified mesocellular silica foams for CO 2 capture. *Chemical Engineering Journal*, *168*, 918–924. doi:10.1016/j.cej.2011.01.066

Yan, X., Zhang, L., Zhang, Y., Yang, G., & Yan, Z. (2011). Amine-Modified SBA-15 : Effect of Pore Structure on the Performance for CO 2 Capture. *Industrial & Engineering Chemistry Research*, *50*, 3220–3226.

Yang, S.-T., Kim, J.-Y., Kim, J., & Ahn, W.-S. (2012). CO2 capture over amine-functionalized MCM-22, MCM-36 and ITQ-2. *Fuel*, *97*, 435–442. doi:10.1016/j.fuel.2012.03.034

Yeh, J. T., Pennline, H. W., & Resnik, K. P. (2004). Aqua ammonia process for simultaneous removal of CO2, SO2, and NOx. *International Journal of Environmental Technology and Management*, *4*, 89–104.

Yokoi, T., Yoshitake, H., Yamada, T., Kubota, Y., & Tatsumi, T. (2006). Amino-functionalized mesoporous silica synthesized by an anionic surfactant templating route. *Journal of Materials Chemistry*, *16*(12), 1125. doi:10.1039/b516863e

Young, P. D., & Notestein, J. M. (2011). The role of amine surface density in carbon dioxide adsorption on functionalized mixed oxide surfaces. *ChemSusChem*, *4*(11), 1671–8. doi:10.1002/cssc.201100244

Yu, C.-H. (2012). A Review of CO2 Capture by Absorption and Adsorption. *Aerosol and Air Quality Research*, 745–769. doi:10.4209/aaqr.2012.05.0132

Yue, M. B., Chun, Y., Cao, Y., Dong, X., & Zhu, J. H. (2006). CO2 Capture by As-Prepared SBA-15 with an Occluded Organic Template. *Advanced Functional Materials*, *16*(13), 1717–1722. doi:10.1002/adfm.200600427

Yue, M. B., Sun, L. B., Cao, Y., Wang, Y., Wang, Z. J., & Zhu, J. H. (2008). Efficient CO2 capturer derived from as-synthesized MCM-41 modified with amine. *Chemistry European Journal*, *14*(11), 3442–51. doi:10.1002/chem.200701467

Zeleňák, V., Badaničová, M., Halamová, D., Čejka, J., Zukal, a., Murafa, N., & Goerigk, G. (2008). Amine-modified ordered mesoporous silica: Effect of pore size on carbon dioxide capture. *Chemical Engineering Journal*, *144*(2), 336–342. doi:10.1016/j.cej.2008.07.025

Zelenak, V., Halamova, D., Gaberova, L., Bloch, E., & Llewellyn, P. (2008). Amine-modified SBA-12 mesoporous silica for carbon dioxide capture: Effect of amine basicity on sorption properties. *Microporous and Mesoporous Materials*, *116*(1-3), 358–364. doi:10.1016/j.micromeso.2008.04.023

Zeng, P., Zajac, S., Clapp, P. C., & Rifkin, J. A. (1998). Nanoparticle sintering simulations. *Science*, *252*, 301 – 306.

Zhang, Y., Zhang, S., Lu, X., Zhou, Q., Fan, W., & Zhang, X. (2009). Dual amino-functionalised phosphonium ionic liquids for CO2 capture. *Chemistry European Journal*, *15*, 3003–3011. doi:10.1002/chem.200801184

Zhao, G., Aziz, B., & Hedin, N. (2010). Carbon dioxide adsorption on mesoporous silica surfaces containing amine-like motifs. *Applied Energy*, *87*(9), 2907–2913. doi:10.1016/j.apenergy.2009.06.008

Zhao, J., Simeon, F., Wang, Y., Luo, G., & Hatton, T. A. (2012). Polyethylenimine-impregnated siliceous mesocellular foam particles as high capacity CO2 adsorbents. *RSC Advances*, *2*(16), 6509. doi:10.1039/c2ra20149f

Zheng, F., Tran, D. N., Busche, B. J., Fryxell, G. E., Addleman, R. S., Zemanian, T. S., & Aardahl, C. L. (2005). Ethylenediamine-Modified SBA-15 as Regenerable CO 2 Sorbent. *Industrial & Engineering Chemistry Research*, *44*(9), 3099–3105. doi:10.1021/ie049488t

APPENDIX A

SYNTHESIS OF TETRAETHYLENEPENTAMINE WET IMPREGNATED PARTICUALTE AEROGELS

1. Place Cabot MT-1100 Nanogel into an oven and heat treat for 8 hrs at 400 ^{o}C with a heating rate of 5 ^{o}C/min. Labeled as MT400

2. To prepare the impregnation solution, add the appropriate amount of TEPA to 70 mL of methanol in a 250 mL filtering flask and mix for 10 min using a magnetic stirring rod. Refer to Table A.1 for the appropriate amount of TEPA for desired wt% of TEPA in the aerogel support.

Table A.1: Amount of TEPA to add to Methanol for desired weight percentage of sorbent

Amount of TEPA (g)	**Weight % of TEPA in Aerogel**
1.33	40
2.00	50
3.00	60
4.67	70
8.00	80
11.3	85

3. Add 2.0 g of the MT400 to the impregnation solution in flask and stir for 10 min.

4. Place a rubber stopper in mouth of the flask and attach vacuum source to the vacuum spout of the flask. Apply a slow stir while vacuuming until the slurry becomes a thick paste then discontinue stirring and vacuum for 24 hrs.

5. After vacuuming period is finished remove aerogel sorbent from the flask into a air-tight container.

6. For hydrophobic aerogel, repeat steps 2-5 with the original Cabot Nanogel

APPENDIX B

SYNTHESIS OF TETRAETHYLENEPENTAMINE MODIFIED AEROGEL USING THE CONTROLLED EVAPORATIVE PRECIPITATION METHOD

1. First a saturated TEPA/n-hexane solution was prepared by adding TEPA (9 mL) to 100 mL of n-hexane in a 150 mL Erlenmeyer flask at room temperature.

2. The mixture was then heated with stirring to a light boil (~68 ^{o}C, hexane's boiling temperature). TEPA has a solubility of approximately 7 and 40 mg/mL at 23 ^{o}C and 68 ^{o}C, respectively.

3. In a 50 mL Erlenmeyer flask, 1 g of hydrophilic aerogel MT400 (Appendix A) and 20 mL of n-hexane were mixed and heated to approximately 60 ^{o}C. This aerogel/hexane slurry was reduced due to evaporation of n-hexane until a paste developed weighing approximately 4.0 g (1.0 g of MT400 and 3.0 g of n-hexane)

4. At this point, 5 mL of the TEPA/n-hexane solution at 68 ^{o}C was removed by a glass pipette and added into a 25 mL beaker heated by a second hot plate. Perform this step as fast as possible to prevent too much precipitation and loss of TEPA in pipet.

5. Once the TEPA is re-dissolved, add the 5 mL of TEPA/n-hexane solution in the 25 mL beaker to the aerogel/hexane paste and then mix by hand swinging the flask in a circular fashion until the solution and paste is well mixed.

6. Keep contents heating until the weight of the sample reaching approximately 4.0 g and has the same paste consistency as before.

7. Continue steps 4-6 according to Table B.1 to reached the desired TEPA content immobilized in the aerogel support. Each 5 mL addition contains approximately 200 mg of TEPA. For a 50 wt% TEPA/aerogel sample, 5 additions of 5 mL of TEPA/n-hexane (25 mL total, equivalent to 1 g of TEPA) are required. Note some TEPA precipitates in pipette and therefore the desired wt % of TEPA will be slightly lower than that desired.

Table B.1: Amount of 5 mL additions for a desired TEPA content in Aerogel

Number of Additions	Wt % of TEPA in Aerogel
2.0	30
3.5	40
5.0	50
8.0	60
11.5	70
20.0	80
45.0	90

8. The final paste is then cooled to room temperature and then vacuumed dried at 25 ^{o}C for 24 hrs.

APPENDIX C

SYNTHESIS OF AMINE GRAFTED AEROGEL BY ANHYDROUS LIQUID PHASE SILANE METHOD

1. For anhydrous grafting, a calculated amount of MT400 (Appendix A) was activated by placing in an oven at 150 ^{o}C for 2 hrs to remove any adsorbed species, and then placed in a 250 mL teflon flask with a PTFE cap.

2. Anhydrous toluene was then added to the aerogel. The amount of toluene should be in a ratio equal to 1.0 g to 75 mL of toluene. For example if the desired amount of aerogel added in 0.5 g, the amount of toluene should be approximately 37 mL. Mix for 10 min.

3. A solution of toluene and aminosilane (e.g. tri, di, or mono-amine silane) is then prepared by adding a calculated amount of silane to 50 mL of toluene. The amount of silane added is up to ones decision. I recommend a 2:1 silane to aerogel ratio for adequate grafting. Also the amount of toluene in this solution should be in a ratio of 1.0 g to 50 mL. Therefore the total ratio of aerogel to toluene is approximately 1.0 g to 125 mL.

4. Added the silane/toluene solution to the aerogel/toluene mixture in the teflon flask and mix for 1-2 min.

5. With the PTFE cap on the flask tightly, place in an oil bath at a designated temperature for 18 hrs. Make sure a stir bar is present in both the oil bath and Teflon flask for homogenous mixing and temperature distributions.

6. After 18 hr period, the contents are then filtered and washed with 100 mL of toluene twice and 100 mL of n-hexane once. Use Grade 5 filter paper.

7. Filtered samples were then dried in flowing argon in an oven at 150 ^{o}C for 2 hrs.

APPENDIX D

SYNTHESIS OF AMINE GRAFTED AEROGEL BY HYDROUS LIQUID PHASE SILANE METHOD

1. For hydrous grafting, a calculated amount of MT400 (Appendix A) was activated by placing in an oven at 150 ^{o}C for 2 hrs to remove any adsorbed species, and then placed in a 250 mL teflon flask with a PTFE cap.

2. Anhydrous toluene was then added to the aerogel. The amount of toluene should be in a ratio equal to 1.0 g to 75 mL of toluene. For example if the desired amount of aerogel added in 0.5 g, the amount of toluene should be approximately 37 mL. Mix for 10 min.

3. Then a calculated amount of water was added to the toluene/MT400 mixture in Teflon flask by drop wise under vigorous mixing. I recommend a ratio of 300 mg of water to 1.0 g of aerogel. The Teflon flask was then tightly capped and then placed in a oil bath at 80 ^{o}C for 3 hrs with vigorous mixing to homogenous the water/toluene/MT400 mixture.

4. A solution of toluene and aminosilane (e.g. tri, di, or mono-amine silane) is then prepared by adding a calculated amount of silane to 50 mL of toluene. The amount of silane added is up to ones decision. I recommend a 2:1 silane to aerogel ratio for adequate grafting. Also the amount of toluene in this solution should be in a ratio of 1 g to 50 mL. Therefore the total ratio of aerogel to toluene is approximately 1 g to 125 mL.

5. Added the silane/toluene solution to the aerogel/water/toluene mixture in the teflon flask and place immediately in an oil bath at the desired temperature of grafting for 18 hrs. Make sure a stir bar is present in both the oil bath and Teflon flask for homogenous mixing and temperature distributions.

6. After 18 hr period, the contents are then filtered and washed with 100 mL of toluene twice and 100 mL of n-hexane once. Use Grade 5 filter paper.

7. Filtered samples were then dried in flowing argon in an oven at 150 ^{o}C for 2 hrs.

APPEDNIX E

SYNTHESIS OF AMINE GRAFTED AREOGELS BY ATOMIC LAYER DEPOSITION OF AMINO SILANE PRECURSORS

1. First place approximately 15 mL of the desired silane into the reagent vessel in the ALD setup (Figure 5.1)

2. The silane reagent vessel needs to be activated (i.e. all air and water vapor removed from vessel. Therefore place vessel on ALD apparatus and purge the entire system with Argon for 30 min with the vessel valve open.

3. Then vacuum the entire system with the vessel valve remaining open. Make sure the apparatus is at room temperature. Repeat this process two times ending with the vacuum so the pressure inside the vessel is approximately 5 mbar. Then close the vessel valve.

4. Repeat this process for the water reagent vessel.

5. Then place approximately 30 mg of MT400 (Appendix A) in the sample pan and activate in two sequential steps. First the reactor chamber was heated to 150 ^{o}C with a purge flow of Argon at 100 mL/min for 30 min. Then holding this temperature the reactor chamber was vacuumed to less than 5 mbar and held here for 30 min.

6. At this time heat the silane reagent vessel to 130 ^{o}C.

7. With the reactor chamber at 5 mbar and 150 ^{o}C, close needle valve between silane and water reagent vessels and also valve at end of reactor on opposite side. Then open the silane reagent vessel and allowed to react for 24 hrs.

8. Once complete, close the vessel valve and purge the reactor chamber with Argon for 30 min while heat remains at 150 ^{o}C. To perform this purge and prevent any condensation to occur in the areas where no heating tape exists, first open valve to gas to pressurize the water vessel section of the reactor (note: keep pressure below 2 bar). Then open needle valve between the two vessel slightly to allow some argon to flow through for 1-2 min. Don’t allow pressure on the water vessel portion to be below 1 bar. Then

turn on vacuum and open valve at other end of reactor. Make sure flow is going through the cold trap. Continue this vacuum with Argon flow purge for 30 min.

9. Close valve to Argon gas and allow the system to reach 5 mbar again.

10. Then close valve at the end of reactor and open the water reagent vessel. The temperature of the water vessel should be 25 ^{o}C. Allow to react for 3 hrs.

11. After water introduction the reactor chamber was purged and vacuumed as explained previously after silylation.

12. The repeated introduction of silane and then water is repeated until the desired number of cycles is reached.

APPENDIX F

CARBON DIOXIDE ADSORPTION MEASUREMENT BY GRAVAMETRIC MICROBALANCE

1. Remove the glass sample chamber from the microbalance. Be sure to only touch the end of the sample chamber for static can developed where touched and therefore can produce fluctuations in weight during testing.

2. Run the microbalance software package and establish a connection with the balance. With the sample pan still attached make sure the reading of the weight is 0.00000. A fluctuation of +/-0.00050 is fine. If weight does not read near zero, tare the weight. Make sure the sample pan is steady during the tare to obtained an accurate base weight.

3. Place approximately 10 mg of the desired sorbent in the sample pan of the microbalance chamber. Read the weight to obtained approximately 10 mg.

4. Carefully reattached the glass sample chamber to microbalance and close the tube furnace around the chamber. Be sure the sample pan is not touching the inside wall of the glass chamber.

5. First activate the sample by heating the furnace to the desired chamber and purging the chamber with Argon. Argon must be used for the densities of Argon and CO_2 are close and therefore buoyancy effects negligible. For amine based sorbents, activation was performed by heating the sorbent to 100 ^{o}C at a rate of 10 ^{o}C/min with Argon flowing at 100 mL/min for 30 min.

6. After activation, reduce temperature of the chamber to the desired adsorption temperature.

7. Once adsorption temperature is reached and stable, start the data acquisition in the software to being weight recording. The time of recording and rate of data acquisition was 3 hrs and 5 sec intervals.

8. Introduce CO_2. The flow rate was commonly set at 100 mL/min.

9. After 1 hr of adsorption or until the weight has stabilized and equilibrium has been reached, end the data acquisition and remove the sample.

10. The data is recorded in absolute weight of sample. Therefore in order to know how many ‘mmol/g’ was adsorbed use the equation below.

$$q\left(\frac{mmol}{g}\right) = \frac{Final\ weight - Initial\ weight}{Initial\ weight} * 1000/Mw_{CO2}$$